Differentiating Common Workplace Postures through Plantar Pressure: Laying the Groundwork for a Low-Cost Instrumented Insole

by

Kohle James Merry

B.A.Sc., The University of British Columbia, 2015

Thesis Submitted in Partial Fulfillment of the
Requirements for the Degree of
Master of Applied Science

in the
School of Mechatronic Systems Engineering
Faculty of Applied Science

© Kohle James Merry 2017
SIMON FRASER UNIVERSITY
Fall 2017

Approval

Name:	**Kohle James Merry**
Degree:	**Master of Applied Science**
Title:	**Differentiating Common Workplace Postures through Plantar Pressure: Laying the Groundwork for a Low-Cost Instrumented Insole**

Examining Committee: **Chair: Siamak Arzanpour**
Associate Professor

Carolyn Sparrey
Senior Supervisor
Associate Professor

Edward Park
Supervisor
Professor

Michael Ryan
Supervisor
Adjunct Professor
Biomedical Physiology and Kinesiology

Stephen Robinovitch
Internal Examiner
Professor
Biomedical Physiology and Kinesiology

Ethics Statement

The author, whose name appears on the title page of this work, has obtained, for the research described in this work, either:

a. human research ethics approval from the Simon Fraser University Office of Research Ethics

or

b. advance approval of the animal care protocol from the University Animal Care Committee of Simon Fraser University

or has conducted the research

c. as a co-investigator, collaborator, or research assistant in a research project approved in advance.

A copy of the approval letter has been filed with the Theses Office of the University Library at the time of submission of this thesis or project.

The original application for approval and letter of approval are filed with the relevant offices. Inquiries may be directed to those authorities.

Simon Fraser University Library
Burnaby, British Columbia, Canada

Update Spring 2016

Abstract

Prolonged weight bearing (WBR) at work is a suspected risk factor for the development of musculoskeletal disorders that commonly occur in the feet. No objective measure to quantify time spent in different WBR postures currently exists, creating a barrier in investigating the connection between WBR and foot pain. This study aimed to develop a prototype design for a low-cost instrumented insole system capable of differentiating workplace postures (sitting, standing and walking). Three objectives were defined: 1) quantify and differentiate the pedobarographic characteristics associated with each posture, 2) classify the postures from plantar pressure characteristics and 3) develop an insole system with off-the-shelf sensors capable of classifying workplace postures. Pressure measures near the hindfoot and central/lateral forefoot were found to simultaneously differentiate the postures, and machine learning algorithms accurately classified the postures using plantar pressure metrics. This foundational work facilitates the deployment of a low-cost instrumented insole for workplace studies where it will provide the objective evidence needed to resolve the link between WBR and foot pain.

For my parents, Wendy and James Merry.

When I set my sails, you were my wind.

Acknowledgements

First and foremost, I would like to acknowledge the abundant and steadfast support of my senior supervisor Dr. Carolyn Sparrey. Carolyn has always trusted my judgement and allowed me control over the direction of the research enclosed in this thesis; although challenging at first, I have come to appreciate the wisdom in her way—it encouraged me to think for myself and trust my own capabilities, which was not, and is still not, always easy. To me, Carolyn is a mentor, a mother, a strong woman in STEM, slightly terrifying, and hopefully a lifelong friend. This experience would not have been the same without her.

Dr. Michael Ryan, representing *Kintec Footlabs Inc*., provided me with consistent support and guidance throughout my tenure. Michael brought an unparalleled clinical insight that has not only helped my work, but will facilitate future works as this project transitions into the next phase: workplace deployment.

Refayet Siam, an undergraduate student out of Mechatronics, has also contributed significantly to this work. A true "Engineer's Engineer," Refayet has an amazing set of hands-on skills, and I have no doubt he will go on to do great things.

My lab mates, both current and former, were always willing to lend an ear. Tim Bhatnagar, Shervin Jannesar, Ehsan Daneshi, Matt Courtemanche, Loiuse Thomas, and Garrett Kryt, thank you for the support.

And last, but by no means least, thank you to my family, my partner Megan (who painstakingly edited every word of every document), and Suzy and Stew MacPherson. Having unconditional support through the ups and downs of graduate school and beyond is a privilege which I am fortunate enough to have, and one I won't soon forget.

Table of Contents

List of Tables

List of Figures

List of Acronyms

ASTD	Activity-Related Soft Tissue Disorder
BTLE	Bluetooth Low Energy
BTD	Bagged Decision Tree
BMI	Body Mass Index
CFS	Correlation Feature Selection
COP	Center of Pressure
DIP	Distal Interphalangeal Joint
DT	Decision Tree
FSR	Force Sensitive Resistor
FTI	Force-Time Integral
IMU	Inertial Measurement Unit
KNN	K-Nearest Neighbour
LDA	Linear Discriminant Analysis
LOOCV	Leave-One-Out Cross-Validation
MCP	Metatarsophalangeal Joint
ML	Machine Learning
MLA	Medial Longitudinal Arch
MRMR	Minimum-Redundancy Maximum-Relevance
NB	Naïve Bayes
NTS	Not to Scale
OSPAQ	Occupational Sitting and Physical Activity Questionnaire
PA	Physical Activity
PCB	Printed Circuit Board
PIP	Proximal Interphalangeal Joint
PF	Plantar Fasciitis
PTI	Pressure-Time Integral
PWS	Preferred Walking Speed
SVM	Support Vector Machine
TMT	Tarsometatarsal Joint
WBR	Weight Bearing
WMSD	Work-Related Musculoskeletal Disorder

Executive Summary

Prolonged weight bearing (WBR) at work is a widely suspected risk factor for the development of musculoskeletal disorders, which most commonly occur in the feet and low back. The absence of an objective tool to quantify time spent in different WBR postures is a significant barrier in establishing evidence to either support or refute the connection between WBR and foot pain. Development of such a tool is impeded by the lack of data characterizing different workplace postures through pedobarographic patterns. The goal of this study was to develop a prototype design for a low-cost instrumented insole system capable of differentiating workplace postures (sitting, standing and walking). To achieve this goal, three objectives were defined: 1) to quantify and differentiate the plantar pressure locations and characteristics associated with each workplace posture, 2) to classify workplace postures from plantar pressure characteristics and 3) to develop an insole system with off-the-shelf force sensitive resistors (FSRs) capable of classifying workplace postures. The plantar pressure patterns of three common workplace postures – sitting (static non-WBR), standing (static WBR), and walking (dynamic WBR) – were characterized using a high-resolution, laboratory grade, in-shoe pressure measurement system. A regional breakdown of the plantar aspect of the foot was modified to enable the isolation of specific foot regions and measurement parameter combinations which significantly differed between the three postures. Following differentiation of sitting, standing and walking using selected plantar pressure measures, a machine learning classification algorithm was employed to determine the locations and number of discrete FSRs necessary to differentiate the three postures. Outcomes from the machine learning study were then built into a prototype low-cost instrumented insole. Overall, pressure measures in the medial and lateral hindfoot as well the lateral midfoot best differentiated the three postures simultaneously; the medial and central forefoot also differentiated the three postures concurrently using pressure and contact area measures, but to a lesser extent. These results were then validated through machine learning, which independently selected sensors around the midfoot/hindfoot boundary, and central/lateral forefoot, as most indicative of the posture; three sensor locations – the central forefoot and the medial and lateral midfoot – correctly classified the three postures 98% of the time while sampling at 15Hz using a three second overlapping sliding window approach. To build in redundancy to the low-cost insole prototype, five sensor locations were required based on the

machine learning study: two sensors in the central forefoot, one in the lateral forefoot, and one in each of the medial and lateral heel regions. By Nyquist Theory, a minimum sampling rate of 3Hz was selected for the system based on a slow step frequency of 1.41Hz. Additionally, sensor resolution was selected on the basis of avoiding sensor saturation under loading conditions found on the plantar aspect of the foot. Initial testing of the low-cost insole prototype revealed that this standalone system can collect in-shoe plantar force data over an extended duration. Further testing of the insole prototype coupled with refinement of the machine learning classification scheme will allow this system to classify sitting, standing and walking in a similar fashion to the commercial in-shoe measurement system. This work demonstrates that it is possible to accurately classify common workplace postures based on pedobarographic patterns, and these postulations were physically confirmed through development of the insole prototype. This foundational work facilitates the deployment of a low-cost instrumented insole for workplace studies, where it will provide the objective evidence needed to confirm or dispute the causal link between WBR and foot pain. Further research using the system could also identify which characteristics of an individual's pedobarographic pattern may predispose an individual to plantar fasciitis or other WBR-related disorders; evidence suggesting atypical pedobarographic patterns leading to PF or other WBR-related disorders is not currently substantiated in the field.

Chapter 1.

Introduction

1.1. Background and Motivation

Prolonged weight bearing (WBR) in the working population is commonplace; it is believed that approximately 47% of employees stand for more than 75% of their workday [1]. A suspected consequence of this loading is the development of work-related musculoskeletal disorders (WMSDs), which are most common in the feet and the low back [2]. In particular, plantar fasciitis (PF) is a debilitating foot disorder that presents as pain in the plantar heel region of the foot which can migrate throughout the entire plantar aspect of the foot and calf. It is estimated that approximately 10% to 24% [3-6] of the general population will be affected by plantar foot pain at some stage in their life; however, studies have shown that this estimate rises in working populations where prolonged WBR is unavoidable, such as retail salespeople (50% [2]), factory workers (52% to 69% [7,8]), and healthcare professionals (11% to 74% [9,10]). The national economic burden of plantar fasciitis in the US is estimated to be approximately $284 million US/yr. with 1,005,000 patient-visits per year [11].

WorkSafeBC policy designates PF as a non-traumatically induced activity-related soft tissue disorder (ASTD) and notes it as a common cause of musculoskeletal pain among workers in British Columbia. Despite various studies suggesting a causal link between prolonged WBR and the development of plantar foot pain, it is extremely difficult to attribute the disorder directly to work-related WBR because of the lacking evidence related to the etiology of PF [12-15]. A diagnosis of PF is often associated with a variety of factors making it challenging to determine whether intrinsic factors (e.g., BMI, age, gender) or extrinsic factors, such as prolonged WBR, are more influential in the development of PF. Due to this ambiguity, justifying workers' compensation for plantar fasciitis is problematic and highly subjective, resulting in most claims being denied. Between 2009 and 2013, WorkSafeBC accepted an average of 13 claims and denied 38 claims for PF per year, resulting in an average time lost cost of $194,000 per year (approximately $15,000 per claim) [16]. In 2015, WorkSafeBC amended that PF be subsequently defined as an occupational hazard, while still noting that the current evidence does not relate PF to any one process or industry; evaluations of causality are still conducted on

a case-by-case basis [17]. Quantifying and linking prolonged exposure to physical risk factors in the workplace and PF is not as immediate as a traumatic injury, such as a fall. Therefore, the prevalence of WMSDs like PF are frequently underestimated from workers' compensation claims as many cases go unreported [18,19].

Attributing work causality to the development of PF is challenged by the bias and inaccuracy associated with reporting time spent WBR at work, and more specifically, time spent standing (static WBR) versus walking (dynamic WBR). Use of self-report measures to determine time spent in workplace activities has had varying results and its utility in estimating workplace physical activity (PA) has been cautioned [20]. For example, one study comparing objective to self-report measures found that self-report was moderately accurate in measuring sitting and standing time, but not walking time [21], whereas another study found self-reporting workplace activity to underestimate standing time and overestimate walking time [22]. This variability is problematic, as research has shown prolonged standing to be particularly damaging to the plantar fascia [4,5,23,24]. Although no definitive answer exists as to why static WBR may be more causal in the development of PF than dynamic WBR, recent evidence suggests that soft tissue metabolism is mechanosensitive and modulated by the frequency of applied load [25]. Therefore, the constant load applied during prolonged standing theoretically places the worker at a greater risk of developing PF. This underlying ambiguity regarding the etiology of PF coupled with the established inaccuracies associated with self-reporting PA at work suggests that direct measurement of time spent WBR would yield more significant correlations between prolonged WBR and PF [9,26-28].

When compared to more direct measures of activity (e.g. accelerometer based inertial technologies, biometric tracking, video-monitoring, etc.), criticism has emerged regarding the accuracy and reliability of using self-report methods to collect activity data due to recall bias and other limitations [29-34]. However, direct measures of activity also have several shortcomings. Inertial measurement units (IMUs) and biometric technologies have been proven to differentiate complex activities quite reliably (ascending/descending stairs, cycling, walking/jogging, etc.) [35,36]; however, they have limited capabilities when distinguishing between various static activities (i.e. standing from sitting) [37,38]. IMU sensors are also limited by bias (i.e. drift) which can affect the accuracy and reliability of the sensors over time [39-41]. Although orientation data from multi-IMU systems [42,43] and single IMUs placed in select locations [44,45] can distinguish certain static postures, multi-IMU systems are of limited use in everyday life and

single IMUs are often placed in uncomfortable or impractical locations (e.g. chest, waist, thigh) [45] which can interfere with work in some professions. Problematic drift and intrusive single IMU locations make this technology infeasible for the widespread deployment proposed in this work. Additionally, other methods such as video-monitoring can reliability quantify PA at work, but sacrifice worker privacy and are resource-intensive to implement.

The first step to investigate the potential link between WBR and PF is to develop a technology capable of differentiating PA at work. Specifically, time spent walking (dynamic WBR), standing (static WBR) and sitting (static non-WBR) are of primary interest. Because of the explicit activities of interest, many current technologies on the market are beyond the scope of what is needed to characterize activities thought to contribute to PF. Additionally, many systems are not designed to characterize these more subtle passive postures (e.g. sitting from standing) and are therefore often not designed with the sensitivity required to differentiate the postures. Preliminary testing of working prototypes have shown that embedding activity sensors within a shoe insole can quantify activity type and duration with minimal discomfort [36,46]. The high fidelity and temporal resolution associated with deploying an instrumented insole to a worker population allows for more valid conclusions to be drawn about the association (and ultimately relationship) of prolonged WBR at work and PF.

This thesis lays the groundwork for the development of a novel insole technology to be used for differentiating sitting, standing and walking at work. The long-term goal of this project is to utilize this technology to track periods of WBR at work to establish an evidence-based link between WBR and incidence of PF. The focus of this thesis is quantitatively characterizing the plantar pressure distribution patterns between WBR postures (walking and standing) and static postures (standing and sitting). Through machine learning, this research aims to minimize the plantar pressure data needed to accurately differentiate these three postures. By distilling the necessary input data down to only essential measurements, this research will assist in the initial development of a cost-effective, purpose-driven activity differentiation insole ready for deployment to a worker population.

1.2. Foot and Ankle Anatomy

To better quantify the biomechanics of plantar tissue loading, it is necessary to have a basic understanding of foot and ankle anatomy and how external loading on the foot can translate to and affect specific tissue structures.

1.2.1. Bony Structures

In the context of human osteology, the foot can be subdivided into three major areas of interest [47]:

1. **Tarsus**: The tarsus, or tarsal bones, are a collection of seven articulating bones beneath the distal tibia and fibula of the shank.

2. **Metatarsus:** The metatarsus, or metatarsal bones, are a series of five long bones connecting the tarsal bones to the phalanges.

3. **Phalanges:** The phalanges are a series of five digital bones also classed as long bones.

The three major regions of the foot are shown below in Figure 1.
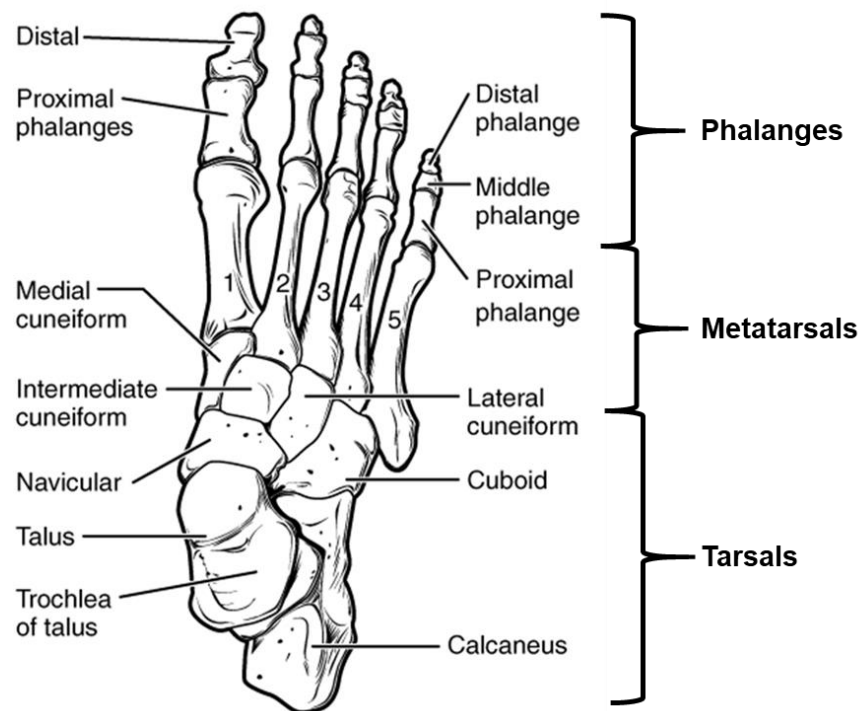
Figure 1   **Superior view of a right foot. Emphasis placed on the three main regions of the foot: Tarsus ('Tarsals'), Metatarsus ('Metatarsals') and Phalanges.**

Figure adapted from [48].

The Tarsus

The tarsus contains seven bones: the calcaneus, talus, cuboid, navicular and the three cuneiform bones, labeled medial, intermediate and lateral (Figure 1). The calcaneus is the largest of these bones, and it is situated at the most posterior end of the foot primarily serving to transmit load to the ground [47]. The talus, or ankle bone, is the second largest bone of the tarsus and acts as a socket to provide a connection between the shank and the foot. The talus is supported mediolaterally by the malleoli and anteriorly by the navicular; the tibia rests on the superior surface of the talus while the inferior surface rests on the calcaneus. The remaining tarsal bones serve to provide an articulating connection between the calcaneus, talus and the metatarsal bones.

The Metatarsus

The five long bones of the metatarsus are numbered from medial to lateral (I-V) (Figure 1) and each demonstrates typical long bone characteristics—two rounded extremities and an

elongated body [47]. The metatarsal bones articulate with four of the tarsal bones (cuboid, three cuneiforms) at their bases, and individually connect to a specific phalange at the head [47].

The Phalanges

Common to both the hands and feet, the phalanges are a series of connected long bones which make up the fingers or toes. The phalanges are also labeled in a similar fashion to the metatarsal bones numbering I-V starting on the medial side with the hallux. Primarily for articulation purposes, the toes are made up of multiple phalanges; the great toe, or hallux, is comprised of two phalanges whereas all other toes have three, labeled proximal, middle and distal (Figure 1). In contrast to the phalanges of the hands, those of the feet have shorter bodies [47].

Generalized Foot Regions

In addition to the three anatomical divisions, the foot can also be subdivided into the hindfoot, the midfoot and the forefoot (Figure 2a). Typically, the bones included in each region are as follows [47]:

1. **Hindfoot**: The hindfoot is comprised of the talus and the calcaneus.

2. **Midfoot**: The midfoot is comprised of the cuboid, navicular and medial, intermediate and lateral cuneiforms.

3. **Forefoot**: The forefoot is comprised of the metatarsal bones (I-V) and the phalanges (I-V).

To increase specificity, this work further subdivides the forefoot region into a forefoot and a toe region (Figure 2b), as detailed below:

1. **Forefoot**: The forefoot is comprised of the metatarsal bones (I-V).

2. **Toe Region**: The toe region is comprised of all the phalanges.
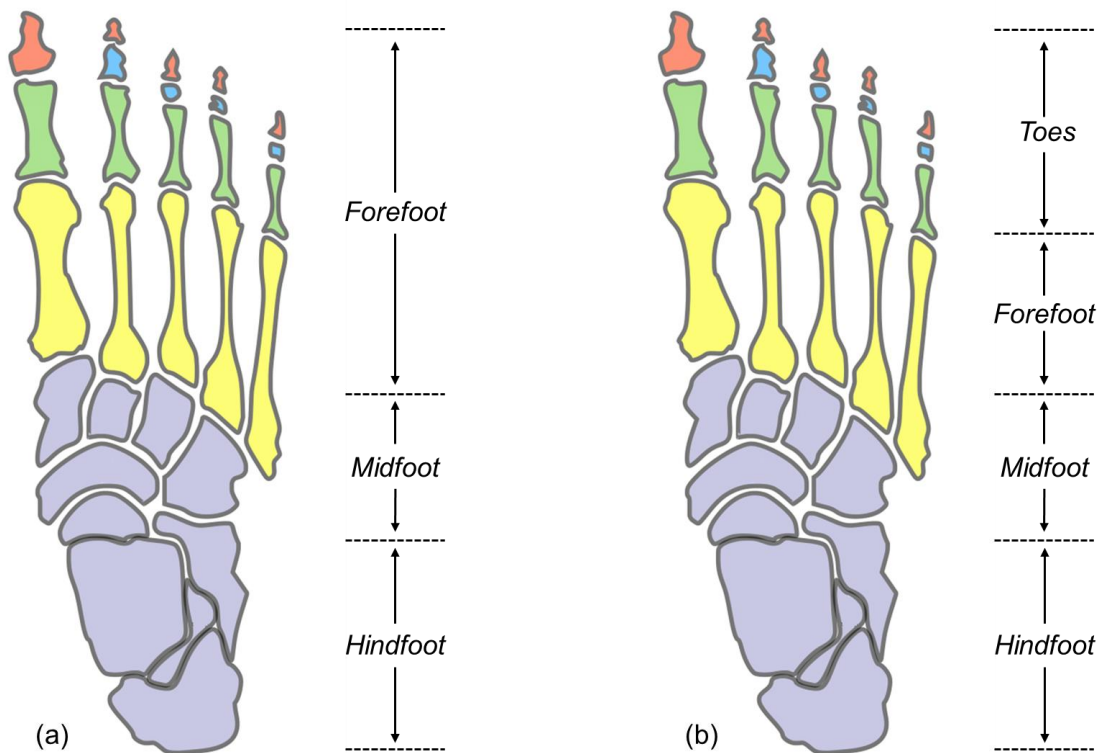
Figure 2   **(a) Generalized foot regions prior to modifications made in this work (b) Generalized foot regions defined in this work; note that the forefoot has been subdivided to a smaller forefoot region and a toe region ('toes'). Tarsal bones are coloured purple, while the metatarsals are coloured yellow. Proximal phalanges are coloured green, middle phalanges blue, and distal phalanges orange. Bolded bone outlines denote overlap due to superior view.**

Figure adapted from [49].

1.2.2. Musculature and Connective Tissues

The Dorsal Tissues of the Foot

The two main muscles of note near the superior surface of the foot are the extensor digitorum brevis and the extensor hallucis brevis. The extensor digitorum brevis originates at the dorsal surface of the calcaneus and inserts at the proximal dorsal region of phalanges II, III and IV; the extensor hallucis brevis originates at the calcaneus and inserts at the proximal phalanx of the hallux [47]. While the extensor digitorum brevis functions to extend digits II, III and IV, the extensor hallucis brevis extends the hallux. The fifth toe is not moved by either of these

muscles, and is instead manipulated by the abductor digiti minimi and the flexor digiti minimi. Although many additional tissues lie deep to the extensor digitorum brevis and the extensor hallucis brevis, their actions are beyond the scope of what is necessary to interpret this work.

The Plantar Tissues of the Foot

The plantar aspect of the foot, similar to the dorsal region, is made up of a series of musculature, and this complexity exceeds the context of this work. The main tissue on the plantar aspect of the foot is the plantar fascia, also known as the plantar aponeurosis. The plantar fascia primarily functions to support the arch of the foot by supporting a tensile load during WBR, and also acts as a shock absorber during the stance phase of gait. A strong connective tissue, the plantar fascia originates at the tuberosity of the calcaneus and inserts at the individual heads of the metatarsal bones. White in colour, the tissue is comprised of collagen fibres oriented primarily parallel to the long axis of the foot. Longitudinally, the plantar fascia can be segmented into medial, lateral and central portions; the medial and lateral portions are thinner than the central portion and span the sides of the plantar aspect of the foot [47]. Additionally, the medial and lateral portions insert at the hallux and fifth toe, respectively, whereas the central portion inserts at the second to fourth toes. The plantar fascia originates as a uniform fibrous band of tissue near the calcaneus then widens anteriorly in the transverse plane, culminating in a division into five processes which insert into the respective metatarsals [47].

1.2.3. Joints

Hindfoot Joints

The hindfoot region is the site of three joints important for dynamic foot function and load distribution, these joints are:

1. **The Talocrural Joint**: Connecting the distal ends of the tibia and fibula to the proximal end of the talus, the talocrural joint is a synovial hinge joint permitting dorsiflexion and plantarflexion of the foot [47]. The Talocrural joint is typically what is referred to as the ankle joint (Figure 3).

2. **The Subtalar Joint**: Connecting the talus to the calcaneus, the subtalar joint plays a fundamental role in load transfer and allows for inversion/eversion of the foot; the

subtalar joint does not assist in the dorsiflexion or plantarflexion of the foot [47] (Figure 3).

3. **The Inferior Tibiofibular Joint**: Connecting the distal ends of the tibia and fibula, the inferior tibiofibular joint is a fibrous joint which enables minor articulation between the distal tibia and fibula [47]. The inferior tibiofibular joint contrasts with the superior tibiofibular joint, which is a synovial joint as opposed to a fibrous joint (Figure 3).
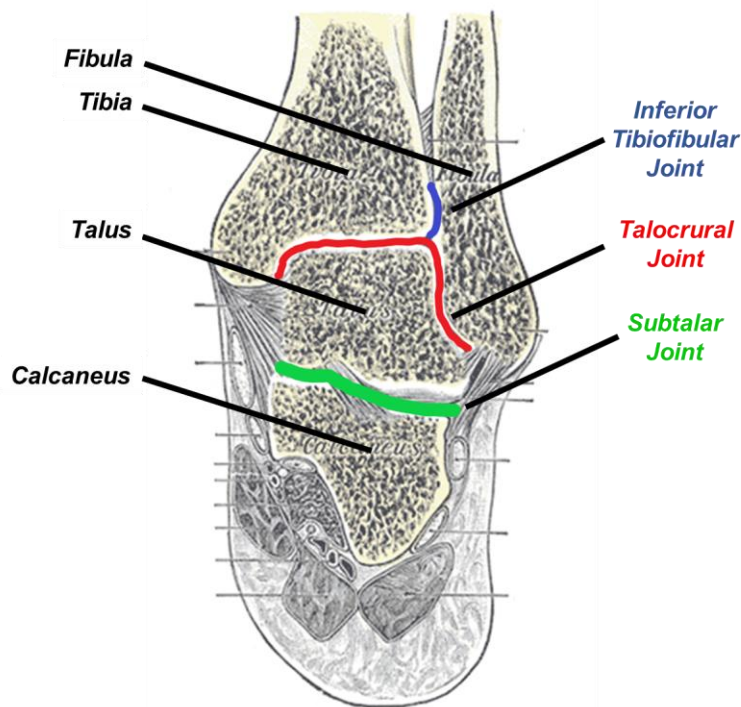
Figure 3   **Posterior view of the foot and ankle complex. The blue line designates the Inferior Tibiofibular Joint, red denotes the Talocrural Joint and green the Subtalar Joint.**

Figure adapted from [47].

Midfoot, Forefoot & Toe Joints

The midfoot, forefoot and toe regions share a number of similar joints, due to the similarities in the five metatarsal and various phalangeal bones, which combine to enable various articulations of the anterior part of the foot (Figure 4). The midfoot extends from the hindfoot through five tarsometatarsal (TMT) joints, which connect the proximal metatarsal bones to the three cuneiform bones and the cuboid [47]. Moving anteriorly, the proximal ends of the metatarsals

9

connect to the distal phalanges through five metatarsophalangeal (MCP) joints, and the phalanges are linked through interphalangeal joints; note that the hallux has a single interphalangeal joint while toes II-V have both proximal (PIP) and distal (DIP) interphalangeal joints [47].

Distal Interphalangeal
(DIP) Joints

Proximal Interphalangeal
(PIP) Joints

Metatarsophalangeal
(MCP) Joints

Tarsometatarsal
(TMT) Joints
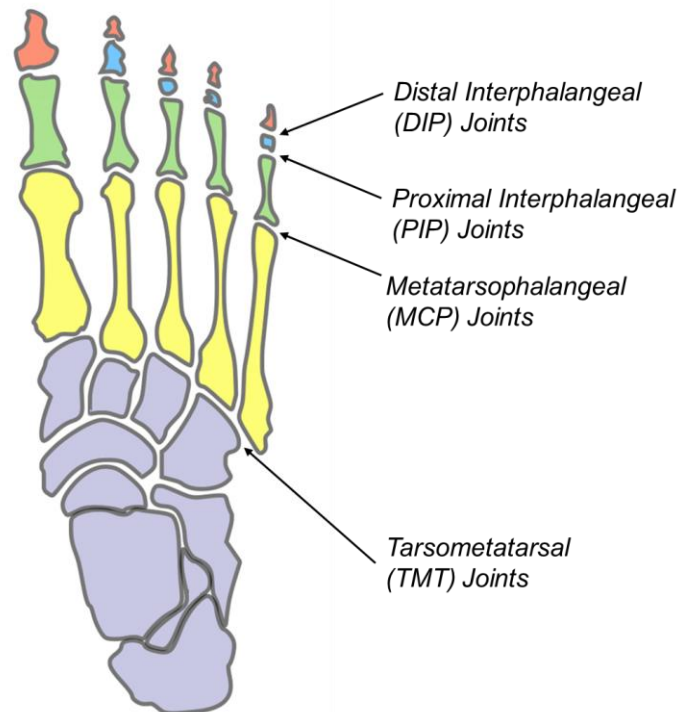
Figure 4   Superior view of selected forefoot, midfoot and toe joints.

Figure adapted from [49].

1.2.4. Arches

The arches of the foot facilitate static WBR in an erect posture and elicit elastic characteristics which aid in dynamic movements [47] (Figure 5). The arches are composed of the tarsal and metatarsal bones with supportive connective tissues strengthening the structure. There are three primary arches of the foot:

1. **The Medial Longitudinal Arch:** Comprised of the calcaneus, talus, navicular, cuneiforms I-III and metatarsals I-III, the medial longitudinal arch is the most

prominent of the arches and provides a significant amount of elasticity due to its height [47].

2. **The Lateral Longitudinal Arch:** Comprised of the calcaneus, cuboid, metatarsals IV and V, the lateral longitudinal arch is shorter than its medial counterpart and is more structurally rigid [47].

3. **The Anterior Transverse Arch:** Comprised of the heads of the five metatarsal bones, the anterior transverse arch sits primarily in the frontal plane and contributes to what is widely known as the 'ball of the foot'.
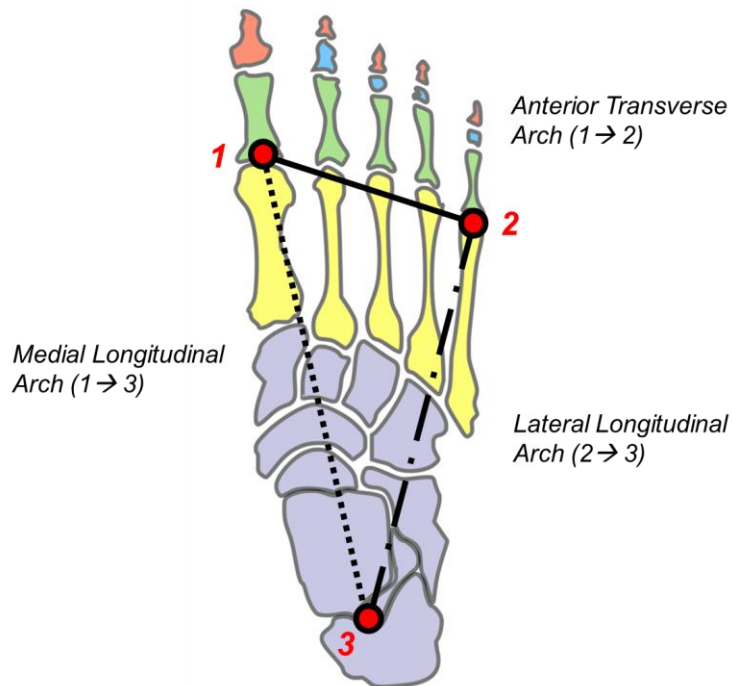
Figure 5   **Superior view of the three arches of the foot.**

Figure adapted from [49].

1.3. Foot Biomechanics

1.3.1. Shock Absorption and Load Distribution

The foot structure has evolved to support upright bipedal walking including the cyclic loading and unloading of gait, the shock loading of sudden movements and the passive loading of constant standing. Further, during erect standing the feet play a fundamental role in balance and through minor articulations of the musculature, permit dynamic load redistribution to keep the individual upright. In addition to static WBR, the foot is also extremely important for dynamic movements, specifically gait. Gait is the manner and style of walking and is comprised of a series of synchronized movements which place various impulses on the plantar aspect of the foot through the entire stride. To adequately distribute such dynamic loads, the foot employs several innate techniques to act as a spring-damper system for softening both the typical and atypical loading regimes experienced throughout everyday life. However, the foot is also the primary propulsion device enabling human locomotion; resultantly, tissues of the foot must strike a balance between being soft enough to adequately attenuate loads, while being rigid enough to enable push off when transitioning from a static to dynamic posture (e.g. standing to walking).

The primary biological solution to this trade-off is a structural technique the foot employs known as the 'windlass mechanism' (Figure 6). The windlass mechanism utilizes the triangular-like structure of the medial longitudinal arch (MLA) to modulate the stiffness of the plantar fascia, enabling it to act as both a spring-damper system (Figure 6a) and a push block (Figure 6b). The MLA is similar to a three-bar linkage, where the plantar fascia constitutes a flexible 'bar', spanning the distance from the tuberosity of the calcaneus to head of the first metatarsal bone. The two rigid 'bars' of the linkage may be thought of as the bony pathways starting at the attachment points of the plantar fascia and terminating at the center of the talus. The three bars approximate a triangle, as shown in (Figure 6c). Fundamentally, the term 'windlass mechanism' details the elongation of the plantar fascia as the hallux is dorsiflexed; the plantar fascia wraps around the first metatarsophalangeal joint during dorsiflexion of the hallux, resulting in the tensioning of the plantar fascia [50] (Figure 6b). By tensioning the plantar fascia, the calcaneus is drawn closer to the forefoot thus lifting the MLA without direct muscle action [51]; raising the MLA aids the re-supination of the foot, which is a fundamental step in creating the propulsive force necessary for locomotion [52,53]. An ineffective windlass mechanism would hinder the foot's capacity to return from its pronated position, thus culminating in decreased propulsive

force and the elevated potential for foot pain and/or dysfunction [51]. During static WBR, the neutral position of the hallux keeps the plantar fascia taut, but does not apply extra tensile loads to the fascia like gait does. In this neutral position, the body weight is distributed over the entire plantar aspect of the foot, with load concentrations acting on the hindfoot and medial forefoot. Load concentrations at these two locations tend to flatten the MLA; however, this is counteracted by the plantar fascia, which preserves the structure of the arch while providing some energy absorption, rebound, and flexibility in conjunction with minor articulations within select tarsal bones [54,55].
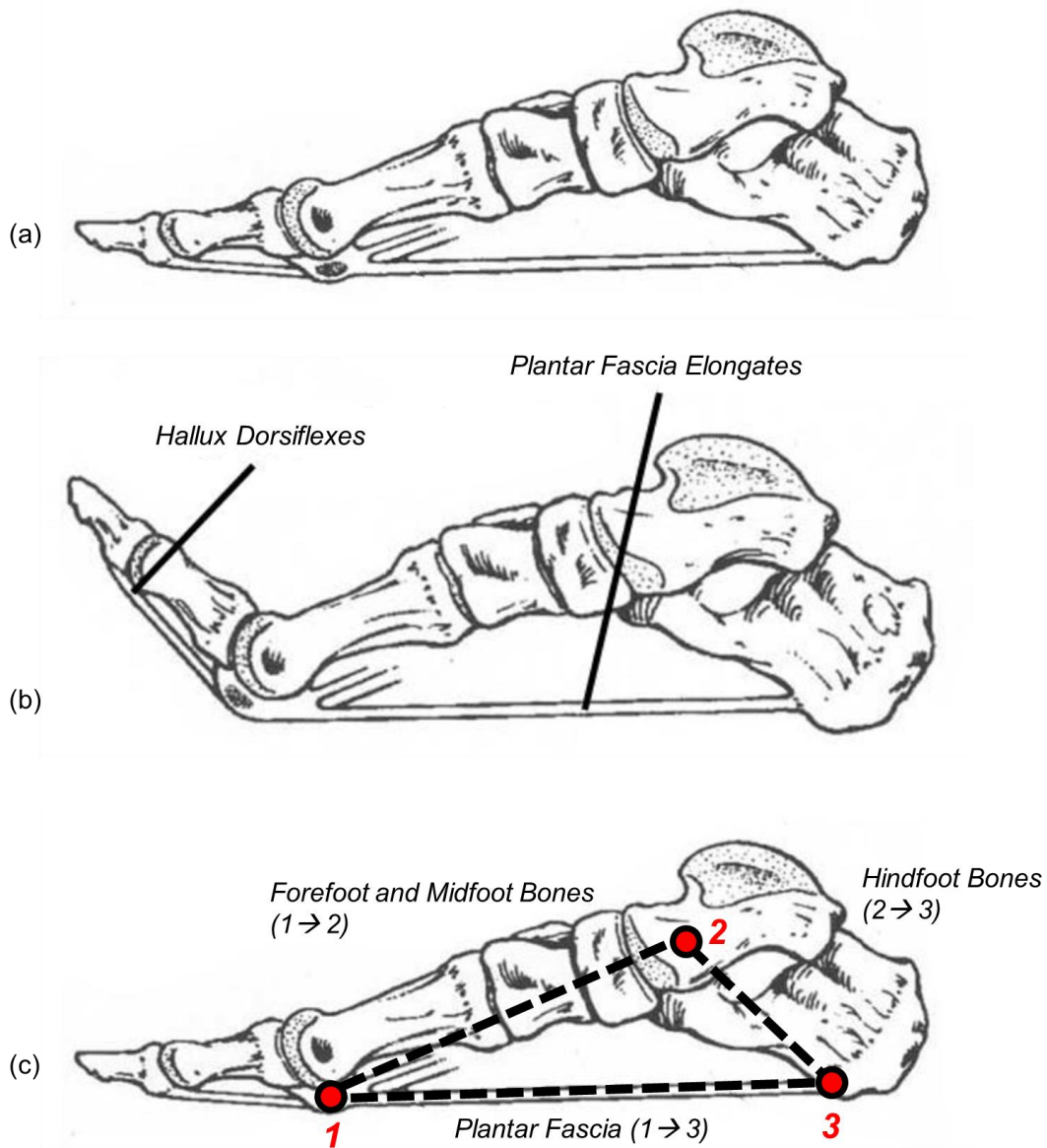
Figure 6   **(a) Windlass mechanism with hallux in a neutral position (b) Windlass mechanism with hallux dorsiflexed; plantar fascia elongates raising medial longitudinal arch (c) Truss-like structure of the foot.**

Figure adapted from [56].

1.3.2. The Gait Cycle

In 2006, it was reported that walking was the second most prevalent form of transportation in the United States and Europe after the private car [57]. The locomotor pattern demonstrated during bipedal walking amongst humans, also known as gait, has been reported to be quite

14

stable when observing both kinematic [58,59] and kinetic [59] features over level ground. At the highest level, the gait cycle can be broken down into two phases, stance, occupying the first 60% of the cycle whilst the foot is in contact with the ground (Figure 7a), and swing, occupying the latter 40% whilst the foot is airborne (Figure 7b); the gait cycle during typical walking at a preferred walking speed (PWS) is approximately 1050ms in healthy individuals below thirty years of age, and increases slightly with age [60]. The stance phase of gait can be further deconstructed into a series of five positions:

- **Initial Contact:** Typically referred to as 'heel strike', this is the first phase following swing where the heel is the first part of the foot to contact the ground.

- **Loading Response:** The period of stance phase during which weight is completely transferred onto the referenced leg.

- **Mid Stance:** This phase is marked by the alignment of the referenced leg with the opposite leg in the sagittal plane.

- **Terminal Stance:** Primarily distinguishable by the heel of the reference leg rising off the ground, terminal stance phase consists of a weight transfer in the anterior direction loading the forefoot and toes and unloading the heel.

- **Toe-Off:** The last phase of swing, toe-off describes the rising of the forefoot and toes off the ground initiating the transition of the reference leg into the swing phase of the gait cycle.

The swing phase of gait can be further deconstructed into a series of three positions:

1. **Initial Swing:** The reference leg is not at all in contact with the ground, and lies posterior to the opposite leg when viewed in the sagittal plane.

2. **Mid Swing:** The reference leg lies approximately parallel to the opposite leg when viewed in the sagittal plane.

3. **Terminal Swing:** The reference leg is just about to contact the ground, and lies anterior to the opposite leg when viewed in the sagittal plane.
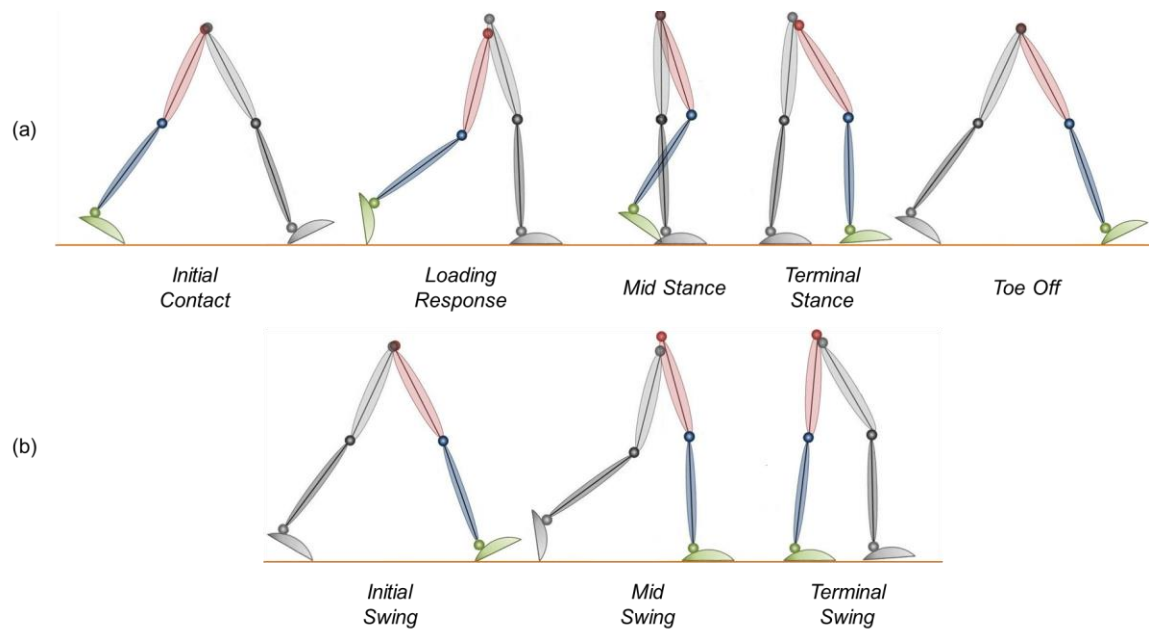
Figure 7   **(a) Stance phase of gait broken into five positions (b) Swing phase of gait broken into three positions. The right leg is considered the referenced leg, and is pictured in colour. The left leg is considered the opposite leg, and is shown in grayscale.**

Figure adapted from [61].

Loading of the plantar aspect of the foot during the stance phase of gait parallels the posterior to anterior weight transfer in the sagittal plane, with a slight lateral to medial load transfer in the transverse plane [62]. Pressure concentrations have shown to exist in the heel and the ball of the foot [62], which coincide with the main contact regions of heel strike and toe off, respectively. Additionally, the plantar fascia has been reported to transfer a large amount of load between the hindfoot and forefoot during the stance phase of gait [63]; this load transfer is often repeated many times during prolonged walking, placing cyclic stress on the fibres of the plantar fascia.

1.3.3. Plantar Tissue Biomechanics

The plantar fascia plays a fundamental role in load distribution within the foot, both during erect standing and in more dynamic movements such as walking or stair ascent/descent. As demonstrated in Figure 6c, the plantar fascia acts as a structural element which directly attributes to the medial longitudinal arch conformation [64]. Different overuse pathologies can

contribute to the breakdown of the plantar fascia, which thereby compromises its mechanical functionality [65]. The plantar fascia is comprised of collagen fibres oriented parallel to the long axis of the foot (Figure 8a) [47,66]; loading of the tissue is primarily tensile and acts in the same direction along the major foot axis. Various studies have examined the elastic properties of the plantar fascia. One study found that for a progressive load applied axially, the plantar fascia exhibited nonlinear behaviour with an elastic limit of approximately 6-7% of the initial length [67]. Another work identified an 11-12% elastic limit due to an axial load of approximately 900N [68]. The plantar fascia measures approximately 12 ± 1.5cm along the main longitudinal axis (from the medial tubercle of the calcaneus to the first MTP joint) [66]; this demonstrates the potential for a 0.72cm to 1.44cm (6% and 12% elastic limit respectively) elongation prior to plastic deformation. Additionally, the stiffness of the plantar fascia has been shown to be independent of loading rate [69]. The elongation capability coupled with the constant response over various loading rates makes the plantar fascia a dynamic spring-damper system for various loading regimes experienced throughout daily life.

Ideally, the plantar fascia will maintain its intrinsic elastic properties throughout the duration of one's life; however, this is not always the case. Evidence has demonstrated that the stiffness of the plantar fascia decreases with age [70], thereby decreasing the energy absorbing capabilities of the tissue. Additionally, various pathologies of systemic origin [71] can also compromise the mechanical functionality of the plantar fascia. If the elastic potential of the plantar fascia is compromised, loading regimes that were previously tolerable can potentially damage the plantar fascia. Damage to the plantar fascia is realized through micro-tearing of the collagen fibres resulting in some fibres deviating from their initial parallel orientation (Figure 8). Typically, these micro-tears are found near the calcaneal attachment of the plantar fascia where loads are more concentrated. Once the collagen fibres comprising the plantar fascia begin to tear, an increase in load is seen in the remaining collagen fibres, often culminating in a cascading effect which is felt as a sharp pain near the site of the micro-tearing (generally near the heel); the sharp pain in the heel is a condition known as *plantar fasciitis* (PF).

(a)	(b)
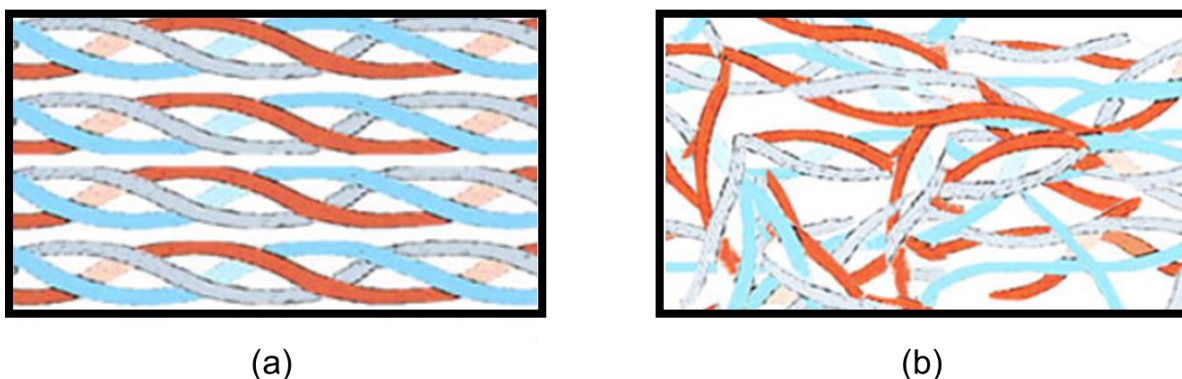
Figure 8   **(a) Collagen fibres comprising the plantar fascia in a healthy state; fibres are parallel and organized (b) Collagen fibres comprising the plantar fascia after micro-tearing has occurred; fibres are scattered and disorganized.**

Figures adapted from [72].

1.4. Plantar Fasciitis: Characterization and Etiology

1.4.1. Overview of Plantar Fasciitis

One of the main causes of the overarching condition known as 'plantar heel pain' is plantar fasciitis [12,73,74]; described as a degenerative condition similar to tendinosis [75], PF is primarily characterized by micro-tears in the plantar fascia leading to fascial thickening and inflammation [24]. Studies have shown that degeneration of the fascia is primarily due to chronic mechanical overloading [76-78], although the exact etiology is multifaceted and varies between individuals [12-14,79]. Presenting as excruciating pain in the plantar heel region, PF has been estimated to affect 1 in 10 [3-5] people during their lifetime, with some estimates of up to 1 in 4 [6]. Typically, patients first complain of pain in the medial heel, particularly after long periods of inactivity; such pain tends to decrease as activity level increases throughout the day, but often pain resurfaces towards the end of the day [79,80]. Many treatment modalities are available for PF, including but not limited to rest, ice/heat cycling, stretching, orthotics, taping, nonsteroidal anti-inflammatory drugs (NSAIDs), steroid injections, radio or shockwave therapy, and surgical intervention [3,13,14,74,78,80-86]. Often considered to be a self-limiting condition (a condition with no long-term harmful effects) [80] symptoms of PF are often resolved with conservative methods of treatments and tend to resolve within a year [83].

1.4.2. Intrinsic Risk Factors

Intrinsic risk factors predisposing an individual to plantar fasciitis refer to features within the body which may act alone, or in conjunction with other features, to place excessive strain on the plantar fascia damaging it over time. In 2014, Beeson [24] wrote a critical review examining the etiology of PF; a summary of intrinsic risk factors associated with PF is provided (Table 1). The review concluded that there is not enough data to rank the relative importance of each intrinsic risk factor; however, several reviews have listed obesity as a particularly influential intrinsic factor, often noting its importance and prevalence in PF diagnoses [5,24,87].

1.4.3. Extrinsic Risk Factors

Extrinsic risk factors predisposing an individual to plantar fasciitis refer to features outside the body which may act alone, or in conjunction with other features, to place excessive strain on the plantar fascia damaging it over time. In 2014, Beeson [24] wrote a critical review examining the etiology of PF; a summary of extrinsic risk factors associated with PF is provided (Table 2). As with intrinsic risk factors there is insufficient evidence to assign the relative importance of each extrinsic risk factor; however, several reviews noted overuse due to prolonged WBR as an important and prevalent extrinsic factor in PF diagnoses [5,24].

Table 1   Intrinsic risk factors for Plantar Fasciitis

Risk Factor	Description	Relevance to this Study
Age	- Degenerative processes naturally occurring during the aging process [80,88] - Heel fat pad thickness varies with age which can change forces seen by the plantar fascia [89-91] - Lack of muscle strength and decreased bodily healing capabilities increase potential for damage [81]	Because this work intends to target a working population (approximately 25-65 years old), age will need to be considered in future works. A solution to this is age-matching the groups across different workplace activity groups to negate any age effects. In the current study, a young population was used (29 ± 4.8 years old).
Obesity	- Elevated BMI levels [4,80,92-95] - Heel fat pad thickness varies with body weight, which can change forces seen by the plantar fascia [96]	Because this work intends to target an average working population, BMI will need to be considered in future works. A solution to this is matching the groups across different workplace activity groups to negate any effects associated with elevated BMI. In the current study, a population on the border of normal/overweight was used (24.8 ± 4.1 kg m^{-2}).
Gender	- Women have a higher incidence than men [91,93]	Because this work intends to target an average working population, gender will need to be considered in future works. A solution to this is matching the groups across different workplace activity groups to negate any effects associated with gender. In the current study, a primarily male population was used (8 male, 2 female).
Anatomical Abnormalities	- Faulty foot mechanics (flat feet, restricted ankle joint mobility and/or excessive foot pronation) [8,77,80,81,92,97] - Strain induced on the plantar fascia by tightness in the lower limb muscles [98] - Existing calcaneal spur present [99]	Although anatomical abnormalities have been rigorously studied as a risk factor for PF, future works will initially study asymptomatic populations so individuals with anatomical abnormalities will be excluded at this point. In the current study, individuals with anatomical abnormalities were not admitted to the study through the exclusion criteria.
Acquired Systemic Diseases	- Rheumatoid arthritis [100] - Diabetes mellitus [85]	In the current study, individuals with acquired systemic diseases were not admitted to the study through the exclusion criteria.
Genetics	- Various genetic variants [101]	In the current study, genetic predispositions for PF were not investigated and can therefore not be commented on further.

Table 2   Extrinsic risk factors for Plantar Fasciitis

Risk Factor	Description	Relevance to this Study
Occupation	- Prolonged weight bearing [4,8,12,77,81,88,102] - Weight bearing on hard surfaces [8,97]	Occupational exposure is the primary independent variable this work is attempting to study. Further details relating to this risk factor is expanded upon below.
Footwear	- Insufficient, diminished or poor-fitting footwear [4,12,76,103]	Although footwear issues have been rigorously studied as a risk factor for PF, this factor will only be addressed on a surface level in future works; instrumented insoles will be manufactured flat so as to not intrude on the structural integrity of the shoe, and shoes will be initially examined to ensure they are in good condition sufficient for studies examining activity at work. In the current study, specific shoe type was not specified and each participant provided their own shoes during testing. Shoes were not examined for fit or wear prior to inclusion in this study.
Lifestyle	- Change in activity level [4,12]	Because this work intends to target an average working population, activity level will need to be considered in future works. A solution to this is matching the groups across different workplace activity groups to negate any effects associated with change in activity level. Additionally, participants included in future works will be asked to maintain their current activity level outside of work. In the current study, lifestyle factors were not considered as participants were asymptomatic and were only sampled once.
Sport	- Anatomical abnormal exacerbated by running [104] - Excessive running distance or intensity [12,105] - Running surface [105]	Exclusion criterion of future works will be used to selectively exclude individuals with extensive running backgrounds as this sport has been noted to predispose individuals to PF. In the current study, history of sport was not considered as participants were asymptomatic and were only sampled once.

1.4.4. Weight Bearing and Plantar Fasciitis

Several studies have looked at the correlation between work-related musculoskeletal disorders (WMSDs) and physical risk factors in the workplace; generally, the studies vary by examining different populations, types of work, or using different collection techniques and reporting strategies. Many of the studies suggest that ankle and foot disorders may be associated with prolonged standing at work [4,28,73,106-108]. One study sampled grocery store employees from different departments to determine the correlation between exposure to physical risk factors and the presentation of pain symptoms [2]. A total of 254 participants were sampled, and approximately 78% of grocery store workers reported WMSD symptoms, with 50% reporting foot pain, a substantial increase compared to estimations of the general population prevalence of foot pain (24%) [6]. Additionally, foot pain was more prevalent in workers who stood for most of the day when compared to counterparts who walked more [2]. Long-term fatigue can develop in individuals standing more than five hours a day, even with regular short (less than five minute) rest breaks [109]. Long-term fatigue is thought to be a precursor to more serious pain and degenerative conditions of the feet [109]. Nurses are cited as one of the most at-risk populations for foot pain, with some studies suggesting a prevalence of plantar fasciitis of up to 33% in nurses [110], a full 9% to 23% above estimates of PF prevalence in adults [3-6]. Nurses typically work more hours per week than other at-risk populations and primarily stand and walk during their shifts, which could contribute to the increased risk and development of plantar foot pain [110] .

1.4.5. Weight Bearing and Workplace Exposure

In some professions, individuals spend the majority of their workday on their feet; although breaks are provided in most industries. An analysis conducted on the European Survey of Working Conditions concluded that approximately 47% of employees spend over 75% of their workday on their feet [1]. One proposed solution employed in many companies includes offering shock-absorbing 'anti-fatigue' mats which are supplemental flooring surfaces made of softer materials that rest on top of a hard floor (e.g. cement). Such mats have been shown to improve both subjective (e.g. discomfort/fatigue ratings) and objective (e.g. lower-extremity swelling) measures when compared to standing on hard floors [111]. Key factors that contribute to these measures include flooring elasticity, stiffness, and thickness, with the suggestion that softer floors reduced discomfort [112]. The use of such cushioning mats may lower the risk for PF,

although due to the multifaceted nature of PF etiology, it is challenging to draw comprehensive conclusions [8].

Additionally, workplace exposure is difficult to characterize due to the dynamic nature of some professions which constantly vary between several primary postures. Of 32 perioperative nurses and technicians (PNTs) surveyed, 84% reported that at least half of their time was spent in some sort of WBR posture during their shift, primarily because sitting or resting is not allowed for PNTs once they are scrubbed in for surgery [9]. Another work studied the effect of standing in factory workers in varying departments within the same work site; it was concluded that workers standing in one place during the day (e.g. operating tools/stationary machines) were more likely to overload tissues when compared with workers in other areas where motion was more prevalent (e.g. the shipping department) [7]. Though compelling, both studies identify self-reporting workplace posture durations as a limitation [7,9]. Another study found standing for the majority of the workday to yield an approximate three-fold increase in risk of developing plantar heel pain when compared to not standing for the majority of the day at work [4]; however, similar works have found no evidence suggesting a link between plantar heel pain and occupational WBR in the general population [28,92]. Because of the reliance on self-report measures and contradictory evidence, it is still not possible to substantiate a definitive link between prolonged WBR and PF due to the current inability to accurately track WBR at work [27].

1.5. Monitoring Weight Bearing in the Workplace

Two primary options exist for tracking physical activity in the workplace: subjective measures or objective measures [113]. A third option, measuring energy expenditure through criterion standards, such as direct observation, doubly labelled water (DLW) and indirect calorimetry, also exists, but are typically carried out in a laboratory setting, making it inapplicable for this work [113]. Subjective measures of workplace activity level, or 'self-reporting,' include both written surveys/questionnaires as well as oral interviews. Objective measures of workplace activity level, or 'activity trackers,' include accelerometers, pedometers and other technologies which use inertia and other biometrics to infer activity type. Other objective measures, such as video monitoring and motion trackers, while effective, are resource-intensive and difficult to implement in most industries and can only be used in small participant populations. Video monitoring and motion trackers have been excluded from further review because of the divergence from the long-term goals of this work.

1.5.1. Self-Reporting

Self-reporting is appealing on a surface level largely due to the simplicity and low resource requirements. Resultantly, self-reporting has been employed in a variety of workplace activity studies with acceptable levels of reported reliability [114-117]. A 2011 review on measurement of PA and sedentary behaviour at work cited questionnaires as the most common tool used for reporting [113]. Conversely, several studies have emerged questioning the accuracy and reliability of self-reporting workplace activity [29-34]. A 2008 systematic review [118] compared direct versus self-report measures in assessing PA in adults though not specifically within the workplace; the authors concluded that 38% of the 173 articles had low quality scores in a risk of bias assessment, identifying them as particularly subject to bias [118]. The authors postulated that self-report response bias may exist due to social desirability, and can cause overweight/obese individuals to over-report their PA levels leading to skewed results. The mixed opinions in the literature regarding the efficacy and accuracy of self-reporting are concerning and make it difficult to use self-reporting as a primary workplace PA measurement tool.

When specifically examining self-reporting of sitting, standing and walking at work compared to objective measurements, the results are generally positive when using the *Occupational Sitting and Standing Physical Activity Questionnaire* (OSPAQ) [119]. Wick et al. [22] sampled 38 office employees and reported a modest underestimation of standing time (4.6%) and an overestimation (7.7%) of walking time. Pedersen et al. [21] sampled 34 desk-based employees and reported an underestimation of sitting time (3.2%) and standing time (0.2%), and an overestimation of walking time (3.4%). Despite the promise that these results demonstrate with respect to self-reporting of common workplace postures, several underlying issues hinder usability in the current line of research. Firstly, the OSPAQ is completed at the end of a workweek and asks users to estimate the percentage of time spent sitting, standing and walking over a typical workday; the percentage breakdown is then used to estimate the time spent in each posture. Although evidence [21,22] demonstrates that daily classification resolution is quite good, the OSPAQ, and most self-reporting questionnaires in general, lack specificity in the data collected. Daily or weekly totals are indicative of the high-level workplace physical activity profile, but identifying exactly how often an individual changes postures or information about the duration typically spent in each posture is lacking. The inadequate temporal resolution is problematic; although research has shown prolonged standing to be particularly damaging to the plantar fascia [4,5,23,24], recent evidence suggests that tissue metabolism is

mechanosensitive and therefore responsive to the frequency of the applied load [25]. Without temporal clarity, it may be challenging to draw specific conclusions about the connection between WBR and PF and comment as to why this connection may exist.

Additionally, many self-report surveys and questionnaires exist making it difficult to compare results when so many non-standard methods are employed. One study [120] noted the importance of questionnaire phrasing and distinct separation of exposure categories when self-reporting working posture [120]; therefore, it is difficult to determine which self-report measure of sitting, standing and walking at work is best, as to the authors knowledge, no studies to date have compared the validity and reliability of multiple self-reporting questionnaires to determine a single 'gold standard'. Overall, these results suggest that although self-reporting does have potential when distinguishing sitting, standing and walking postures at work, self-reporting should be used as a secondary measure in conjunction with an objective measure to ensure accurate results are obtained.

1.5.2. Activity Trackers

Recent advancements in sensing technologies, embedded systems, wireless communication technologies and microelectromechanical systems (MEMS) have enabled continuous monitoring of health behaviours for commercial, personal and research purposes [121]. In 2013, fitness devices made up approximately 97% of the wearable electronics market [121], although many industries are starting to employ wearables as the technology is refined. In the medical field, technological advancements have made it possible to track a number of biomarkers, such as body temperature, heart rate, brain activity, and muscle motion, which are ideal for remote monitoring by a clinician [122,123]. Fall detection systems for older adults are also an area of ongoing research [124-126] which tend to employ various sensor-based wearables for monitoring human movement. One of the most widely used sensor types for monitoring human activity are accelerometers [121]; accelerometers have been employed for a multitude of activity-tracking purposes, such as the detection of falls [125-128], human movement analysis [127,128], and postural detection [36,129]. One of the fundamental challenges in working with wearable technologies, and specifically inertial-based technologies, is being able to provide the user with a comfortable, unobtrusive system which can be worn over extended durations without limiting the individual or causing them any discomfort [121]. Additionally, issues may arise surrounding user privacy, power consumption, on-node processing, wireless interference (if

applicable), and storage of the large amount of data obtained while collecting over an extended time-frame [121]. Although inertial based technologies do provide reliable feedback when differentiating complex dynamic postures [35,36], they have limited potential differentiating subtler static postures typical of a working environment (e.g. distinguishing sitting from standing) [37,38], making them difficult to employ for distinguishing sitting, standing and walking at work. Although orientation data from multi-IMU systems [42,43] and single IMUs placed in select locations [44,45] can distinguish certain static postures, multi-IMU systems are of limited use in everyday life, and single IMUs are often placed at positions on the body which may interfere with workplace activities (e.g. chest, waist, hip) [45]. Problematic drift [39-41] and intrusive single IMU locations make this technology infeasible for the widespread deployment proposed in this work. Additionally, IMUs provide no data on the loading patterns an individual may place on their feet throughout various day-to-day activities. Although differentiating the postures may be possible through select IMU placement, resolving why PF or WBR-related disorders occur in selected individuals may be best accomplished by an analysis of pedobarographic patters ascertained using instrumented insoles.

1.5.3. Instrumented Insoles

Custom Instrumented Insoles

One solution that has been proposed to circumvent some of the issues associated with tracking human movement over an extended duration is to build the electromechanical system into an insole. If designed correctly, insoles can maintain a relatively unobtrusive feel for the user while providing more space to house various electronic components. Obvious issues of user discomfort, gait modification due to the added weight of the insole, and electronic durability may arise, but several studies have designed and tested instrumented insoles for varying applications [36,130-135]. Similar to the issues associated with inertial activity trackers, the majority of these custom instrumented insoles have been designed to monitor and/or distinguish more complex movements (Table 3). Additionally, almost all of the systems cited encompass wireless data transmission capabilities. Such capabilities may interfere with or be disrupted by work equipment and are unnecessary for the extended duration data collection proposed by the author for future studies.

An instrumented insole system developed in 2013 [130] appears to be closest to the desired applications of the system proposed in this work. The 'SmartStep' system developed by

Sazonov and company has previously been validated in people with stroke, classifying sitting, standing and walking using a Support Vector Machine (SVM) classifier; the system achieved an accuracy of 95% when classifying the three postures [46,136]. However, these results represent optimal lab accuracies which would likely vary if data acquisition was conducted in the real world. Despite the promising results obtained by this novel insole system, several critical differences exist between Sazonov's SmartStep and the system proposed in this work:

1. **Unilateral/Bilateral Collection:** The SmartStep system collects data from two instrumented insoles worn by the same participant (bilateral collection). The proposed system aims to collect unilaterally in order to decrease system cost and reduce redundancy. Sazonov and colleagues [36] highlighted that unilateral collection could yield similar classification accuracies to those ascertained with both sides.

2. **Sensor type:** The SmartStep contains 3 FSRs as well as a 3D accelerometer; the proposed system intends to only use FSRs and avoid integration of an accelerometer to reduce complexity and system cost.

3. **Location of sensors:** The SmartStep developers placed FSRs under 'biomechanically important' support points on the plantar aspect of the foot (i.e. hallux, 1st metatarsal head, heel center). Although this sensor layout seems logical, assumptions of these key locations are not evidence based. The proposed system and the work encompassed in this thesis attempt to substantiate why specific sensor locations are selected when placing FSRs.

4. **Number of sensors:** The SmartStep has been developed with 3 FSRs [130] as well as 5 FSRs [36,46,131,136,137], with an additional 3D accelerometer. The proposed system and the work encompassed in this thesis attempt to substantiate why a specific number of FSRs are required for posture classification.

5. **Sensor Calibration:** The SmartStep system uses calibrated FSRs to classify postures, which is difficult and costly if intending to mass-manufacture the insoles. The proposed system aims to use an on/off signal for classification, which may avoid the technical complexities and costs associated with FSR calibration.

6. **Wireless Capabilities:** The SmartStep wirelessly transmits data to an associated smartphone via a Bluetooth Low Energy (BTLE) module. The proposed system will store all data collected on-board for later collection by appropriate personnel.

7. **Sampling Frequency:** The SmartStep collects pressure and acceleration signals at 25Hz while the proposed system intends to sample at less than 15Hz, thus reducing power consumption.

Overall, the SmartStep system developed by Edgar et al. [137] and refined by Sazonov, Hegde and Tang [130] has largely contributed to demonstrating the potential for posture classification using in-shoe sensors [46,136]. Currently, the SmartStep technology is being prepared for commercialization through *SmartMove Inc.*, a company founded in part by Dr. Edward Sazonov in 2008 aiming to combat sedentary behaviours through activity tracking. Compared with the wider body of instrumented insole systems, the novel aspects of the proposed system can be summed up in three main points:

1. **Single Uncalibrated Sensor Type:** The proposed system intends to only use uncalibrated FSRs to classify workplace postures; by removing other sensors (e.g. accelerometers) and avoiding sensor calibration, this stands to simplify data integration and minimize sensor costs.

2. **Unilateral Data Collection:** The vast majority of current systems collect bilaterally. By collecting unilateral data, the proposed system will have lower electronic costs.

3. **Physiologically Relevant Sensor Locations:** This work contributes physiologically relevant sensor locations specifically identified for differentiating sitting, standing and walking; use of these sensor locations could aid in differentiating typical from atypical loading patterns.

Research-Grade Instrumented Insoles

In addition to the custom insoles (Table 3), many research grade technologies are also available for plantar pressure measurement; a summary of these commercially available technologies is provided (Table 4). Additional information on options for research-grade plantar pressure measurement systems can be found in a 2012 review by Razak et al. [138].

Of the commercial systems, no single system is universally accepted as best for all applications; each of the systems has various pros and cons depending on the application. For the work encompassed in this thesis, the F-Scan system by Tekscan was the most desirable based on several factors:

1. **Superior Number of Sensors:** As the F-Scan system has the highest number of pressure sensors amongst the noted commercial systems, it is advantageous for this work as it allows for the most comprehensive pressure field to be used as a basis for sensor localization within the novel insole.

2. **Thinnest Insole:** The F-Scan insole offers the thinnest option when compared to other systems. A thin insole was advantageous for this work as it was the least obtrusive to the participants, allowing for the most natural activities to be recorded using their preferred footwear**.**

3. **Lightest System:** The F-Scan insole and wireless transmission belt offers the lightest option when compared to the other systems; a light insole system was advantageous for this work as it was the least obtrusive to the participants, allowing for the most natural activities to be recorded**.**

Table 3   Summary of research with custom instrumented insoles

Study	Sensors Used	Wireless Data Transmission (Yes/No)	Insole Target Function
Edgar et al., 2010 [137]	5 Force Sensitive Resistors (FSRs); 1 3D accelerometer	Yes	Characterize postures in stroke patients to facilitate rehabilitation
Sazonov, Hegde and Tang, 2013 [130]	3 FSRs; 1 3D accelerometer	Yes	Measure pressure differences between WBR and non-WBR postures and capture pressure differences during walking
Sazonova, Browning and Sazonov, 2011 [131]	5 FSRs; 1 3D accelerometer	Yes	Predicting energy expenditure.
Chen et al., 2006 [132]	8 FSRs	Yes	Measure plantar pressure under the 8 specified regions and measure mean plantar pressure during walking
Hellstrom et al., 2016 [133]	4 FSRs	Yes	Measure walking intensity
Jacobs and Ferris, 2016 [134]	8 custom neoprene bladders	No	Measure localized plantar pressure
Shu et al., 2010 [135]	6 Custom fabric resistive pressure sensors	Yes	Characterize normal walking using various measurement parameters (e.g. mean and peak pressure, center of pressure (COP) shift speed)

Table 4   **Selected in-shoe, comercially available, plantar pressure measurement systems**

Company	Tekscan	Novel	Paromed	Moticon	Noraxon
Model	F-Scan	Pedar	paroTec	Science	Medilogic
Approximate Cost (CAD)	23,000 (inc. software + insoles)	21,000 (not inc. software or insoles)	Unspecified	20,000 (inc. software + insoles)	17,500 (inc. software + insoles)
Number of Pressure Sensors	960	85-99	24 or 36	13	240 (max)
Sampling Frequency [Hz]	Up to 100Hz	Up to 235Hz	Up to 300Hz	Up to 100Hz	Up to 300Hz
Wireless [Y/N]	Y (some models)	Y (some models)	N (data stored onboard)	Y	Y
Technology	Resistive	Capacitive	Resistive	Capacitive	Resistive
Resolution [kPa]	4	2.5	Unspecified	10	Unspecified
Pressure Range [kPa]	862 (max)	15-600	625 (max)	400 (max)	6-640
Insole Thickness [mm]	0.15	1.9	3.5	Unspecified	1.6
System Weight [g]	322	400	Unspecified	Unspecified	180 (Transmitter Only)

1.6. Machine Learning

The development of smart technologies and wearable devices to track activities requires intelligent algorithms to be used to differentiate activities based on measurable characteristics. Machine learning (ML) employs a variety of unique algorithms to analyze a series of training examples to then make predictions about new examples of the same form.

Machine learning is a broad field which uses computational power and statistics as a basis for prediction-making. The power of ML is derived from the efficiency of modern computing, which is able to compile observations from known training examples, retain the information, and make predictions about new observations according to the learned data at a rate far superior than possible by humans. However, there are numerous techniques for implementing these algorithms, control parameters that must be assumed, and a wide range of specific ML algorithms that can be applied. While a comprehensive review of these factors and algorithms is beyond the scope of this thesis, the components which relate to the implementation of ML for classifying workplace activities using plantar pressure measurements are briefly discussed. The reader is directed to [139-141] for a more comprehensive discussion of ML methods.

1.6.1. The Overlapping Sliding Window Approach

When sampling streams of continuous data, it is difficult to characterize the temporal characteristics of the data if only one time point is observed. One solution to this is a 'sliding window' approach, which observes several time points simultaneously to account for the temporal characteristics of data (Figure 9). However, the operator must then determine the most effective representation of the data within the window. A variety of descriptive statistics and data measures can be used to characterize the data within the window (e.g. mean, median, sum, maximum or minimum, Fourier transform, etc.). The window length can also affect the accuracy of the ML algorithm, especially when forecasting time series data [142-144]. Selecting an appropriate window length and degree of overlap between consecutive windows has been identified as a critical step of physical activity classification. The window should be selected to cover the full length of the activity of interest [145]. Sliding window methods have been used in many ML algorithms classifying human biomechanics [141,145-152].The effect of the metrics and window length on the accuracy of the classification algorithms should be evaluated.
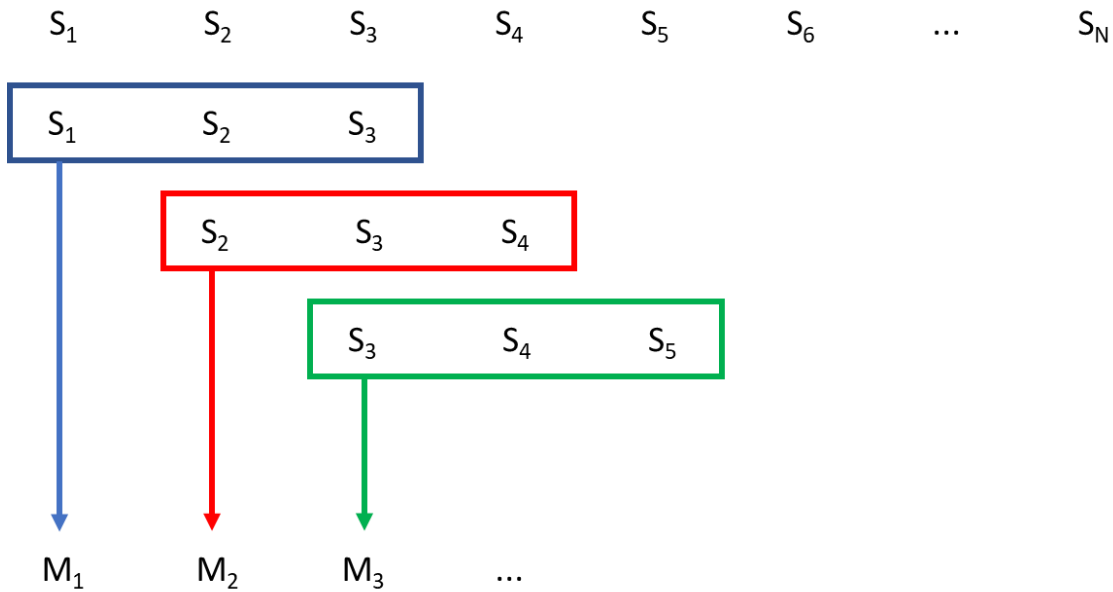
Figure 9 **Overview of the overlapping sliding window approach. S-variables denote the input data set, and M-variables denote the output dataset. Colours denote different windows.**

1.6.2. Selected Feature Selection Methods

The goal of the work presented in this thesis is to identify the least number of sensors and the location of sensors necessary to record plantar pressure characteristics that are able to classify workplace postures. Therefore, reducing the number of features used in the machine learning algorithms is important. However, this reduction must be done in a systematic and robust way. Feature selection is the process of reducing a set of input features to a subset of the most significant features for use in the construction of a model. Feature selection attempts to minimize the amount of information 'lost' by removing features in logical ways to reduce redundancy and repetition of features. Two common feature selection methods are either a filter method or a wrapper method.

Filter Methods

A filter method is a feature selection tool which uses a proxy technique to comparatively score features, as opposed to directly using the classification error rate to score the features against each other. There are many filter methods available, however, five common methods are easily accessible through predefined Matlab scripts; a brief description of each method is described in Table 5.

Wrapper Methods

A wrapper method is a feature selection tool which uses a predictive model to score and subsequently rank features. Wrapper methods primarily differ from filter methods in that they evaluate subsets of variables, thus allowing them to account for interactions between variables. Wrapper methods intersect feature selection with algorithm selection; features are selected based on the relative value they add to the classification scheme as evaluated by their impact on the classification accuracy. Using both methods staged is an effective way to maximize accuracy of the output, increase the robustness of the feature selection protocol, and also limit the computational cost.

Table 5   Selected filter methods for feature selection

Method	Description
Chi-Squared Based Feature Selection	The Chi-Square test statistic is calculated between every feature variable and the class label. If the class label is found to be independent of the feature variable, the feature is not selected.
Information Gain Based Feature Selection	The information gain ('information entropy') describes a statistic which can be calculated for each feature variable in relation to the class label. Feature variables which contribute more information (on a 0 to 1 scale) will be ranked higher than those which do not add much information.
Gini Index Feature Selection	The Gini index is a measure of statistical dispersion, which, in the context of feature selection, analyses the distribution of a feature across the specified classes. Features most-representative of specific classes are ranked highest compared to those that are dispersed amongst several class labels.
Minimum-Redundancy Maximum-Relevance (MRMR) Feature Selection	MRMR feature selection attempts to select features which bear the strongest correlation to the class label, while maintaining sufficient separation from other feature variables.
Fisher Score Feature Selection	The Fisher score ('Fisher information') describes a method of measuring the specific amount of information a feature variable carries about a specific class label. Fisher scoring method used in statistics to answer maximum likelihood equations.

1.6.3. Selected Classification Algorithms

Machine learning algorithms are used in a broad range of applications. While there are hundreds of algorithms, and thousands of variants, we explored the most common algorithms available in packaged computational software (e.g. Matlab). Five machine learning algorithms were reviewed for their ability to classify biological systems and biomechanical behaviours (Table 6):

Table 6   Selected machine learning algorithms

Machine Learning Algorithm	Description	Uses in Biomechanics
Support Vector Machine (SVM)	The SVM algorithm centers on using an optimization scheme to identify the optimal separating decision hyperplanes between the specified classes, as made up by a series of training examples mapped out as points in space. Any new examples are then mapped into the same space and are subsequently classified depending on which side of the hyperplane they fall. A further 'kernel trick' can be used to perform non-linear classification by implicitly mapping inputs to another higher dimensional space.	- PA classification using motion sensors [153] - PA classification using shoe-based wearables [36,154] - PA classification using inertial technologies [154]
Decision Trees (DT)	Similar to a process flow chart, decision trees utilize a series of connected 'tests' which result in distinct outcomes depending on the result at any node. The original decision tree construction is an automated process in which the algorithm examines the discriminatory ability of each feature to create a set of rules from the training data, which can then be used on subsequent classification of new examples.	- PA classification using shoe-based wearables [146,148] - PA classification using inertial technologies [145,150,152]
Linear Discriminant Analysis (LDA)	LDA is a statistical method used to find a linear combination of features which characterizes or separates multiple classes of objects or events. The resulting feature set can be subsequently used as a linear classifier.	- Classifying causes of falls [125,147]
Naïve Bayes (NB)	NB is a probabilistic classification scheme in that instead of providing the user a guess to the most likely class a specific example belongs, the NB algorithm will yield a probability distribution over the set of classes. The NB classification scheme is based upon 'Bayes theory,' which describes the probability of an event given knowledge about the conditions that may be related to that specific event.	- PA classification using shoe-based wearables [154] - PA classification using inertial technologies [145,151,154]
K-Nearest Neighbour (KNN)	The KNN algorithm begins by populating a space with a series of training examples, each of which identifies as a specific class based on the features associated with that example. Upon identifying a new example, the k-closest training examples are identified by their degree of similarity to the new example, and the class is determined based on the classes of the k-closest training examples.	- PA classification using shoe-based wearables [148] - PA classification using inertial technologies [145,149]

1.6.4. Training and Testing the Algorithms

Once a feature set and an algorithm have been selected, the process of evaluating the model can begin. At its core, the fundamental purpose of machine learning is to generalize from learned experiences, allowing the developed model to make predictions on new, unseen examples; the accuracy of these predictions is one of the evaluation statistics used to assess the model. Two central processes facilitate the appraisal of a model—training and testing. In the context of supervised machine learning, training is when a model is presented with example inputs and their desired outputs. The goal of this is for the model to learn a general rule, or set of rules, that maps the inputs to the outputs. Once the model has 'learned' the appropriate mapping rules, testing can take place. Testing involves presenting the model with new example inputs and asking the model to predict an associated output. There are a number of possible outputs for a model trained using machine learning, most of which are beyond the scope of this thesis. Within the context of this work, the trained model is known as a *classifier*; classification describes the process where inputs are partitioned into two or more classes, and the algorithm must produce a model which assigns new inputs to one (or more) of these classes. In this work, multi-label classification was used to train a model able to label new inputs into three discrete postures: sitting, standing or walking. Labels proposed by the model for the new inputs are then compared to the correct labels for evaluation.

To increase the robustness of testing when evaluating a model, it is advantageous to test the model with multiple sets of new examples, and subsequently evaluate the model based on multiple sets of performance statistics [155,156]. If the model was appraised using only one test set, the evaluation statistics could be biased due to possible abnormalities associated with that one set. The alternative approach is to use multiple test sets and average the evaluation statistics over all tests, thus creating more generalizable outcomes from which to compare models. Leave-one-out cross-validation (LOOCV) is a training and testing method used in machine learning to vary the test set within multiple folds of the same data set (Figure 10). In LOOCV, one set of observations is used as the test set, and the remaining observations form the training set. The process is then repeated until all observation sets have been used as the test set [157-159]. Prior to shuffling the testing and training set, the model is evaluated and performance statistics are extracted. At the end of the process, performance statistics are then averaged yielding a robust set of evaluation statistics from which to compare different models (denoted as P_{Avg} in Figure 10).
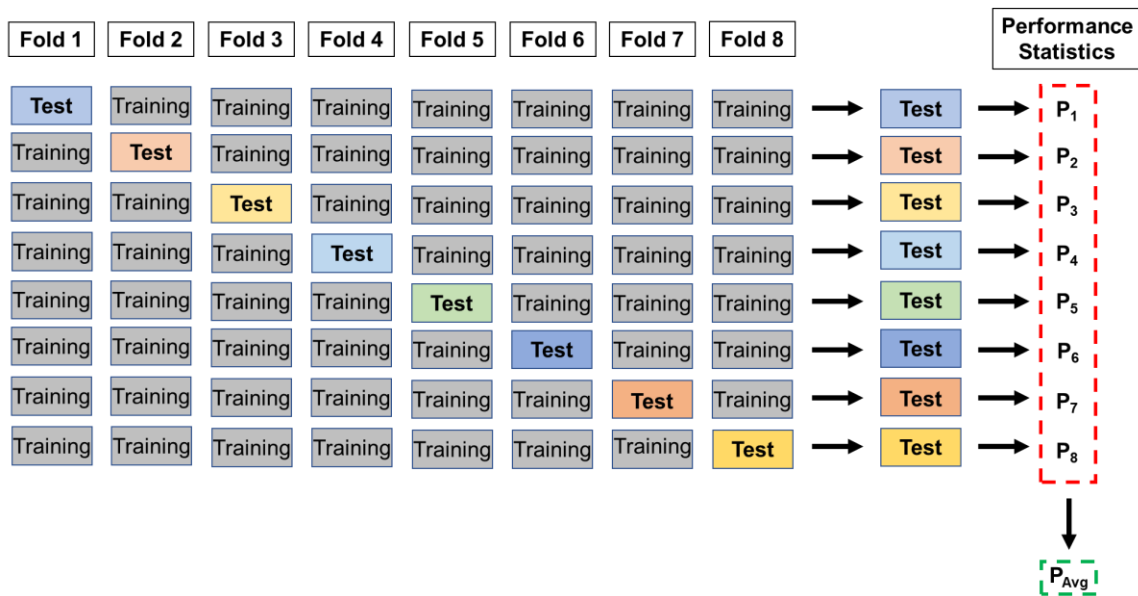
Figure 10 **Leave-one-out Cross-validation scheme denoted for a sample of 8 observation sets. Fold numbers denote the eight particular ways of subdividing the original data set into training and testing subsets. Performance statistics (P_x) may include measures such as classification accuracy, error rate, sensitivitiy, and specificity. P_{Avg} represents the average performance statistics of the model, which are averaged across all performance statistics obtained from each classifier test.**

1.7. Organization and Objectives of the Thesis

1.7.1. Objectives

The goal of this study was to develop an initial prototype design for a low-cost instrumented insole system capable of differentiating workplace postures (sitting, standing and walking). To achieve this goal, three objectives were defined.

1. Quantify and differentiate the plantar pressure locations and characteristics associated with each workplace posture.

2. Classify workplace postures from plantar pressure characteristics.

3. Develop an insole system with off-the-shelf force sensitive resistors capable of classifying workplace postures.

1.7.2. Organization

This thesis is comprised of five chapters, which are organized as follows:

Chapter 1 provides the background information necessary for interpretation of this work and explains the motivation behind the work.

Chapter 2 (Study 1) focuses on the characterization of three common workplace postures – sitting, standing and walking – through pedobarography. A laboratory study was conducted to collect plantar pressure data from ten asymptomatic participants while they demonstrated each of the postures; a commercial-grade in-shoe pressure measurement tool was used to collect the pressure data. Pressure data was assessed to identify regions and measurement characteristics (e.g. peak pressure, average contact area, etc.) which most differed between the three postures.

Chapter 3 (Study 2) details the development and validation of a posture classification scheme to classify sitting, standing and walking using machine learning methods based only on selected plantar pressure measures.

Chapter 4 (Study 3) describes the development of a low-cost novel insole system; the intended use for this system is to selectively capture selected plantar pressure measures based on the outcomes from Study 2. This study details the development of the insole system to date, while also providing a comparison between classifying workplace posture using data from the commercial-grade in-shoe pressure measurement tool and classification using data from the novel system.

Chapter 5 provides conclusions and implications as well as future works that may stem from this work.

Chapter 2.

Differentiating sitting, standing and walking through regional plantar pressure characteristics

The following journal paper will be submitted for review in *Gait & Posture*.

2.1. Extended Methods

Please refer to Appendix B for further details regarding the methods associated with developing this work.

2.2. Prepared Journal Manuscript

Title Page

Differentiating sitting, standing and walking through regional plantar pressure characteristics

Kohle Merry[a], Michael Ryan[b,c], Carolyn J. Sparrey[a]

[a] Mechatronic Systems Engineering, Simon Fraser University, Surrey, BC Canada

[b] Biomedical Physiology and Kinesiology, Simon Fraser University, Burnaby, BC Canada

[c] Kintec Footlabs Inc, Surrey, BC Canada

Corresponding Author:

Carolyn J. Sparrey, PhD
Associate Professor
Simon Fraser University
250-13450 102 Ave, Surrey, BC, V3T 0A3, CANADA
phone: (778) 782-8938
email: csparrey@sfu.ca

Abstract

Prolonged static weight bearing is thought to aggravate plantar heel pain; however due to a lack of available technologies, there is insufficient empirical evidence to conclusively prove causation or correlation. Likewise, prolonged periods of static weight bearing, common in the workplace, may put workers at greater risk of developing plantar heel pain. However, objective measures of physical activity and sedentary behaviours in the workplace are lacking making it difficult to establish or refute the connection between work exposure and plantar heel pain. Characterizing loading patterns during common workplace postures will enhance the understanding of foot function and inform the development of new measurement tools. Plantar pressure data during periods of sitting, standing and walking was measured in ten healthy participants using the F-Scan in-shoe measurement system (Tekscan Inc, Boston, USA). Peak and average pressure, peak and average contact area, and average pressure range, were analyzed in ten different regions of the foot. A two-way repeated measures ANOVA assessed the posture by foot region interaction for each measurement parameter; significant effects of posture by foot region were identified for all five measurement parameters. Ten foot-region by measurement parameter combinations were found to significantly differentiate all three postures simultaneously; seven used pressure measures to differentiate while three used area measures. The heel, lateral midfoot, and medial and central forefoot encompassed nine of ten areas capable of differentiating all postures simultaneously. This work demonstrates that plantar pressure is a viable means to characterize and differentiate three common workplace postures. The results of this study can inform the development of a measurement tool for quantifying posture duration at work.

Keywords: Pedobarography, Plantar Pressure Patterns, Posture Differentiation, Plantar Heel Pain, Weight Bearing

1. Introduction

Plantar heel pain (PHP) is a common musculoskeletal disorder (MSD) of the foot [1] prevalent in 10% [2] to 25% [3] of adults. Although the etiology of PHP is considered multifactorial [1], evidence has shown a greater prevalence in working populations where prolonged static weight bearing (WBR) (i.e. standing) is necessary [4,5]. Prolonged static WBR in the working population is commonplace; approximately 47% of employees stand for more than 75% of their workday [6]. Professions with prolonged standing show a higher than average prevalence of MSDs in the feet and low back [4]. However, establishing the causality of WBR and differentiating dynamic and static WBR postures in the development of PHP has been hampered by poor reporting methods [7]. Elongation of plantar soft tissue during static loading creates a concentration of stress at the medial calcaneal tubercle [8]. Furthermore, bioreactor studies showed soft tissue metabolism is mechanosensitive and modulated by the frequency of applied load [9]. Collectively this suggests that passive WBR postures increase the risk of PHP [1,10]. Quantifying plantar pressure patterns during WBR (walking, standing) and non-WBR postures (sitting) will provide important clarity into the loading characteristics that may adversely affect the plantar soft tissue. Further, contrasting dynamic WBR and static WBR will provide valuable insights for the development of more effective PHP prevention strategies, interventions and workplace measurement tools.

Plantar pressure distributions vary between individuals with and without foot-related MSDs during common activities such as walking, running, and stair ascent [11-14]. Evidence shows high pressure concentrations on the hallux [15] and heel [12,15] during walking; however, little consideration has been given to the pedobarographic patterns during standing [16]. Research into pressure distributions during sedentary activities have typically used force plates under barefoot conditions [13,16,17], which lack ecological validity for simulating workplace environments when compared to insole-based pressure measurement systems, as insole systems allow for plantar pressure measurement while wearing shoes [18]. Other studies have brief (3 - 10s) collection periods [11,13,14,19], which may not allow for natural

relaxation into a steady-state posture which can occur over longer duration WBR. These investigations suggest that different plantar pressure distributions exist between sitting, standing and walking; however, there has not been simultaneous study of walking and static postures representative of a typical working environment over an extended duration [20].

Objective measures of physical activity and sedentary behaviours in the workplace are lacking [20]. Differentiating static postures such as sitting and standing are important for understanding plantar loading conditions, but are often not distinguished by commercial inertial-based technologies [21]. To develop better objective measurement tools, it is critical to first clarify the pedobarographic characteristics that differentiate sitting, standing and walking in an asymptomatic population.

This study aimed to quantitatively characterize the plantar pressure distribution between WBR postures (walking, standing) and contrast those with a non-WBR posture (sitting). Further, this study investigated the differentiability of dynamic WBR (walking) from static WBR (standing). It was hypothesized that forefoot contact as well as toe contact may show the greatest contrast between the WBR and non-WBR postures as these regions are largely inactive during sitting and active for balance during standing. Additionally, the cyclic loading of walking was hypothesized to be a reliable method for differentiating dynamic from static WBR postures.

2. Methods

I. Participants

Data from ten healthy subjects (two females and eight males; mean age = 29 years) with no current or prior lower limb injuries or abnormalities were included in the current study (Table 1). Written informed consent was obtained from each participant. This study was approved by the Simon Fraser University Office of Research Ethics.

Table 1. Subject characteristics for individuals (N=10) included in the study. Values expressed as mean ± SD.

Gender (M/F)	Age (years)	Height (cm)	Weight (kg)	BMI (kg m^{-2})	Shoe Size (mm)	Dominant Foot (R/L)
8/2	29.0 ± 4.8	172.0 ± 10.3	74.2 ± 18.4	24.8 ± 4.1	260.1 ± 19.0	10/0

II.   *Protocol*

A pair of appropriately sized pressure-measurement insoles was placed into each participant's personal shoes. Data collection was structured into two distinct trials performed twenty minutes apart, each consisting of a six-minute collection phase. Each trial consisted of six, one-minute activity blocks (sitting, standing, or walking) in which each activity was executed twice and the order of activities was randomized. Sitting was conducted in a standard plastic office chair (46cm floor-seat height) while walking was performed at a self-selected speed over a 10m walkway; upon reaching the end of the walkway, participants turned in a self-selected manner and continued this repetition until the completion of the activity block. Participants were warned approximately five seconds before the conclusion of each activity. At the start of each activity the participant performed a right-footed stomp. Video of the participant's feet was captured over the entire test and was used to validate the activity classifications.

III.   *Plantar Pressure Measurement*

Plantar pressure was recorded bilaterally using an F-Scan in-shoe system (Tekscan Inc, Boston, USA) at 75 Hz. In-shoe pressure measurement was utilized to allow for static and dynamic plantar pressure measurements while wearing shoes, which is not feasible with force plates [18]. Additionally, F-Scan provides continuous data collection throughout the activity.

To subdivide the plantar aspect of the foot into anatomical areas of interest, a modified version of the PRC masking method, developed by Novel (Novel GmbH, Munich, Germany) was implemented [22,23]. The PRC method segments the plantar aspect of the foot into ten regions: hallux (HA), second toe (T2), third to fifth toes (T35), medial forefoot (MFF), central forefoot (CFF), lateral forefoot (LFF),

medial midfoot (MM), lateral midfoot (LM), medial heel (MH) and lateral heel (LH) (Figure 1). The definition of the toe regions were modified because no description of how they are defined by Novel was found [22,23]; the toe-forefoot boundary was defined by the sensor with the lowest cumulative pressure under the proximal interphalangeal joint of the hallux and continued laterally to the CFF/LFF boundary. HA and T2 were separated by an extension of the MFF/CFF boundary. The T35/LFF boundary was defined by a diagonal from the T2/T35/CFF/MFF intersection to a point on the most lateral aspect of the foot at a distance corresponding to 10% of the foot length below the toe-forefoot boundary.

To assess the physiological plantar loading differences between the three activities, five parameters were calculated: peak pressure, average pressure, average pressure range (95th-5th CI), peak contact area and average contact area, in each of the ten foot-regions. Pressure measurements were spatially averaged across each region at each time increment; peak pressure was defined as the highest pressure at a single time point for a given region during the activity, average pressure was the mean region pressure over the entire activity, and average pressure range was defined as the maximum minus the minimum pressure for a given region during an activity. Contact area was determined by the number of active sensors within a region multiplied by the sensor area; peak contact area was determined by the highest area recorded for a given region during an activity while average contact area was defined as the mean area within a region for an entire activity.
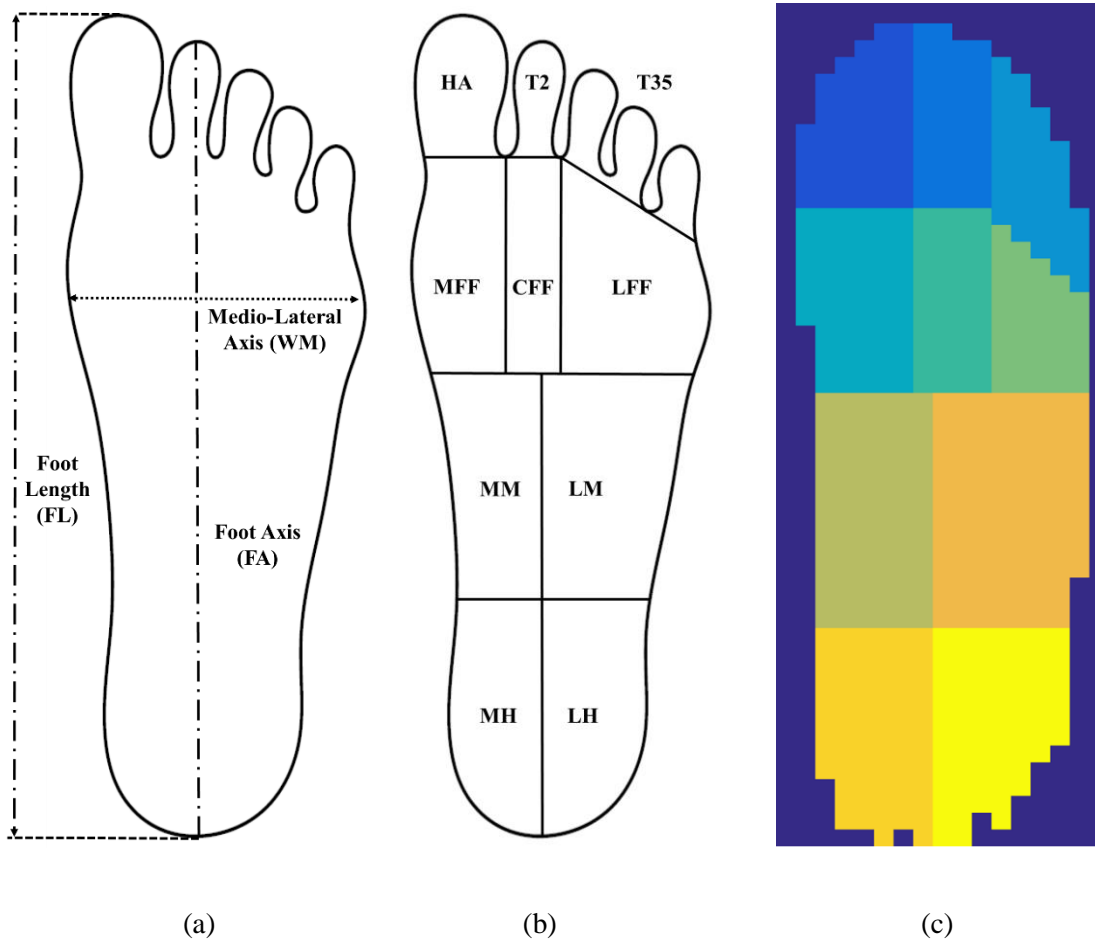
Figure 1. Regional breakdown of the foot conducted per the PRC mask method. (a) Foot characteristics defined as foot length (FL) measured from leading toe to heel, foot axis (FA) running vertically from center of heel to center of second toe, and medio-lateral axis (WM) running horizontally across the widest part of the metatarsals. (b) Heel-midfoot boundary is located 0.73(FL) measured from the leading toe, midfoot-forefoot boundary is located 0.45(FL). Medial and lateral heel and midfoot are distinguished by the foot axis (FA). Medial, central and lateral forefoot are defined as 0.3:0.25:0.45 of the medio-lateral axis (WM), respectively. (c) Exemplary footprint with ten anatomical masks displayed.

IV.   Data processing and statistical analysis

All analyses were run using the JMP statistics software package, (v13.1.0, SAS Institute Inc., Cary, NC). Investigation of the three conditions excluded any transition periods which were defined as the time when an activity was completed until the participant was comfortably in position to begin the subsequent activity denoted through a stomp of their right foot; consequently, activity durations were non-uniform and typically were reduced from one-minute blocks to 40-50 second blocks after removing transitions.

Video data was used to identify and remove transitional activity periods from the data set. Average pressure was compared between dominant/non-dominant feet across all ten anatomical masks using paired t-tests with Bonferroni corrections for multiple comparisons.

The goal of this analysis was to investigate which combinations of foot regions and measurement parameters significantly differed across postures. Differences in specific pedobarographic patterns for each of the five parameters measured were first analyzed across both posture and foot region using a two-way repeated measures analysis of variance (ANOVA) to identify potential activity by foot region interactions. Assumptions associated with the repeated measures ANOVA (multivariate normality and sphericity) were tested; violations of sphericity were amended by implementing the Greenhouse-Geisser Correction. Post hoc analyses to assess pair-wise differences were carried out through Tukey's HSD test at a significance level of 0.017 after a Bonferroni adjustment. Effect size was characterized based on differences between means using Cohen's d.

3. Results

Paired t-tests on the average contact pressure data found that a difference between the dominant and non-dominant sides only existed in the lateral heel region. Kim and colleagues also reported no significant differences in peak pressure between the dominant and non-dominant side during walking [11]. Therefore, similar to other studies [14,15], only one foot was used for all further analyses; the dominant foot (the right side for all participants) was used.

Differences in plantar pressure patterns were observed between WBR and non-WBR postures as well as dynamic versus static WBR (Figure 2). Significant effects of posture by foot region were identified for all dependent variables: peak pressure, average pressure, average pressure range, peak contact area and average contact area. Effects contrasts show that it is possible to differentiate a dynamic WBR posture (walking), a static WBR posture (standing) and a non-WBR posture (sitting) within a single metric (Table 2 and 3). Ten foot-region by measurement parameter combinations were found to significantly differentiate all three postures; four of these interactions were found at the lateral midfoot and heel, with

another four in the medial and central forefoot. Seven of the ten differentiating combinations used pressure measures. Within the ten significant combinations, 28 of 30 two-way comparisons noted large to very large effects [24] with only two noting medium effects, specifically differentiating walking from standing using average pressure in the lateral midfoot and heel (Table 3).
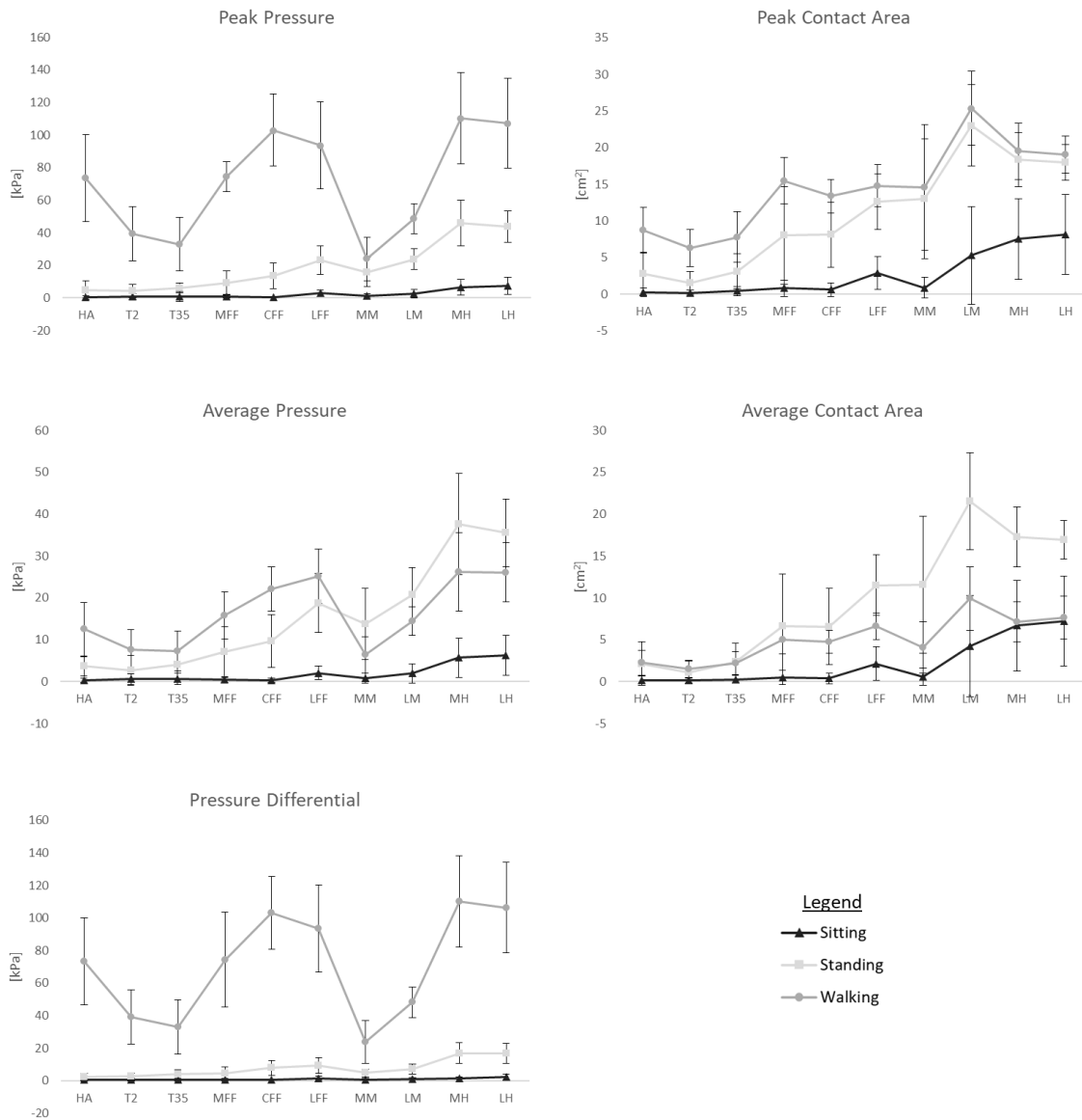
Figure 2. Plantar loading characteristics of posture by foot region for each of the five dependent variables. Values reported designate mean with error bars denoting standard deviation.

Table 2. Pairwise comparisons for each of the dependent variables in the ten foot regions. Values reported designate mean (standard deviation). Bold indicates metrics where all three postures were statistically different from each other.

Variable	Condition	HA	T2	T35	MFF	CFF	LFF	MM	LM	MH	LH
Peak Pressure (kPa)	Sitting	0.54 (0.77)	0.80 (1.76)	0.88 (3.16)	0.93 (1.04)	0.55 (0.21)	2.90 (1.93)	1.21 (1.40)	**2.47 (2.53)**	**6.51 (4.79)**	**7.47 (5.29)**
	Standing	4.82 (5.81)$^{\$}$	4.12 (4.01)$^{\$}$	6.17 (3.16)$^{\$}$	9.26 (7.37)$^{\$}$	13.45 (7.76)$^{\$}$	23.06 (8.85)$^{\$}$	15.92 (8.82)*	**23.72 (6.47)$^{*\$}$**	**45.94 (13.85)$^{*\$}$**	**43.58 (9.61)$^{*\$}$**
	Walking	73.44 (26.71)$^{*\$}$	39.27 (16.64)$^{*\$}$	32.97 (16.52)$^{*\$}$	74.37 (9.26)$^{*\$}$	103.10 (22.21)$^{*\$}$	93.67 (26.62)$^{*\$}$	23.88 (13.25)*	**48.59 (9.40)$^{*\$}$**	**110.28 (28.06)$^{*\$}$**	**107.33 (27.54)$^{*\$}$**
Average Pressure (kPa)	Sitting	0.34 (0.52)	0.61 (1.32)	0.63 (1.38)	**0.56 (0.68)**	**0.36 (0.48)**	2.10 (1.66)	0.88 (1.17)	**1.99 (2.29)**	5.73 (4.71)	**6.30 (4.72)**
	Standing	3.67 (4.94)$^{\$}$	2.72 (3.53)$^{\$}$	4.14 (3.64)$^{\$}$	**7.07 (6.04)$^{*\$}$**	**9.70 (6.32)$^{*\$}$**	18.73 (7.06)$^{\$}$	13.73 (8.55)$^{*\$}$	**20.81 (6.42)$^{*\$}$**	37.64 (12.07)*	**35.52 (8.04)$^{*\$}$**
	Walking	12.50 (6.46)$^{*\$}$	7.58 (4.86)$^{\$}$	7.33 (4.72)$^{\$}$	**15.82 (5.65)$^{*\$}$**	**22.20 (5.28)$^{*\$}$**	25.15 (6.47)$^{*\$}$	6.37 (4.29)$^{\$}$	**14.44 (3.47)$^{*\$}$**	26.22 (9.43)*	**26.10 (7.04)$^{*\$}$**
Avg. Pressure Differential (kPa)	Sitting	0.37 (0.57)	0.42 (0.87)	0.42 (0.52)	0.73 (0.87)	0.45 (0.52)	1.62 (1.00)	0.70 (0.56)	1.19 (0.80)	1.58 (0.58)	2.27 (1.84)
	Standing	2.40 (2.32)$^{\$}$	2.67 (2.02)$^{\$}$	4.09 (2.71)$^{\$}$	4.74 (3.73)$^{\$}$	7.85 (4.51)$^{\$}$	9.51 (4.83)$^{\$}$	4.88 (2.38)$^{\$}$	7.09 (3.04)$^{\$}$	16.90 (6.38)$^{\$}$	16.80 (5.92)$^{\$}$
	Walking	73.43 (26.71)$^{*\$}$	39.27 (16.64)$^{*\$}$	32.97 (16.52)$^{*\$}$	74.37 (29.29)$^{*\$}$	103.10 (22.21)$^{*\$}$	93.47 (26.72)$^{*\$}$	23.88 (13.25)$^{*\$}$	48.30 (9.37)$^{*\$}$	110.26 (28.02)$^{*\$}$	106.40 (27.74)$^{*\$}$
Peak Contact Area (cm^2)	Sitting	0.29 (0.58)	0.18 (0.36)	0.41 (0.62)	**0.82 (1.11)**	**0.60 (0.91)**	2.87 (2.27)	0.86 (1.43)	5.28 (6.70)	7.53 (5.48)	8.14 (5.42)
	Standing	2.77 (2.96)$^{\$}$	1.55 (1.51)$^{\$}$	3.12 (2.36)$^{\$}$	**8.01 (6.69)$^{*\$}$**	**8.10 (4.47)$^{*\$}$**	12.59 (3.80)*	13.00 (8.15)*	23.06 (5.53)*	18.35 (3.67)*	17.99 (2.45)*
	Walking	8.75 (3.11)$^{*\$}$	6.29 (2.54)$^{*\$}$	7.78 (3.44)$^{*\$}$	**15.48 (3.16)$^{*\$}$**	**13.36 (2.32)$^{*\$}$**	14.81 (2.88)*	14.58 (8.55)*	25.36 (5.08)*	19.49 (3.87)*	19.03 (2.55)*
Average Contact Area (cm^2)	Sitting	0.19 (0.46)	0.14 (0.29)	0.27 (0.48)	0.52 (0.83)	0.38 (0.64)	**2.16 (2.03)**	0.55 (1.03)	4.27 (6.06)	6.68 (5.41)	7.22 (5.37)
	Standing	2.14 (2.58)	1.11 (1.36)	2.40 (2.19)	6.64 (6.19)$^{\$}$	6.57 (4.57)*	**11.53 (3.64)$^{*\$}$**	11.58 (8.16)$^{*\$}$	21.53 (5.79)$^{*\$}$	17.26 (3.56)$^{*\$}$	16.95 (2.32)$^{*\$}$
	Walking	2.26 (1.50)	1.53 (1.05)*	2.22 (1.38)*	5.01 (1.68)$^{*\$}$	4.77 (1.39)*	**6.62 (1.57)$^{*\$}$**	4.10 (3.05)$^{\$}$	9.92 (3.82)$^{\$}$	7.14 (2.41)$^{\$}$	7.68 (2.54)$^{\$}$

* Significant differences compared to sitting

$^{\$}$ Significant differences between standing and walking

The largest effects differentiating WBR from non-WBR were seen across all pressure-based metrics with the greatest contrasts seen in peak pressure and average pressure in the lateral midfoot and hindfoot (Table 3). Average pressures in the midfoot and hindfoot differentiate WBR postures from non-WBR with almost all comparisons noting very large effects [24]. However, average pressure only notes one large effect (medial midfoot) when contrasting walking from standing within the midfoot and hindfoot. Additionally, peak contact area had very large effect sizes between WBR and non-WBR postures in the midfoot and hindfoot [24].

Dynamic and static WBR were best distinguished by average pressure differentials across all foot regions. Peak pressure across the entirety of the foot differentiated static from dynamic WBR with only one of twenty comparisons having less than a very large effect size; the rapid increase in pressure across all foot regions during the stance phase of gait is unequaled in static WBR. Peak contact area in the toes also differentiated static from dynamic WBR; while being unable to significantly contrast standing from sitting.

Table 3. Effect size comparisons for each posture combination of the dependent variables, in the ten foot regions (Cohen's d score). A value of 0.5 represents a medium effect while a value of 1.2 is a very large effect [24].

Variable	Comparison	HA	T2	T35	MFF	CFF	LFF	MM	LM	MH	LH
Peak Pressure (kPa)	Walking - Sitting	1.96	1.91	1.86	1.96	2.13	2.13	1.74	**2.28**	**2.21**	**2.21**
	Walking - Standing	1.84	1.75	1.55	1.74	1.86	1.66	0.61	**1.23**	**1.37**	**1.41**
	Standing - Sitting	0.11	0.16	0.31	0.22	0.27	0.47	1.13	**1.05**	**0.84**	**0.8**
Average Pressure (kPa)	Walking - Sitting	1.76	1.54	1.52	**1.94**	**2.14**	2.05	0.72	**1.38**	1.27	**1.42**
	Walking - Standing	1.28	1.07	0.73	**1.11**	**1.23**	0.57	0.97	**0.71**	0.71	**0.67**
	Standing - Sitting	0.48	0.47	0.8	**0.83**	**0.92**	1.48	1.7	**2.09**	1.98	**2.09**
Avg. Pressure Differential (kPa)	Walking - Sitting	1.94	1.91	1.86	1.93	2.09	2.05	1.82	2.14	2.11	2.11
	Walking - Standing	1.89	1.8	1.65	1.83	1.94	1.87	1.49	1.87	1.82	1.81
	Standing - Sitting	0.05	0.11	0.21	0.11	0.15	0.18	0.33	0.27	0.3	0.29
Peak Contact Area (cm^2)	Walking - Sitting	1.94	1.95	1.9	**1.99**	**2.11**	1.98	1.51	1.87	1.72	1.77
	Walking - Standing	1.38	1.51	1.2	**1.01**	**0.87**	0.37	0.17	0.21	0.16	0.17
	Standing - Sitting	0.57	0.44	0.7	**0.97**	**1.24**	1.61	1.33	1.66	1.56	1.6
Average Contact Area (cm^2)	Walking - Sitting	1.07	1.22	1.1	1	1.17	**0.97**	0.53	0.63	0.07	0.08
	Walking - Standing	0.06	0.36	0.1	0.37	0.48	**1.06**	1.11	1.3	1.61	1.6
	Standing - Sitting	1.01	0.86	1.21	1.37	1.64	**2.03**	1.63	1.93	1.68	1.68

4. Discussion

I. Biomechanics/Physiology of Movement

The central finding of this study is that plantar pressure in a healthy population is a viable means to both characterize and differentiate the common workplace postures of walking (dynamic WBR), standing (static WBR) and sitting (static non-WBR). The results of this study quantify the unique plantar contact characteristics of each posture for the first time. As expected, average pressures better distinguish WBR from non-WBR postures while peak pressures better distinguish dynamic from static WBR. Peak heel pressures during walking were double those observed during standing; whereas, average pressure metrics had limited ability to differentiate dynamic and static WBR postures, due to the cyclic loading/unloading of walking. Stance phase was distinguishable from standing using peak contact pressures, peak contact area and peak pressure differential due to the movement of the load from the hindfoot (heel strike) to the toes (toe-off) when compared to the more constant and distributed hindfoot and midfoot load of standing. Lower magnitude peak contact forces in the forefoot are seen during standing when compared with walking. During erect sitting forefoot and toe loading is even lower than standing. The biomechanical differences noted between the three postures and further demonstrated through the pedobarographic patterns suggest that plantar pressure is a viable way to distinguish between walking, standing and sitting.

To the authors' knowledge, no previous studies have investigated which pedobarographic characteristics can differentiate walking, standing and sitting in an asymptomatic population. Previous studies have, however, assessed plantar pressure characteristics within the individual postures; such studies often focus on the effects of a disease or condition [13,14], gender, age or foot differences [11,15,17], or contrasting dynamic activities [12,15], all using plantar pressure as an outcome measure.

Patterns of pressure distribution during walking are consistent with recent reports, although regional peak pressure values were notably lower when compared to similar works using different measurement systems [12,15]. Previous research on the F-Scan system found lower peak pressures when compared to the absolute pressure [25,26]. However, Chevalier et al., [27] found regional peak pressure

values comparable to values found in this study also using the F-Scan system. The inaccuracy of the F-Scan has been previously investigated [25,26,28] and attributed to sensor temperatures [25,28], preconditioning and damage [25,29], or inaccurate and inadequate calibration protocols [29]. Despite these issues, several works [25,29] have expressed that although accuracy and reliability of absolute pressure values ascertained with the F-Scan system may be skewed, valuable information can still be observed in the relative pressure patterns. Additionally, Price et al. [26] noted that findings are often challenging to compare due to differences in loading conditions and study protocols.

Standing pressure patterns are similar to those previously reported. Pau et al. [13] also studied standing in an asymptomatic population and verified the finding that hindfoot is the most active during standing; however, they noted forefoot loads to be substantially greater than midfoot loads, which conflicts with our study's results where the midfoot was more active than forefoot during standing. Explanations for this include that Pau use a different shoe condition (barefoot), plantar measurement tool (force place), and different method to divide the plantar aspect of the foot - Pau grouped the forefoot with the toes, which moved the forefoot/midfoot and midfoot/hindfoot divisions anteriorly relative to our study. In contrast, Cimolin et al. [30] reported similar pressure and contact area trends using a Pedar-X in-shoe system as found in this study during standing. They noted the hindfoot to be most active, followed by the midfoot and then the forefoot/hallux [30].

II.   *Significance*

Weight bearing has shown to be a risk factor for the development of PF [1,10]. It was hypothesized that the forefoot and toes may elicit differentiable characteristics between WBR and non-WBR postures primarily due to the minimal recruitment during sitting. Our results (Table 2) suggest that all the pressure-based metrics and peak contact area in the toe regions can successfully differentiate walking from sitting. Distinguishing standing from sitting proved more challenging as the large standard deviation in the toe regions during standing reduced the differentiability for most pressure metrics. The forefoot demonstrated

a strong potential for differentiating WBR from non-WBR, particularly in the medial and central forefoot using average pressure and peak contact area. As hypothesized, the low recruitment during sitting contrasts significantly when compared to WBR postures. Pressure-based metrics in the hindfoot also proved to strongly differentiate WBR from non-WBR postures. As Pau et al. [13] showed, the peak and average contact pressures in the hindfoot are greatest during standing and walking. Because of the magnitude of the loading, WBR postures place significantly more load on the hindfoot when contrasted with sitting, as shown by the large to huge [24] effect sizes in this study.

Recent evidence suggests that soft tissue metabolism is mechanosensitive and modulated by loading frequency [9]. This suggests that differentiation of not only WBR versus non-WBR activities, but also dynamic versus static loading regimes, is of the utmost importance when examining the etiology of PF. We hypothesized that when differentiating dynamic from static WBR, the cyclic nature of gait could provide a means of distinguishing dynamic from static postures. Pressure-based metrics proved to distinguish dynamic from static postures across almost all regions; this was especially apparent using the average pressure differential, which had very large effect sizes [24] across all foot regions. However, peak or average pressures may prove more useful metrics as pressure differential was not able to significantly differentiate all three postures simultaneously, whereas peak pressure was able to differentiate the three postures in three foot regions and average pressure in four regions. Average pressure and average contact area demonstrate the impact of the cyclic nature of gait when distinguishing dynamic from static weight bearing. Average standing metrics were greater than that of walking, especially in the midfoot and hindfoot; although walking has higher peak pressures, the swing phase of walking reduces the average values. This trend is not always apparent in other studies which reported mean pressure or area values [13,15], as they only took an average across the stance phase of gait therefore inflating the average values of walking beyond that of standing across all regions/metrics. Combining both stance and swing and observing the results through average metrics provides a better picture of the overall loading exposure of the plantar fascia during the activity.

III.   *Future Implications of Work*

Minimizing redundancy when analyzing plantar pressure characteristics is critical for the development of cost-effective posture differentiation interventions. By distilling down the number of inputs needed to differentiate the three postures, plantar data collection can be conducted using cheaper instrumentation at only certain plantar locations and over a longer duration without amassing excessive amounts of data. In this study, ten foot-region by measurement parameter combinations were found to significantly differentiate all three postures highlighting the fundamental differences in biomechanics between the postures and the value of plantar pressure metrics for activity classification. Table 2 and 3 demonstrate that although many possible region by parameter combinations exist, they convey the same information. By isolating those which can not only differentiate WBR from non-WBR, but also dynamic versus static postures simultaneously, one can reduce the number of inputs necessary to distinguish these postures. Further research is needed to optimize the number of foot-region by measurement parameter combinations needed to strike a balance between reliable posture differentiation and minimal redundant information; however, this work demonstrates that the medial/lateral hindfoot and the medial/central forefoot regions are good starting points.

IV.   *Limitations*

The findings presented must be considered under several study limitations. First, a small sample size comprised mainly of males was used, although the number of participants included in the current study is similar to other studies investigating physical activity and sedentary behaviours [11,12,23], it may not be representative of plantar pressure distributions in females. Second, although plantar pressure across the feet has been shown as symmetric in standing [17] and walking [11], the current study was comprised of only right-foot dominant individuals. Third, shoe type and model were not controlled, foot type and shape were not restricted and participants were instructed to walk at their preferred speed. Although these choices do introduce variability into the investigation, one underlying goal of the study was to make the

in-shoe posture differentiation robust to eventually monitor ecological conditions. Similar choices have been made in other research; namely non-standardization of shoes [12,15,30] and using preferred walking speed [14]. Lastly, these results can be further validated through replication with other in-shoe pressure measurement systems.

5. Conclusion

It is currently difficult to establish a causal link between weight bearing in the workplace and plantar heel pain due to its multifarious etiology coupled with a lack of available objective evidence [20]. The current study sought to quantitatively characterize the pedobarographic patterns in three common workplace postures to identify how plantar regions and measurement parameters differ between them. Results suggest that ten region/parameter combinations could significantly differentiate the three postures simultaneously, while many more can distinguish between WBR and non-WBR postures or dynamic versus static postures. These results lay the groundwork for optimizing the differentiation of common postures and understanding the physiological implications of these different workplace postures. Above all, differentiating such postures using plantar pressure may allow for the objective evidence to emerge allowing researchers to establish or refute a link between weight bearing and plantar heel pain.

6. Acknowledgements

7. Conflict of Interest Statement

Michael Ryan is a salaried employee of Kintec Footlabs Inc.

References

[1] Beeson P. Plantar fasciopathy: Revisiting the risk factors. Foot & Ankle Surgery (Elsevier Science) 2014;203:160-5.

[2] Tong KB, Furia J. Economic burden of plantar fasciitis treatment in the United States. Am J Orthop 2010;395:227.

[3] Thomas MJ, Roddy E, Zhang W, Menz HB, Hannan MT, Peat GM. The population prevalence of foot and ankle pain in middle and old age: a systematic review. Pain 2011;15212:2870-80.

[4] Anton D, Weeks D. Prevalence of work-related musculoskeletal symptoms among grocery workers. Int J Ind Ergonomics 2016;54:139-45.

[5] Werner RA, Gell N, Hartigan A, Wiggerman N. Risk Factors for Plantar Fasciitis Among Assembly Plant Workers. PM & R 2010;22:110; 110,116; 116.

[6] Parent-Thirion A, Vermeylen G, van Houten G, Lyly-Yrjänäinen M, Biletta I, Cabrita J. Fifth European Working Conditions Survey overview report . 2012;EF1182.

[7] Pedersen SJ, Kitic CM, Bird M, Mainsbridge CP, Cooley PD. Is self-reporting workplace activity worthwhile? Validity and reliability of occupational sitting and physical activity questionnaire in desk-based workers. BMC Public Health 2016;161:836.

[8] Cheng HK, Lin C, Wang H, Chou S. Finite element analysis of plantar fascia under stretch—The relative contribution of windlass mechanism and Achilles tendon force. J Biomech 2008;419:1937-44.

[9] Wang T, Lin Z, Day RE, Gardiner B, Landao-Bassonga E, Rubenson J, Kirk TB, Smith DW, Lloyd DG, Hardisty G, Wang A, Zheng Q, Zheng MH. Programmable mechanical stimulation influences tendon homeostasis in a bioreactor system. Biotechnol Bioeng 2013;1105:1495-507.

[10] Riddle DL, Pulisic M, Pidcoe P, Johnson RE. Risk Factors for Plantar Fasciitis: a Matched Case-Control Study. Journal of Bone & Joint Surgery, American Volume 2003;85-A5:872.

[11] Kim J, Kim K, Gubler C. Comparisons of Plantar Pressure Distributions between the Dominant and Non-dominant Sides of Older Women during Walking. Journal of Physical Therapy Science 2013;253:313-5.

[12] Rao S, Carter S. Regional plantar pressure during walking, stair ascent and descent. Gait Posture 2012;362:265.

[13] Pau M, Galli M, Celletti C, Morico G, Leban B, Albertini G, Camerota F. Plantar pressure patterns in women affected by Ehlers-Danlos syndrome while standing and walking. Res Dev Disabil 2013;3411:3720-6.

[14] Sullivan J, Burns J, Adams R, Pappas E, Crosbie J. Plantar heel pain and foot loading during normal walking. Gait Posture 2015;412:688-93.

[15] Chuckpaiwong B, Nunley JA, Mall NA, Queen RM. The effect of foot type on in-shoe plantar pressure during walking and running. Gait Posture 2008;283:405-11.

[16] Periyasamy R, Anand S. The effect of foot arch on plantar pressure distribution during standing. J Med Eng Technol 2013;375:342-7.

[17] Machado ÁS, Bombach GD, Duysens J, Carpes FP. Differences in foot sensitivity and plantar pressure between young adults and elderly. Arch Gerontol Geriatr 2016;63:67.

[18] Hillier S, Lai MS. Insole plantar pressure measurement during quiet stance post stroke. Topics in stroke rehabilitation 2009;163:189-95.

[19] Periyasamy R, Mishra A, Anand S, Ammini AC. Preliminary investigation of foot pressure distribution variation in men and women adults while standing. The Foot 2011;213:142-8.

[20] Waclawski ER, Beach J, Milne A, Yacyshyn E, Dryden DM. Systematic review: plantar fasciitis and prolonged weight bearing. Occupational Medicine 2015;652:97-106.

[21] Smith L, Hamer M, Ucci M, Marmot A, Gardner B, Sawyer A, Wardle J, Fisher A. Weekday and weekend patterns of objectively measured sitting, standing, and stepping in a sample of office-based workers: the active buildings study. BMC Public Health 2015;151:9-.

[22] Cavanagh PR, Ulbrecht JS. Clinical plantar pressure measurement in diabetes: rationale and methodology. The Foot 1994;43:123-35.

[23] Gurney JK, Kersting UG, Rosenbaum D. Between-day reliability of repeated plantar pressure distribution measurements in a normal population. Gait Posture 2008;274:706-9.

[24] Sawilowsky S. New effect size rules of thumb. Journal of Modern Applied Statistical Methods 2009;82:597-9.

[25] Nicolopoulos CS, Anderson EG, Solomonidis SE, Giannoudis PV. Evaluation of the gait analysis FSCAN pressure system: clinical tool or toy? The Foot 2000;103:124-30.

[26] Price C, Parker D, Nester C. Validity and repeatability of three in-shoe pressure measurement systems. Gait Posture 2016;46:69-74.

[27] Chevalier TL, Hodgins H, Chockalingam N. Plantar pressure measurements using an in-shoe system and a pressure platform: A comparison. Gait Posture 2010;313:397-9.

[28] Koch M, Lunde L, Ernst M, Knardahl S, Veiersted KB. Validity and reliability of pressure-measurement insoles for vertical ground reaction force assessment in field situations. Appl Ergon 2016;53 Pt A:44-51.

[29] Woodburn J, Helliwell P. Observations on the F-Scan in-shoe pressure measuring system. Clin Biomech 1996;115:301-4.

[30] Cimolin V, Veronica Cimolin, Paolo Capodaglio, Nicola Cau, Manuela Galli. Foot-type analysis and plantar pressure differences between obese and nonobese adolescents during upright standing. International journal of rehabilitation research 2015;391:87-91.

Chapter 3.

Classifying sitting, standing and walking using only plantar force data

The following journal paper will be submitted for review shortly.

3.1. Extended Methods

Please refer to Appendix C for further details regarding the methods associated with developing this work.

3.2. Prepared Journal Manuscript

Title Page

Classifying sitting, standing and walking using only plantar force data

Kohle Merry[a], Omar Aziz[a], Edward Park[a], Michael Ryan[b,c], Carolyn J. Sparrey[a]

[a] Mechatronic Systems Engineering, Simon Fraser University, Surrey, BC Canada

[b] Biomedical Physiology and Kinesiology, Simon Fraser University, Burnaby, BC Canada

[c] Kintec Footlabs Inc, Surrey, BC Canada

Corresponding Author:

Carolyn J. Sparrey, PhD
Associate Professor
Simon Fraser University
250-13450 102 Ave, Surrey, BC, V3T 0A3, CANADA
phone: (778) 782-8938
email: csparrey@sfu.ca

Abstract

Prolonged static weight bearing is common in certain workplace environments and is thought to exacerbate plantar fasciitis. Thus, certain occupations may predispose workers to develop plantar fasciitis. Objective measures of physical activities able to distinguish sedentary behaviours in the workplace are lacking, making it difficult to establish or refute the connection between work exposure and plantar fasciitis. Plantar pressure has shown promise as an unobtrusive tool for posture differentiation, yet evidence suggesting the optimal number and locations of sensors required to accurately classify postures is lacking. Plantar pressure data was measured in eight healthy participants using the F-Scan in-shoe measurement system (Tekscan Inc, Boston, USA) during periods of sitting, standing and walking. Data was resampled to simulate on/off characteristics of 24 force sensitive resistors (FSRs) spanning the plantar aspect of the foot. Following feature selection, the top 10 sensor locations were evaluated using leave-one-out cross-validation with five different machine learning algorithms: RBF-Kernel support vector machines (SVM), bagged decision tree (BDT), linear discriminant analysis, naïve bayes, and K-nearest neighbours. The top two algorithms (SVM and BDT) classified sitting, standing and walking at 98.1% and 99.1% accuracy, respectively, with five sensors, and 97.4% and 98.1%, respectively, with three sensors. The central forefoot, and the medial and lateral midfoot were found to be the most important sensor locations for classification. This work demonstrates that a selected number of uncalibrated FSRs positioned at key points could classify sitting, standing and walking at high accuracies. The results of this study can assist in the development of an objective measure for quantifying sedentary posture duration at work.

Keywords: Pedobarography, Pattern Recognition, Posture Differentiation, Plantar Fasciitis, Weight Bearing

1. Introduction

Plantar Fasciitis (PF) is a degenerative foot condition which typically presents as a sharp pain around the heel after long periods of inactivity. PF is the most common cause of inferior heel pain [1] constituting an estimated 11-15% of foot problems requiring professional attention among adults [2]. The etiology of PF is multifactorial, and no clear consensus exists ranking the most causal risk factors. However, prolonged weight bearing (WBR) at work has been reported to increase risk [3]. Some industries require workers to maintain fixed postures to perform tasks, limiting their freedom to sit or move around [4,5]; estimates indicate 47% of employees stand for at least 75% of their workday [6].

Quantitatively monitoring WBR at work is challenging. Questionnaires are the most common tool used to quantify physical activity at work [7], but may be unreliable and prone to bias [8]. Commercial activity trackers can provide more objective measurements of physical activity without user interaction, but tend to focus on differentiating complex dynamic activities and have limited potential differentiating static postures typical in a workplace (e.g. sitting from standing) [9]. Custom activity trackers have been proven reliable at distinguishing static postures [10], but include unnecessary features beyond this application, thus increasing cost and complexity in the system.

Several challenges arise when attempting to quantify workplace postures over an extended duration. First, the system must be minimally invasive and robust enough to deploy into a worker population with minimal to no participant interaction. Second, the system must be cost-effective so it can be manufactured in high volume to gather population data. One method to characterize essential workplace postures unobtrusively is through plantar pressure. Several shoe-based wearable systems have been recently developed targeting gait analysis and rehabilitation [11-15] and have been able to differentiate basic dynamic from static activities (e.g. walking from standing) and different static postures (e.g. sitting from standing) [13,16]. However, to date, these insole technologies have coupled plantar pressure with accelerometer data [13,16-18], increasing the cost and complexity. Purely pressure-based systems have focused on measuring gait biomechanics not activity differentiation [14,15]. In addition,

current instrumented insole designs using force sensitive resistors must calibrate the sensors prior to use [15,16], a costly and time-consuming process that would be prohibitive in a large-scale manufacturing environment. Finally, current designs place sensors in locations thought to be biomechanically important [11,12,14] but have not assessed the validity of other physiologically relevant sensor locations. Identifying the optimal number and locations of pressure sensors for classification of typical workplace postures and developing classification algorithms that can use uncalibrated on/off signals could reduce the complexity and cost of instrumented insole systems.

Machine learning classifications are effective for activity recognition using shoe-based sensors [13,14,16-18]; however, no single classification algorithm is accepted as the standard for activity differentiation. Successful classification has been achieved for a variety of conditions: walking at various speeds [13,14,16-18], running [16], cycling [16], elevator use [18], ascending/descending stairs [13,16,18], standing [13,16,18], sitting [13,16,18] and sit-to-stand/stand-to-sit transfers [14,18].

This study aimed to classify common workplace postures (sitting, standing and walking) through unilateral plantar pressure data. Additionally, the number and location of sensors on the plantar aspect of the foot needed for accurate posture recognition was evaluated through machine learning by reducing high-resolution temporal and spatial data to simulate force sensitive resistor (FSR) characteristics. It was hypothesized that less than five FSRs selectively placed under the foot would be needed to classify sitting, standing, and walking above 95% accuracy.

2. Methods

I.   Participants

Ten healthy subjects (8 male/2 female, body mass = 74.2 ± 18.4 kg, height 172.0 ± 10.3 cm, age = 29.0 ± 4.8 years) were recruited. Written informed consent was obtained from each participant. This study was approved by the Simon Fraser University Office of Research Ethics.

Two appropriately sized F-Scan pressure measurement insoles (Tekscan Inc, Boston, USA) were

fitted into each participant's shoes; data was captured at 75Hz. Data collection was conducted in two

separate trials spaced twenty minutes apart; each trial consisted of a six-minute collection phase in which

each participant demonstrated the postures (sitting, standing and walking) twice, for approximately one

minute each. Activity order was randomized. At the start of each activity the participant performed a

right-footed stomp. Participants were warned five seconds before the completion of an activity and

instructed to assume the next posture. Video data was captured to validate the start and end of an activity

sequence. Participants sat in a plastic office chair (46 cm floor-seat height). Participants walked back-and-

forth over a 10 m walkway at a self-selected speed.

III.   *Data Processing*

Subdivision of the plantar side of the foot was conducted to consistently locate anatomical regions

of interest; a modified version of the PRC mask, developed by Novel (Novel GmbH, Munich, Germany)

was selected based on literature substantiating its usage [19,20]. The subdivision results in the following

ten anatomical regions: hallux (HA), second toe (T2), third to fifth toes (T35), medial forefoot (MFF),

central forefoot (CFF), lateral forefoot (LFF), medial midfoot (MM), lateral midfoot (LM), medial heel

(MH) and lateral heel (LH) (Figure 1a-b).

Following regional division, 24 proposed sensor locations were identified on the plantar aspect of

the foot (Figure 1c) simulating discrete FSRs that are commonly used in instrumented insoles [15,16].

Sensors locations were identified to cover the entire plantar surface, based on the regions, without

overlapping each other or an edge. Each simulated sensor ('simFSR') was comprised of 5 F-Scan sensel

elements in the shape of a cross which simulates the approximate size of common low-cost (< $9 CAD)

FSRs (1.27 cm diameter). To place the sensors, three sensors were first placed at the center of the hallux,

second toe, and third to fifth toe regions (sensors 1,2,3). A fourth sensor was then placed in the third to

fifth toe region at an offset of 10% of the foot length in the posterior direction, and 10% of the foot width

in the lateral direction (sensor 4). Sensors were then placed at the center of the remaining anatomical

masks (sensors 5,8,11,13,16,19,22). Remaining sensors were positioned offset ± 10% of the foot length along the longitudinal axis of the foot from the center sensor in each mask. Two sensor locations (sensors 6 & 9) were moved an additional 8% anteriorly to compensate for the large toe-forefoot sensor gap. Only two sensors were defined for the lateral forefoot to compensate for the diagonal T35/LFF boundary. Sensor 24 was also moved medially 10% of the foot width to avoid edge overlap.

(a)   (b)   (c)
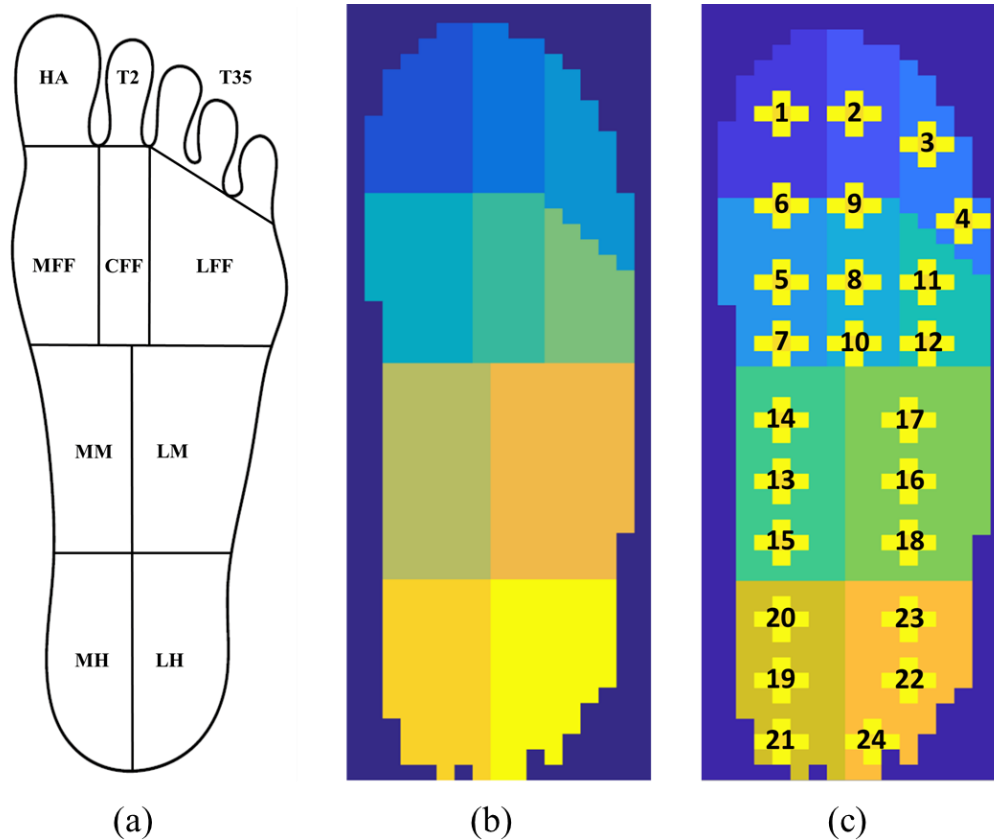
Figure 1 - Regional breakdown of the foot into 10 anatomical regions and 24 perspective sensor locations. (a) Anatomical regions per the PRC masking method (b) Exemplary footprint subdivided using the PRC masking method (c) Exemplary footprint with 24 overlaid sensor locations. Circular FSRs (0.5" diameter) were approximated with 5 F-Scan sensel elements shaped in a cross; sensel elements are spaced 0.51cm apart.

Investigation of the three loading conditions was carried out following the removal of inter-activity transition periods, defined as the time when an activity was completed until the participant was comfortably in position to begin the subsequent activity, denoted through a stomp of the right foot, and

confirmed through video data. Resultantly, activity durations were non-uniform and were reduced from one-minute blocks to approximately 40-50 second blocks after removing transitions.

IV.   *Data Resampling and Reduction*

To simulate low-cost off the shelf sensors and eliminate the need to calibrate the sensors, pressure data was resampled to 15 Hz from the original 75 Hz and data from each of the simFSRs (Figure 1c) was reduced to on/off signals. If any of the five sensel elements comprising a simFSR recorded a pressure value at a single time point, the simFSR was considered 'on'. Pressure readings above the default noise filter threshold for the F-Scan system were deemed on; the default threshold is defined as 1.2% of the saturation pressure determined during calibration, which amounted to 6-12 kPa depending on the size of the participant. This range is similar to previous work by Price and colleagues [21], who defined active sensors of three in-shoe measurement tools as sensors registering pressure >10 kPa. To assist with data consolidation 'on' was assigned a numeric value of 1 and 'off' was assigned a value of 0.

V.   *Machine Learning Classification*

Machine learning algorithms were used to classify each workplace activity using plantar pressure characteristics. The specific machine learning algorithm employed and the various control parameters within the algorithm were systematically explored to maximize classification power and assess the sensitivity of the algorithm to each parameter.

Similar to previous works [13,18], an overlapping sliding window approach was implemented to account for the temporal nature of gait; a sensitivity analysis was conducted for several window lengths (0.5, 0.75 ,1 ,1.5 ,2 ,2.5 and 3s) and window overlap percentages (0%, 25%, 50% and 75%). Window lengths were selected based on a step frequency estimated to be 1.4Hz (0.7s/stride) [22]. Several metrics (mean, mode, median, and sum) were calculated for each of the windows, and a subsequent sensitivity analysis was conducted to determine which data characteristic was best for classification. Data extracted from all 24 sensor locations was used to train five different learning algorithms: RBF kernel type SVM, Bagged Decision Tree (nTrees = 100), Discriminant Analysis, Naïve Bayes, and a k-Nearest Neighbour

(k = 5). A leave-one-out cross-validation scheme was used to test the window characteristics; characteristics were ranked for a given algorithm based on their classification accuracy, defined as the number of correctly classified samples divided by classified samples. Characteristics were compared relative to one another using the mean classification accuracy across all five learning algorithms, and the top characteristic was ultimately selected for subsequent analyses.

Feature selection is a method of variable subset selection where certain characteristics ('features') are selected from a larger set for use in model construction; in this context, feature selection facilitated the reduction of the original 24 simFSRs to a smaller subset by eliminating redundant or irrelevant features while minimizing the loss of information. Twenty-four features were defined as the optimal metric extracted from the sliding window selected from the sensitivity study for each of the 24 proposed sensor locations. Feature selection was conducted using a two-step approach; first, the 24 features were reduced and ranked through five filter-based features selection methods: Chi-Square, Fisher Score feature, Gini Index, Info-Gain and MRMR. The top ten features ranked by each selection method were subsequently compared in rank order, and the most frequently appearing within a given rank were selected as the global feature corresponding to that rank.

Data was split into training and testing data using a leave-one-out cross-validation scheme [23,24]. A sensitivity analysis with five different machine learning algorithms was run. Algorithms used were: RBF kernel type SVM, Bagged Decision Tree (nTrees = 100), Discriminant Analysis, Naïve Bayes, and a k-Nearest Neighbour (k = 5). Using all five of these algorithms, a sensitivity analysis was run on the number of sensors needed to accurately classify the three postures, starting with the top ten features and reducing to the single best feature; this simulated a wrapper-based feature selection method. Confusion matrices were constructed for each algorithm by feature number combination, and then used to calculate accuracy, error rate, sensitivity and specificity. Accuracy was defined as correctly classified samples divided by classified samples. Error rate was defined as incorrectly classified samples divided by classified samples. Sensitivity was defined as correctly classified positive samples divided by true

positive samples. Specificity was defined as correctly classified negative samples divided by true negative samples.

3. Results

I. *Plantar pressure data*

Pressure data was initially captured using the F-Scan system, then resampled to 24 discrete simFSR on/off outputs (Figure 2). During sitting, pressures recorded were low (<10kPa). Consequently, representative sensors at the hallux, medial forefoot and medial midfoot were often inactive or intermittently active during sitting. The sensor at the medial hindfoot, however, demonstrated sustained load during sitting. During standing, the entire foot is used to facilitate balance, so loading is constant across the plantar aspect of the foot. As walking is broken up into two specific phases of gait, stance and swing, activation is cyclical as the foot is constantly loaded and unloaded; this cyclic motion is captured in both the pressure data, and the on/off data, across all regions of the foot.
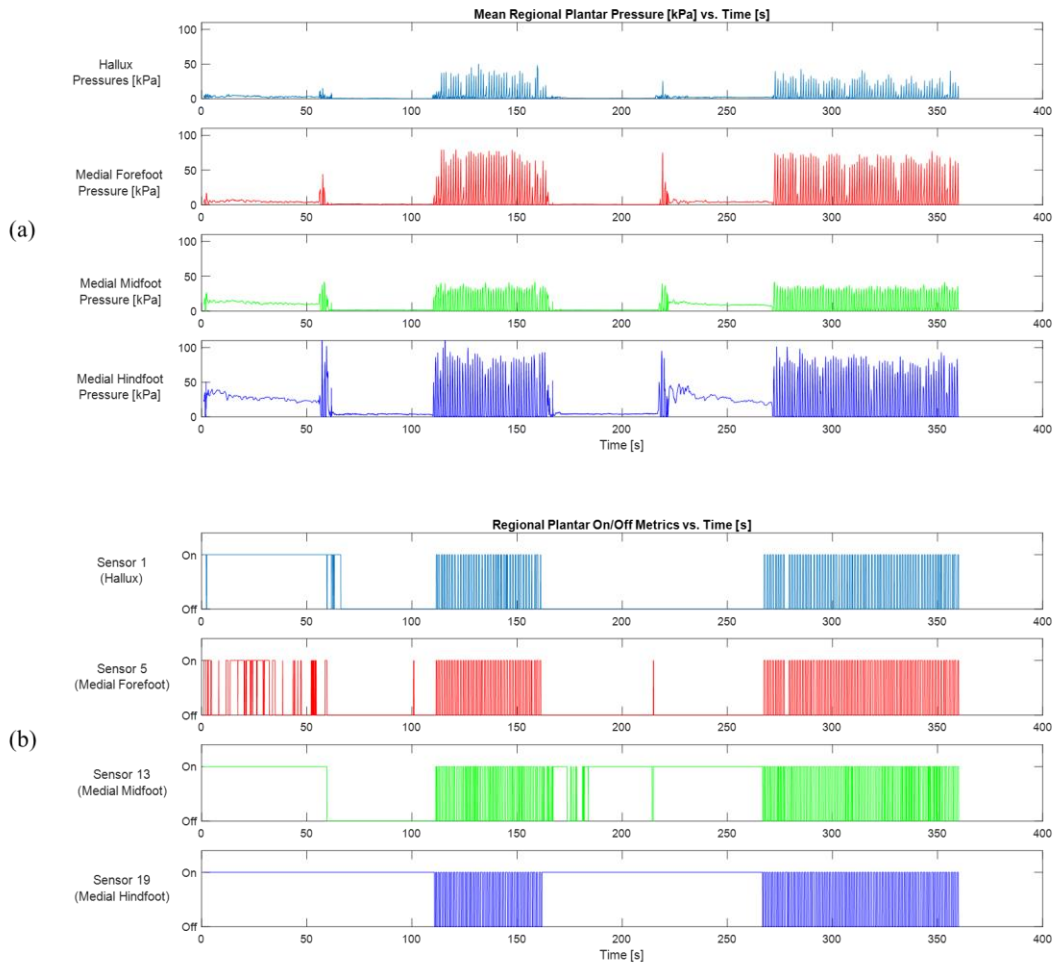
Figure 2 – Exemplary activity collection phase. Order of activities in this case was Standing (approximately 5-55s) - Sitting (65-110s) - Walking (115-160s) - Sitting (170-215s) - Standing (225-270s) - Walking (275 - 360s). Transition periods of approximately 5-10s separate each activity, as can be seen by abnormalities at approximately 60s and 220s. (a) Exemplary plantar pressure data for four major regions of the foot during an activity collection phase. (b) Exemplary on/off data for four simFSRs during an activity collection phase. The four simFSRs shown are representative of the middle of the four major regions of the foot, along the medial side of the foot.

II. Sliding Window Sensitivity Analysis

Three different control parameters were strategically manipulated during this study to optimize the implementation of the overlapping sliding window method for this data set: size of the window, overlap percentage, and data metric extracted from the window (Figure 3). Varying window length demonstrated a plateau effect at lengths greater than 1s, even when different classification algorithms were used (Figure 3a). Deviations in accuracy associated with different window overlaps were minimal (Figure 3b). Mean and sum substantially outperformed mode and median, and mean demonstrated higher accuracies across all classification algorithms when compared to sum using the same algorithm (Figure 3c).
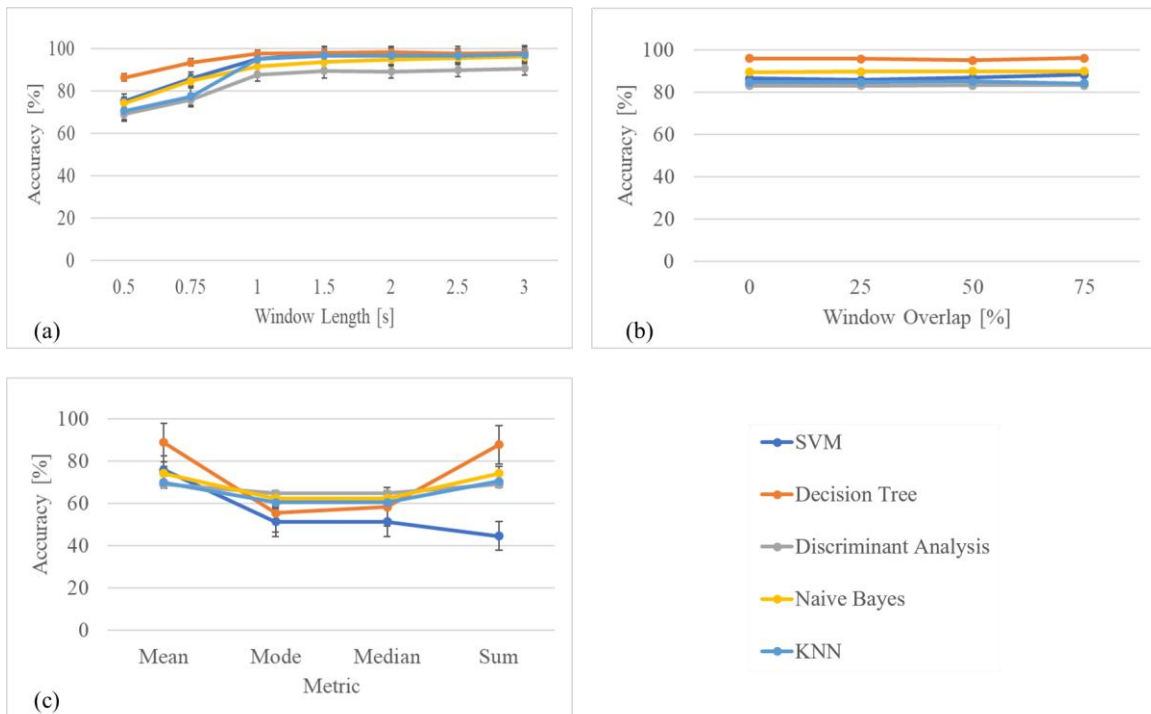
Figure 3 - Sensitivity analysis results for sliding window parameters. Models were trained using a complete feature set (24 features) with five different classification algorithms. (a) Classification accuracies for seven window lengths. (b) Classification accuracies for four different window overlaps. (c) Classification accuracies for four different data metrics. Data represents the mean of all results obtained through leave-one-out cross-validation, across all activities. Error bars denote standard error. Error bars in (b) are smaller than markers and are therefore not visible.

III. Posture Classification

The results show a clear ability to classify posture using only plantar pressure data. The number of sensors necessary for reliable posture classification, varied with classification algorithm (Figure 4).

Classification performance tended to decrease as the number of features used to construct the classification scheme decreased. Different classification algorithms performed similarly except for the K-Nearest Neighbour classifier. The top ten features, in rank order, were: sensor 15, 18, 8, 9, 12, 17, 20, 10, 11, and 16 (Figure 1c). The accuracy, error rate, sensitivity and specificity of the RBF kernel type SVM and the Bagged Decision Tree classifiers outperformed the three other classification algorithms; results from these two algorithms varying from five to a single sensor can be found in Table 1.
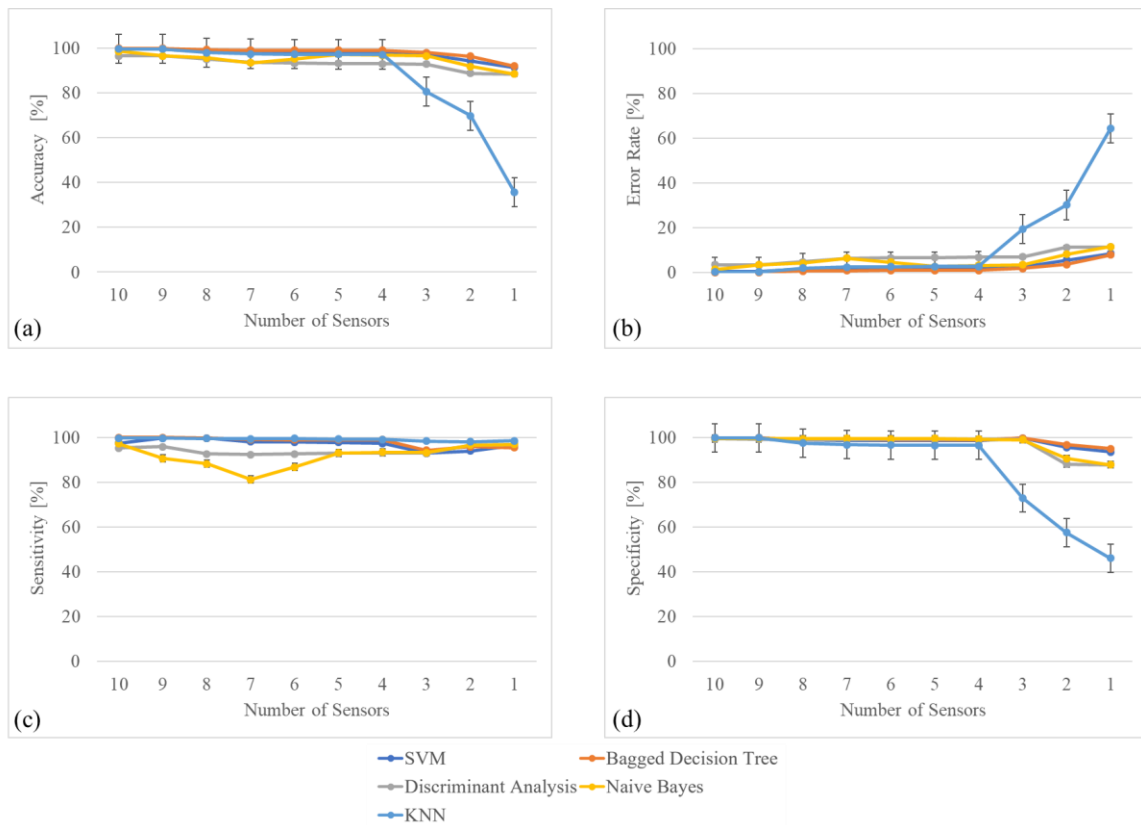
Figure 4 - (a) Classifier accuracy (b) Error rate (c) Sensitivity and (d) Specificity obtained using five different classification algorithms while varying the number of features used. A window length of 3s and window overlap of 75% were used to construct the sliding window, and the mean was extracted from the data within. Data represents the mean of all results obtained through leave-one-out cross-validation, across all activities. Error bars represent standard error. Some error bars in are smaller than markers and are therefore not visible.

72

Table 1 - Classifier accuracy, error rate, sensitivity and specificity for varying sensor combinations and five classification algorithms. Data represents the mean ± standard deviation of all results obtained through leave-one-out cross-validation, across all activities.

Sensors Used	Classification Algorithm	Accuracy (%)	Error Rate (%)	Sensitivity (%)	Specificity (%)
	RBF-Kernel SVM	98.14 ± 2.38	1.86 ± 2.38	97.53 ± 5.58	98.75 ± 2.44
	Bagged Decision Tree	99.09 ± 1.13	0.91 ± 1.13	99.09 ± 2.02	99.09 ± 1.66
	Discriminant Analysis	93.29 ± 7.80	6.71 ± 7.80	93.04 ± 17.60	99.14 ± 1.69
	Naive Bayes	97.28 ± 5.28	2.72 ± 5.28	93.20 ± 17.05	99.57 ± 0.46
	K-Nearest Neighbour	97.31 ± 3.44	2.69 ± 3.44	99.40 ± 0.94	96.60 ± 5.03
	RBF-Kernel SVM	98.12 ± 2.38	1.88 ± 2.38	97.48 ± 5.72	98.77 ± 2.45
	Bagged Decision Tree	99.06 ± 1.25	0.94 ± 1.25	99.09 ± 2.00	99.05 ± 1.84
	Discriminant Analysis	93.12 ± 7.81	6.88 ± 7.81	93.09 ± 17.62	99.18 ± 1.69
	Naive Bayes	96.86 ± 5.33	3.14 ± 5.33	93.45 ± 17.25	99.30 ± 1.49
	K-Nearest Neighbour	97.23 ± 3.42	2.77 ± 3.42	99.24 ± 1.23	96.60 ± 5.03
	RBF-Kernel SVM	97.36 ± 5.64	2.64 ± 5.64	93.04 ± 18.07	99.80 ± 0.58
	Bagged Decision Tree	98.09 ± 4.65	1.91 ± 4.65	94.35 ± 15.03	99.80 ± 0.31
	Discriminant Analysis	92.98 ± 8.18	7.02 ± 8.18	92.94 ± 17.89	99.14 ± 1.53
	Naive Bayes	96.56 ± 5.20	3.44 ± 5.20	93.30 ± 17.36	99.05 ± 1.11
	K-Nearest Neighbour	80.60 ± 12.94	19.40 ± 12.94	98.39 ± 3.50	72.98 ± 18.36
	RBF-Kernel SVM	94.45 ± 5.26	5.55 ± 5.26	94.10 ± 8.36	95.64 ± 7.83
	Bagged Decision Tree	96.42 ± 3.92	3.58 ± 3.92	95.92 ± 6.53	96.85 ± 5.89
	Discriminant Analysis	88.78 ± 17.12	11.22 ± 17.12	96.67 ± 6.99	88.16 ± 22.07
	Naive Bayes	91.83 ± 11.16	8.17 ± 11.16	96.72 ± 6.72	90.72 ± 17.12
	K-Nearest Neighbour	69.85 ± 5.35	30.15 ± 5.35	98.08 ± 2.65	57.53 ± 7.53
	RBF-Kernel SVM	91.51 ± 12.62	8.49 ± 12.62	96.52 ± 7.13	93.63 ± 13.48
	Bagged Decision Tree	92.05 ± 10.74	7.95 ± 10.74	95.51 ± 7.79	95.01 ± 10.68
	Discriminant Analysis	88.53 ± 17.39	11.47 ± 17.39	96.93 ± 6.69	87.84 ± 23.11
	Naive Bayes	88.49 ± 17.20	11.51 ± 17.20	96.93 ± 6.69	87.84 ± 23.11
	K-Nearest Neighbour	35.69 ± 5.64	64.31 ± 5.64	98.64 ± 2.29	46.05 ± 6.66

Classification accuracy was minimally affected by the decrease in sensors from five to three (Table 1). There was a greater decrease in accuracy when further reducing to a single sensor. Both the RBF-Kernel SVM (RBF) and the bagged decision tree (BDT) algorithms showed high accuracy (> 97%) in classifying the three workplace postures when more than three sensors were used. The BDT classification algorithm outperformed the RBF in each of the sensor combinations tested (Table 1). The bagged decision tree classifier produced the highest accuracy in the reduced set, with an accuracy of 99.09% when trained using five sensors; however, when reduced to the top three sensors (sensors 15, 18,

and 8), the accuracy only decreased 1%. Misclassifying a seated activity as standing was the most common error in the predicted behaviours. When reduced to a single sensor for classification standing activities became more frequently confused with walking.
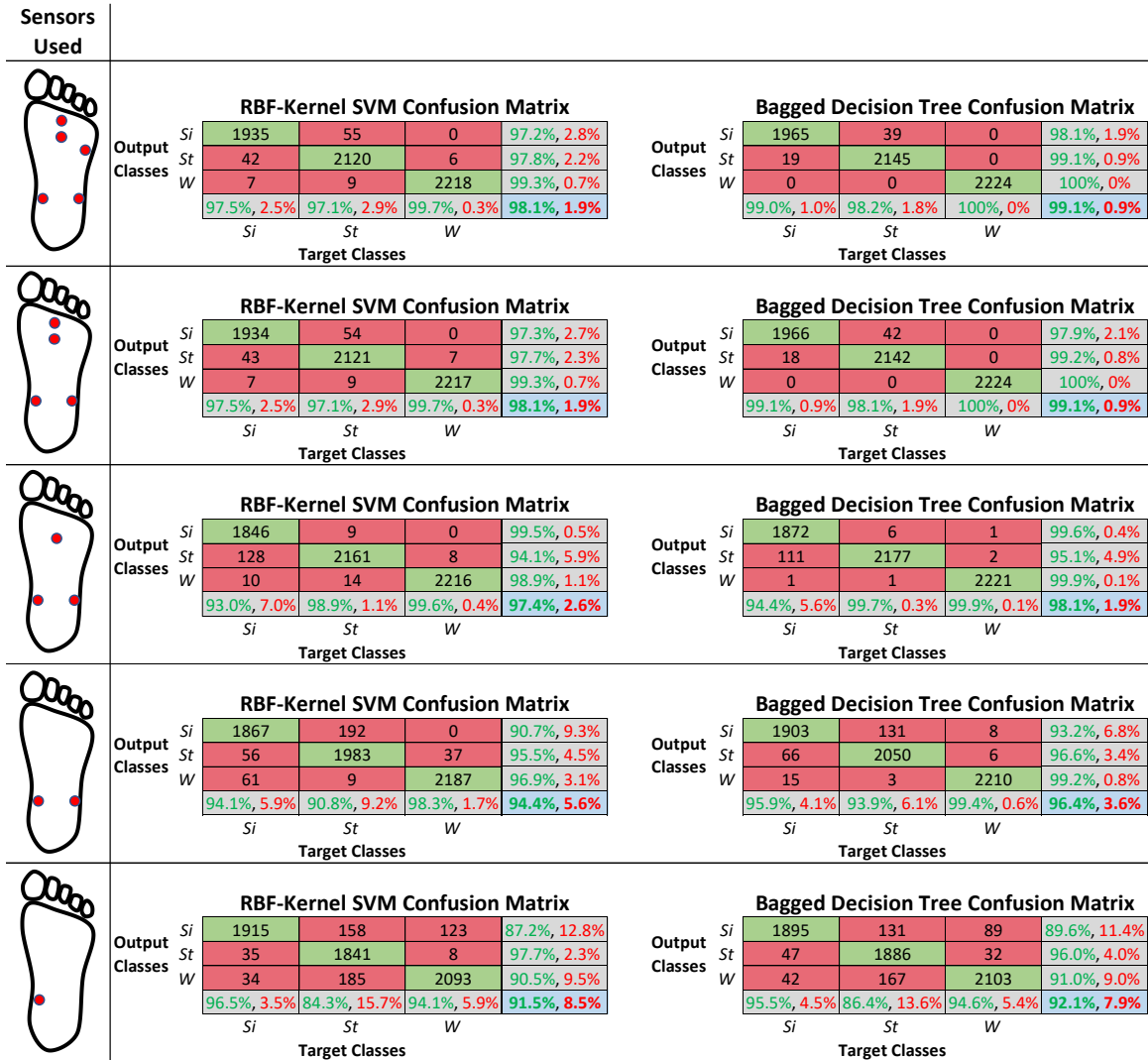
Figure 5 - Confusion matrices, displaying the ability of various sensor combinations to distinguish instances of sitting (*Si*), standing (*St*) and walking (*W*). Green values represent the percent correct while red values show the percent incorrect in each classification. Data represents the sum of all results obtained through leave-one-out cross-validation, across all activities.

4. Discussion

I. Classifier Performance

The classification scheme refined through the sensitivity analysis and subsequent classifier evaluation successfully classified three typical workplace postures. The present work used systematic data

reduction to identify sensor locations on the plantar surface that most effectively classify posture. The results showed that although more plantar force data increased classification accuracy, the number of simFSRs could be reduced significantly without incurring much loss of accuracy in classifying posture. For the top two algorithms, the RBF-Kernel SVM and the Bagged Decision Tree, the classification accuracy was within 1% between three and five sensors used, with sensitivity and specificity changing approximately 5% and 1%, respectively (Table 1). In this study, it was hypothesized that we could achieve above 95% classification accuracy using less than five sensors; using the SVM and DT algorithms, three sensors were identified as the minimum number needed to achieve 95% accuracy. Although the SVM and DT classified at high accuracies with a single sensor location, the standard deviation increased two-fold from three sensors highlighting a substantial increase in variability amongst the LOOCV results. Due to the high variability in classification accuracy associated with a single sensor, one sensor location is not robust enough for classification using multiple participants.

Although body-worn inertial technologies have demonstrated the ability to classify a variety of physical activities and postures [9,10], such technologies can be hindering during extended duration monitoring [18] and provide no information on plantar loading patterns. Previous studies have shown that instrumented shoe systems can classify various activities accurately with minimal disruption to the participant [10,11,13,16,18]. However, FSR-based insole technologies developed to date have coupled FSRs with inertial measurement units (IMUs) to achieve their high classification accuracy [16]. Of these, the most suitable system for the application proposed in this study is the 'SmartStep' developed by Edgar and colleagues [11,16]. Using a classification scheme based on SVMs, the SmartStep classified sitting, standing, walking, running, stair ascent/descent and cycling at a 95.2% average accuracy using a full feature set, and over 98% accuracy on an optimized sensor set [16]. Based on the outcomes of the SmartStep's optimized classification scheme, an accuracy of above 98% was identified as the lower bound for this work; a minimum of 98% accuracy in classification, identified as total correct predictions divided by total predictions, was also reinforced by our industry partner Kintec Footlabs Inc. This

classification accuracy was achieved with sensor combinations using three sensors or more. Several key differences exist between the classification scheme developed here and that of Sazonov and colleagues. Most importantly, using measurement magnitude values from FSRs in the classification schemes requires a time-consuming calibration procedure for each sensor making large scale commercial production of such systems prohibitive. Here we developed a classification scheme using on/off detection only which eliminates the need to calibrate each sensor. By optimizing the positioning of the FSRs in the insole, there is no longer a requirement for an IMU or bilateral data collection which reduces material costs and increase the battery life of the system. While insoles developed to date demonstrate the validity of shoe-based instrumented systems for differentiating postures, the results presented here show opportunities for further simplification of these sensor systems and the potential to transition to large-scale production by eliminating the need for sensor calibration.

II. System Advantages

Quantifying and linking prolonged weight bearing in the workplace and PF is not as immediate as a traumatic injury, such as a fall; therefore, the prevalence of work-related musculoskeletal disorders like PF are frequently underestimated from workers' compensation claims as many cases go unreported [25,26]. A comprehensive review of work related PF found insufficient quantitative evidence linking workplace exposure to the prevalence of PF and consequently identified an immediate need for a low-cost objective measurement tool which can accurately differentiate time spent in various postures at work [27]. Currently, commercial plantar pressure measurement systems such as Tekscan's F-Scan system or the Pedar system by Novel are far too costly for workplace deployment, costing over $20,000 CAD each. Inertial based activity trackers have been proven for posture detection [9,10] and more complex data collection [28], but are often too cumbersome for comfortable long-duration wear [18]. Existing shoe-based systems, although similar [11,16], are overly complex for this application. Through strategic sensor reduction, the classification scheme proposed in this work proves that it is possible to classify sitting, standing and walking at a 98% accuracy using on/off plantar force data at three discrete locations on the

plantar aspect of the foot. If translated to an electromechanical system, these results may provide the foundation for the deployment of such a system into the workplace, allowing for the extended postural tracking at work that is currently lacking.

III.   *Sensor Locations*

Previous work in instrumented insole development have selected sensor locations on the basis of perceived biomechanical importance and strength of contact with the supporting surface [11,12,14]. For example, Sazonov and colleagues [16] assumed five biomechanically important locations and then conducted a backward selection procedure of sensor locations to investigate the contribution of each sensor for posture/activity differentiation. Results of their work found that FSRs at the hallux, medial forefoot, and hindfoot center, were optimal and yielded a 98.1% accuracy when coupled with multiple IMUs in their classification scheme. In our comprehensive analysis of sensor locations, we similarly found the forefoot to be significant in differentiating activities. However, we also identified the medial and lateral midfoot as important activity classifiers. The top two sensor locations were in the medial and lateral midfoot, where most other insole technologies typically embed their electronics under a rigid insole arch eliminating these locations as possible sources of data.

The central forefoot and medial/lateral midfoot may provide the most meaningful data for this application for several reasons. First, the central forefoot is minimally recruited during sitting, constantly used for balance during standing, and cyclically loaded during walking, creating a large differential between the three postures to be classified in this work. The medial and lateral midfoot parallel this, making the combination convey a large amount of information regarding the posture with only three sensors required. Additionally, the medial midfoot, or Sensor 15 (Figure 1c) is on the boundary of the midfoot and the hindfoot making it possible that this sensor may pick up much of the information elicited by the hindfoot. The boundary position may be advantageous in this application because, although the heel has a strong signal due to its constant contact, it is challenging to differentiate sitting from standing

using this area alone (Figure 2b). The loading on the boundary may be intermittent, but the medial

longitudinal arch provides enough variability to differentiate the activities.

IV. *Strengths/limitations of work*

Findings presented in this work must be considered within the study limitations. First, a small sample

size was used, although this is similar to other works in this field [13,16,18,29] further work will be

required to establish the broad applicability of this classification scheme. Secondly, constructing

simulated FSRs from down sampled high spatial and temporal resolution data may not exactly duplicate

FSR performance. However, the simulated FSRs provided an opportunity to comprehensively analyze

sensor characteristics (position and number) from a single trial instead of constructing multiple prototypes

and conducting repeated subject trials. Finally, shoe type and model were not controlled, walking speed

was left up to the participant to select, and all foot shapes were included in the study design. Although

they introduced potential sources of variability, these choices provide ecological validity to the data set,

which ultimately aims to characterize the three postures in an uncontrolled environment, making it

advantageous to leave these factors unrestricted.

5. Conclusion

A current lack of reliable and cost-effective measurement tools for distinguishing postures at work

makes it difficult to link weight bearing at work to the onset of plantar fasciitis [27]. We classified

common workplace postures through unilateral plantar pressure data alone for the first time. Three

locations—the central forefoot and medial and lateral midfoot—were sufficient to classify sitting,

standing and walking through on/off sensor data with an accuracy of over 98%. This work will assist in

making insole-based measurement systems commercially feasible by reducing sensor costs and

eliminating the need for time consuming calibration.

6. Acknowledgements

7. Conflict of Interest Statement

Michael Ryan is a salaried employee of Kintec Footlabs Inc.

References

[1] Singh D, Angel J, Bentley G, Trevino SG. Fortnightly Review: Plantar Fasciitis. BMJ: British Medical Journal 1997;3157101:172-5.

[2] Liden B, Simmons M, Landsman AS. A Retrospective Analysis of 22 Patients Treated with Percutaneous Radiofrequency Nerve Ablation for Prolonged Moderate to Severe Heel Pain Associated with Plantar Fasciitis. The Journal of foot and ankle surgery 2009;486:642; 642,647; 647.

[3] Beeson P. Plantar fasciopathy: Revisiting the risk factors. Foot & Ankle Surgery (Elsevier Science) 2014;203:160-5.

[4] Anton D, Weeks D. Prevalence of work-related musculoskeletal symptoms among grocery workers. Int J Ind Ergonomics 2016;54:139-45.

[5] Werner RA, Gell N, Hartigan A, Wiggerman N. Risk Factors for Plantar Fasciitis Among Assembly Plant Workers. PM & R 2010;22:110; 110,116; 116.

[6] Parent-Thirion A, Vermeylen G, van Houten G, Lyly-Yrjänäinen M, Biletta I, Cabrita J. Fifth European Working Conditions Survey overview report . 2012;EF1182.

[7] Castillo-Retamal M, Hinckson EA. Measuring physical activity and sedentary behaviour at work: a review. Work (Reading, Mass.) 2011;404:345.

[8] Prince SA, Adamo KB, Hamel ME, Hardt J, Connor Gorber S, Tremblay M. A comparison of direct versus self-report measures for assessing physical activity in adults: a systematic review. The international journal of behavioral nutrition and physical activity 2008;51:56-.

[9] Kozey-Keadle S, Libertine A, Lyden K, Staudenmayer J, Freedson PS. Validation of wearable monitors for assessing sedentary behavior. Med Sci Sports Exerc 2011;438:1561.

[10] Klein DA, Levine E, Walsh BT, Sazonov ES. Validation of two novel monitoring devices to measure physical activity in healthy women. In: International Converence of the IEEE Engineering in Medicine and Biology Society; 2014. p. 1727-30.

[11] Edgar SR, Swyka T, Fulk G, Sazonov ES. Wearable shoe-based device for rehabilitation of stroke patients. In: ; 2010. p. 3772-5.

[12] Shu L, Hua T, Wang Y, Li Q, Feng DD, Tao X. In-Shoe Plantar Pressure Measurement and Analysis System Based on Fabric Pressure Sensing Array. IEEE Transactions on Information Technology in Biomedicine 2010;143:767-75.

[13] Archer CM, Lach J, Chen S, Abel MF, Bennett BC. Activity classification in users of ankle foot orthoses. Gait Posture 2014;391:111-7.

[14] Jacobs DA, Ferris DP. Evaluation of a Low-Cost Pneumatic Plantar Pressure Insole for Predicting Ground Contact Kinetics. Journal of applied biomechanics 2016;322:215.

[15] Hellstrom PAR, Åkerberg A, Ekström M, Folke M. Walking Intensity Estimation with a Portable Pedobarography System. Stud Health Technol Inform 2016;224:27.

[16] Sazonov ES, Fulk G, Hill J, Schutz Y, Browning R. Monitoring of Posture Allocations and Activities by a Shoe-Based Wearable Sensor. IEEE Transactions on Biomedical Engineering 2011;584:983-90.

[17] Howcroft J, Kofman J, Lemaire ED. Feature selection for elderly faller classification based on wearable sensors. Journal of Neuroengineering and Rehabilitation 2017;14.

[18] Moufawad el Achkar C, Lenoble-Hoskovec C, Paraschiv-Ionescu A, Major K, Büla C, Aminian K. Instrumented shoes for activity classification in the elderly. Gait Posture 2016;44:12-7.

[19] Gurney JK, Kersting UG, Rosenbaum D. Between-day reliability of repeated plantar pressure distribution measurements in a normal population. Gait Posture 2008;274:706-9.

[20] Cavanagh PR, Ulbrecht JS. Clinical plantar pressure measurement in diabetes: rationale and methodology. The Foot 1994;43:123-35.

[21] Price C, Parker D, Nester C. Validity and repeatability of three in-shoe pressure measurement systems. Gait Posture 2016;46:69-74.

[22] Uematsu A, Inoue K, Hobara H, Kobayashi H, Iwamoto Y, Hortobagyi T, Suzuki S. Preferred step frequency minimizes veering during natural human walking. Neurosci Lett 2011;5053:291-3.

[23] Stone M. Cross-Validatory Choice and Assessment of Statistical Predictions. Journal of the Royal Statistical Society.Series B (Methodological) 1974;362:111-47.

[24] Shao J. Linear Model Selection by Cross-Validation. Journal of the American Statistical Association 1993;88422:486-94.

[25] Major M, Vézina N. Analysis of worker strategies: A comprehensive understanding for the prevention of work related musculoskeletal disorders. Int J Ind Ergonomics 2015;48:149-57.

[26] Stock S, Nicolakakis N, Raïq H, Messing K, Lippel K, Turcot A. Underreporting work absences for nontraumatic work-related musculoskeletal disorders to workers' compensation: results of a 2007-2008 survey of the Québec working population. Am J Public Health 2014;1043:e94-e101.

[27] Waclawski ER, Beach J, Milne A, Yacyshyn E, Dryden DM. Systematic review: plantar fasciitis and prolonged weight bearing. Occupational Medicine 2015;652:97-106.

[28] Chuo Y, Marzencki M, Hung B, Jaggernauth C, Tavakolian K, Lin P, Kaminska B. Mechanically Flexible Wireless Multisensor Platform for Human Physical Activity and Vitals Monitoring. IEEE Transactions on Biomedical Circuits and Systems 2010;45:281-94.

[29] Sazonova N, Browning R, Sazonov E. Accurate Prediction of Energy Expenditure Using a Shoe-Based Activity Monitor. Med Sci Sports Exerc 2011;437:1312; 1312,1321; 1321.

Chapter 4.

Wearable Shoe-Based Device for Posture Differentiation at Work

4.1. Introduction

Development of an objective tool to quantify time spent WBR at work could help fill a longstanding gap in the literature establishing or refuting a causal link between prolonged WBR in the workplace and plantar fasciitis. Currently, subjective methods (e.g. self-reporting), although commonly used [113] are inconsistent [21,22] and prone to bias [118]. Conversely, current objective methods (e.g. inertial based activity trackers) may be uncomfortable for extended use due to form-factor, weight, and position on the body [121]. Additionally, inertial technologies have limited potential differentiating static postures [37,38]. Shoe-based wearables have been proven to circumvent these issues and reliably classify sitting, standing and walking [36,46,136], but are overly complex, costly, and not optimal for large scale deployments required for workplace monitoring [36,131,134,135]. To fill this void, the aim of this work was to develop a prototype design for a low-cost instrumented insole system capable of differentiating workplace postures (sitting, standing and walking) using established plantar pressure patterns, metrics, and machine learning protocols.

Differentiating sitting, standing and walking based on the pedobarographic characteristics associated with each posture was shown to be possible (See Chapter 2: Study 1). Both WBR from non-WBR, and static WBR from dynamic WBR could be distinguished only from the pedobarographic characteristics. Our previous machine learning analysis of down-sampled data defined the lower bound of what was sufficient plantar pressure information to classify these three postures, verifying the use of on/off signals from force sensitive resistors (FSRs) (See Chapter 3: Study 2). Unlike previous works that assumed sensor placements and then applied machine learning algorithms, we considered sensor placement across the entire foot and then assessed the effects of position, data characteristics, machine learning algorithms and settings on the accuracy of classifying three common workplace postures (sitting, standing and walking). It was concluded that three simulated FSR sensors, located at the central forefoot, and the medial and lateral midfoot, could classify the three postures at over 98% accuracy. Five

sensors, located around the medial and lateral midfoot and the central/lateral forefoot, classified the postures at over 99% accuracy.

With a theoretical system design in place, the objective of this work was to develop a prototype insole system with off-the-shelf components capable of collecting plantar force data similar to the simFSR system (Chapter 3). Additionally, the ability of the insole to differentiate sitting, standing and walking using sensor locations determined to be physiologically relevant for these tasks was assessed qualitatively. To be compatible with a range of sensitive workplace applications (e.g. manufacturing, surgery, etc.) all electronics must be onboard and no Wi-Fi or Bluetooth connectivity enabled. This proof-of-concept prototype explores the potential to characterize workplace activities with a low cost, FSR based system. This work lays the foundation for further prototype refinement, more advanced posture characterization (e.g. differentiating fidgeting from quiet standing), as well as pilot testing in a worker population.

4.2. Methods

4.2.1. Technology Development

Design Criteria

To be suitable for workplace applications differentiating sitting, standing and walking the insole technology must meet critical design criteria:

Measurement Accuracy:

- **Minimum of 3Hz Recording Rate**. A slow stride frequency of 1.41Hz, indicative of a slow stride frequency [160] results in minimum capture rate of 3Hz by Nyquist Theory.

- **99% accuracy in classification (i.e. total correct predicted postures/total predicted postures)**, which would result in under a half hour of incorrect postures identified over a standard 40-hour work week; a 40-hour work week results in 2400 minutes of classified data, therefore if 1% was misclassified, 24 minutes/2400 minutes would indicate incorrect postures. This level of accuracy parallels the

SmartStep system's optimized classification accuracy [36] and was further reinforced by our industry partner, Kintec Footlabs Inc.

Form Factor:

- Insole system must fit within any standard footwear.

- Data acquisition unit must attach to lower-limb in a discreet fashion.

- Plantar biomechanics cannot be affected by system (e.g. no stiff arch to hide electronics).

Data Management:

- **Data cannot be transmitted wirelessly (e.g. Wi-Fi or Bluetooth)**; as this technology intends to deploy in a hospital environment, it may be near medical devices with sensitivities to wireless interference [161]. To avoid any complications and liabilities associated with device proximity, no wireless protocols will be employed.

- Minimum undisturbed data acquisition time of 12 hours; this will be affected by both battery life and memory size. Memory is dictated by on-board storage capacity as online data storage (e.g. cloud-based) requires wireless capabilities which are ruled out for this application.

- Data must be easily extracted from device.

Cost:

- Total system cost, including all materials and manufacturing costs, must be less than $100 CAD.

System Description

The physical system developed from this work is known as the '*Posture Differentiating Instrumented Insole*', or the PDI[2] for short. The PDI[2] data acquisition unit (Figure 11a-b) is a standalone system capable of reading outputs from a limited number of FSRs (five or less with the current design), and storing the data within an on-board microSD card. The system is

capable of recording at 19Hz for more than 72 hours with the current battery scheme, although modifications to battery size/type could increase this as needed to suit a variety of study designs. Additionally, the PDI^2 is relatively lightweight, with the data acquisition unit (excluding the insole and embedded sensors) weighing only 65 grams. The data acquisition unit of the PDI^2 can be attached to the participant's shoe via a 3D printed dongle, to ensure the unit does not impact the participant's day-to-day movement in any way. The size of the current PDI^2 data acquisition unit (without the battery) is approximately 6cm x 4cm x 2cm (L x W x H), though this is expected to decrease in subsequent prototypes with the move to a printed circuit board (PCB). The electrical components comprising the data acquisition unit cost approximately $40 CAD. Each FSR used will cost an additional $9 CAD. As the PDI^2 was developed as a one-off prototype, manufacturing costs for production runs have not yet been established.

(a) (b)
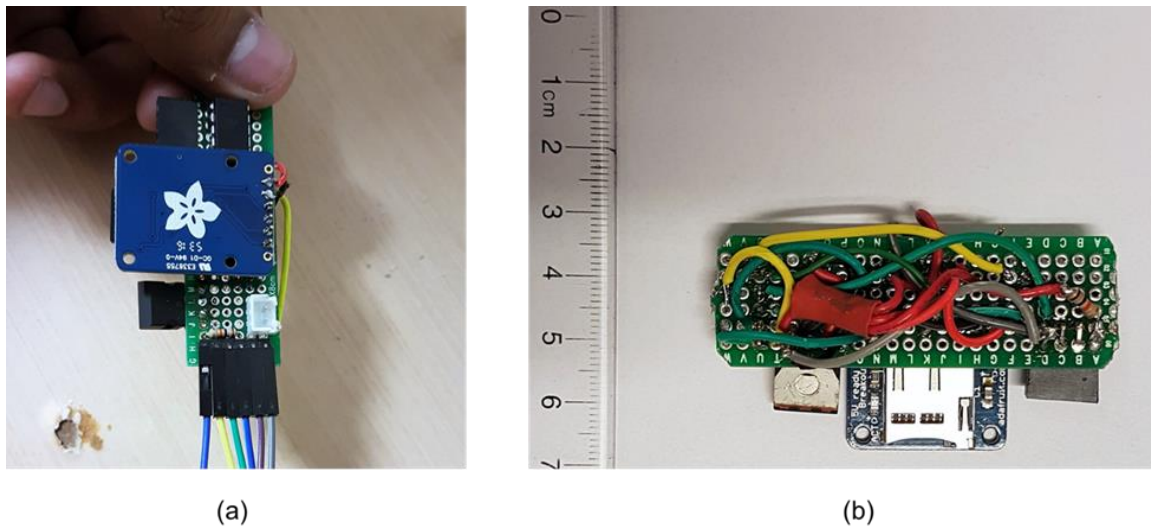
Figure 11   The Posture Differentiating Instrumented Insole Prototype (a) Top view with sensor leads attached (b) Bottom view with no sensor leads present.

Hardware

The complete PDI^2 prototype consists of six major hardware components: a flat insole (thickness = 4mm), one to five force sensitive resistors, a microcontroller, a microSD board & card, a protoboard, and a battery (Table 7).

Table 7   Components of the Posture Differentiating Instrumented Insole

Component	Purpose	Description
Insole (Figure 12)	- Sized to fit in the participants shoe minimizing sensor motion - Houses embedded FSR sensors	The insole is a series of two flat polymer pieces which sandwich FSR sensors. The insole is meant to hide the presence of any sensors to the user, which is particularly challenging given the sensitive nature of the plantar side of the foot. As this is a data acquisition tool and not a custom orthotic meant to treat PF, no contour will be built into the insole to avoid influencing the natural gait of participants.
FSRs (Figure 13)	- Capture data relating to each posture	FSRs are resistors which modify their resistive value when axially loaded in compression. FSRs used in this prototype are *Interlink 402 FSR sensors*, which measure 0.5" in diameter. Sensors are not initially calibrated for rendering force, but are reported to read forces between 0-100N (0-20lbs).
Microcontroller	- Facilitates the read/write channel between the FSRs and the microSD card	A small computing module on a single integrated circuit, the microcontroller acts as the control module for the system, instructing each of the subsystems on their operation.
MicroSD board & card	- Board: Connects the microSD card to the data acquisition unit - Card: Stores information measured by the FSRs	The MicroSD components permit the storage of data within the data acquisition unit, allowing the system to run in isolation. The microSD board & card are the most power-consuming components in the system.
Protoboard	- Backbone of the data acquisition unit; all subsystems are connected via the protoboard	A construction base for the electronic components, the protoboard is the backbone of prototyped system but will be replaced with a custom printed circuit board once the design is finalized.
Battery (Figure 14)	- Power the PDI^2 prototype over an extended duration (~12hrs or one workday at a minimum)	Current battery used in the PDI^2 prototype is a 2,000 mAh Lithium Ion weighing 34g and measuring 6cm x 3.6cm x 0.7cm. Battery life and power requirements were determined assuming peak load of all components; real energy usage will be evaluated in the first prototype and modified in future iterations to determine the smallest cell that is able to meet the 12 hours of continuous run time requirement.
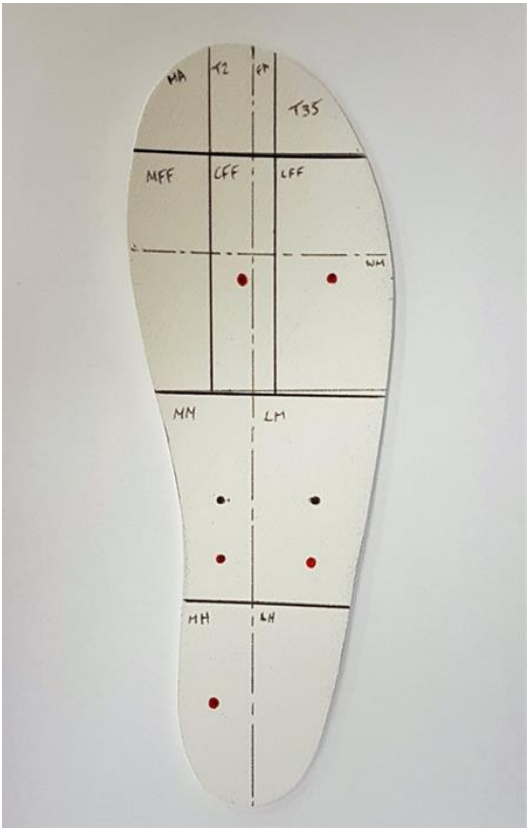
Figure 12   **Representative insole used in the Posture Differentiating Instrumented Insole**
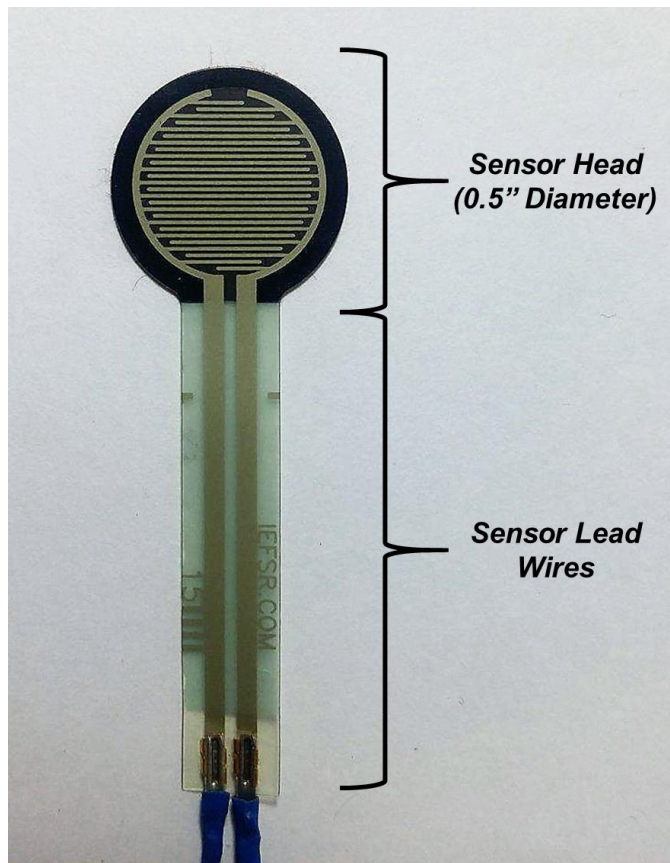
Figure 13   Representative Force Sensitive Resistor used in the Posture Differentiating Instrumented Insole
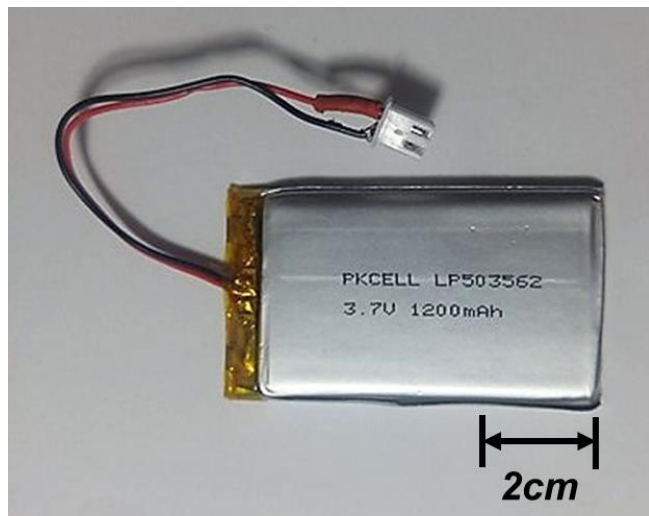
Figure 14   Representative battery used in the Posture Differentiating Instrumented Insole

4.2.2. Pilot Testing

Initial proof-of-concept testing of the system was conducted on a single participant during a simulation of the experimental protocol from Study 1. The trial consisted of six, one-minute activity blocks where each posture was demonstrated twice – sitting, standing, walking, sitting, standing and walking – totaling six minutes of data collection. The PDI^2 prototype was set up to collect data from five FSRs, located strategically at points of the foot identified using preliminary results from Study 2 (Figure 15). Because the simFSR classification scheme (Chapter 3) was conducted in parallel to the development of the PDI^2 system, sensor locations used in the initial testing were based on a preliminary set of results and not on the finalized locations determined as outcomes from the simFSR classification scheme. Therefore, two sensor locations differed between the simFSR classification scheme and the PDI^2 prototype tested; sensor location 11 and 19 were included instead of locations 9 and 12, while all other locations were matched (Figure 16a-b). Comparison of the simFSR system to the PDI^2 prototype was conducted on the three sensor locations common to both systems (sensors 8, 15 and 18, Figure 16a-b). The PDI^2 sampled at 15Hz during the pilot testing, identical to the down sampled data compiled in the simulated FSR analysis.
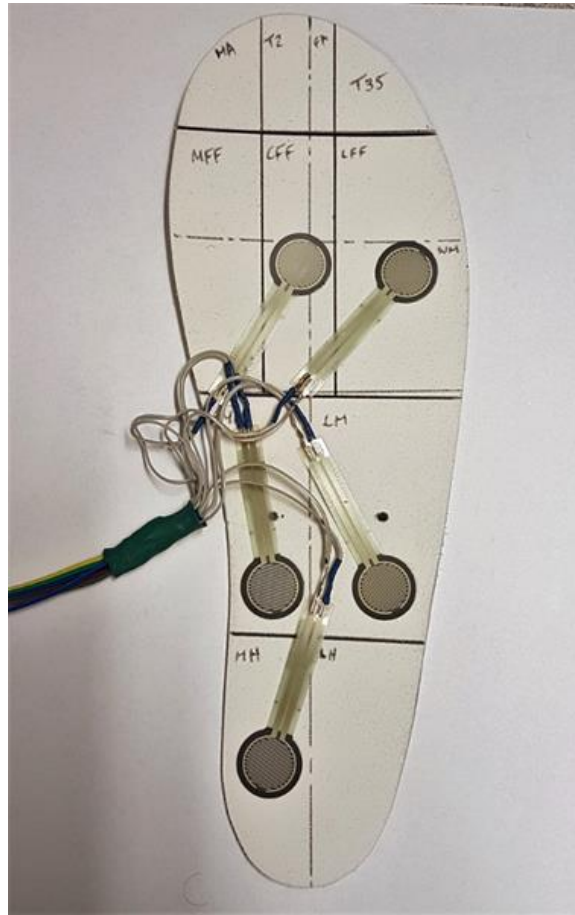
Figure 15 **Posture Differentiating Instrumented Insole system with five FSR sensors localized for testing**
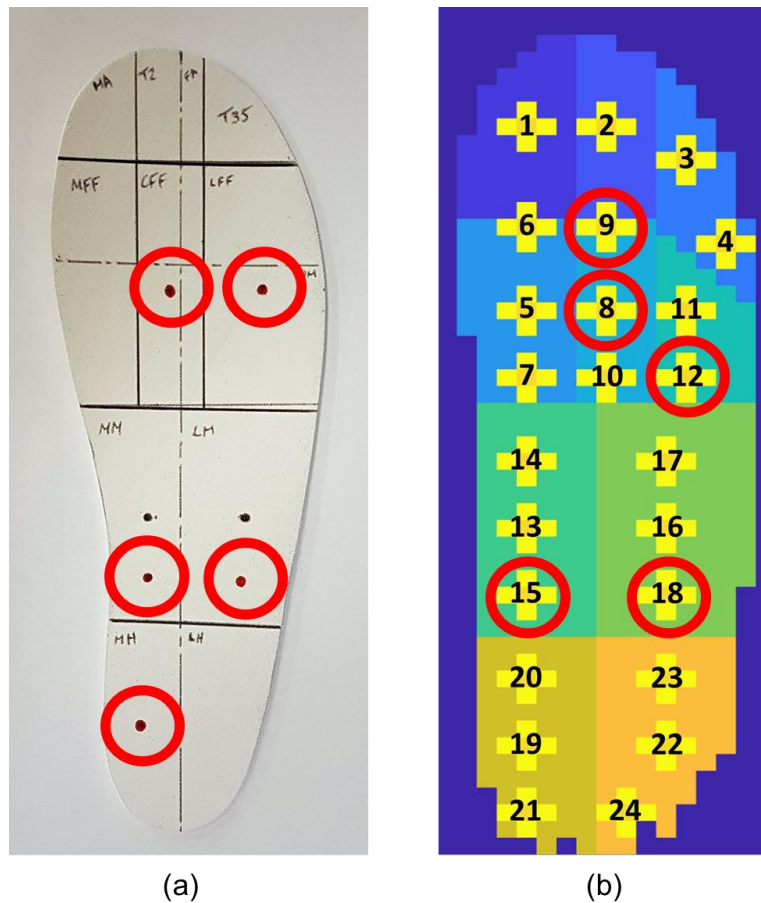
Figure 16 **Comparison of (a) locations used for initial testing of the Posture Differentiating Instrumented Insole and (b) top five sensor locations specified from machine learning outputs. Note that sensor 11 and 19 were used in (a), while sensors 9 and 12 was used in (b).**

4.2.3. Conversion of Raw Data to Binary

Similar to the conversion of the simFSR data into on/off characteristics (chapter 3), the raw FSR data obtained using the PDI^2 was also converted to on/off characteristics. One challenge this presents is identifying the raw threshold value differentiating 'on' from 'off'. Because the PDI^2 system is still in its infancy, a formal analysis and subsequent fine-tuning of this on/off boundary has not been conducted. To compare the initial testing of the PDI^2 system to that of the simFSR system, an on/off boundary value of 50 raw units was selected; anything below 50 raw units represents the bottom 5% of the FSRs range and it is believed that a boundary of 50 units would primarily eliminate noise while maintaining the integrity of the data. In contrast, the on/off boundary used by the F-Scan system, and by extension the simFSR system, had a default noise threshold of 1.2% of the saturation pressure determined during calibration; the saturation

pressure of the F-Scan varies with participant mass, but the system has an upper pressure limit of 825 kPa (125 PSI). Although a lower value percentage-wise, the F-Scan system has a much larger pressure range than the PDI[2] system and therefore 1.2% of the F-Scan data corresponds to a higher pressure reading than 5% of the PDI[2] data. As a result, the noise threshold used for preliminary analysis of the PDI[2] system should be considered conservative.

4.2.4. Comparison of simFSR and FSR data

It was previously determined that plantar pressure data collected using the F-Scan system could be converted to on/off characteristics and subsequently used to classify sitting, standing and walking at high accuracies (Chapter 3). If the data collected using the PDI[2] system resembles that of the simFSR system, a classification scheme using the PDI[2] system should also be able to classify sitting, standing and walking at high accuracies. Because only three of the five sensor locations were common to both systems (central forefoot, medial midfoot and lateral midfoot), the analysis is limited to comparing those three sensors. Additionally, the exemplary data from the simFSR system was taken from a single participant with a mass of 64kg and a foot posture index of +6 (pronated). In contrast, the exemplary trial using the PDI[2] was conducted by a single participant with a mass of 98kg and a foot posture index of -3 (supinated). Because the data was captured at different times using different participants, a qualitative comparison of the data characteristics was used to assess the functionality of prototype system compared to the simFSR system.

4.3. Results

4.3.1. Data Collection

The FSR sensors were not initially calibrated; therefore, a raw value of 0 to 1023 was extracted from all five FSRs individually during each frame of the collection phase. For reference, the FSR response curve is non-linear; variations in force are represented as large changes close to zero, and smaller changes as values draw closer to sensor saturation, found at a raw value of 1023 (~100N). While no calibration was conducted, a benchtop test applying moderate pressure axially through a finger was carried out to verify that all five FSRs were responding to load. All the FSRs reported values between 950-970 raw units as a result of finger contact. Exemplary data for sitting (Table 8), standing (Table 9), and walking (Table 10) over one second

(equivalent to 15 frames) can be found below. Exemplary data for a full six-minute trial (Figure 17) can also be found below.

During sitting (Table 8), no forces were detected in the medial midfoot or lateral forefoot. Additionally, the central forefoot was loaded less than the medial hindfoot and lateral midfoot, showcasing that the majority of load during sitting is in the posterior of the foot. During standing (Table 9), loading was detected across all five sensors consistently, with the highest raw values being recorded in the central forefoot and the medial hindfoot. During walking (Table 10), a clear differential between swing and stance was seen, even within the one second exemplary data set. Additionally, the relative raw values demonstrate visible variations between heel-strike and toe-off. The medial hindfoot is loaded the highest first, followed by a transition into higher midfoot values concluding with highest values in the central and lateral forefoot sensors.

Table 8 **Exemplary sitting data collected using the Posture Differentiating Instrumented Insole; only one second of data is shown.**

	SITTING				
Time [s]	Medial Midfoot - Sensor 15	Central Forefoot - Sensor 8	Medial Hindfoot - Sensor 19	Lateral Midfoot - Sensor 11	Lateral Forefoot - Sensor 18
0.07	0	407	886	596	0
0.13	0	413	887	602	0
0.20	0	406	889	607	0
0.27	0	392	890	609	0
0.33	0	369	892	597	0
0.40	0	371	893	597	0
0.47	0	376	893	599	0
0.53	0	386	893	606	0
0.60	0	388	893	607	0
0.67	0	390	893	606	0
0.73	0	389	894	603	0
0.80	0	389	894	606	0
0.87	0	391	894	607	0
0.93	0	392	894	607	0
1.00	0	388	894	604	0

Table 9 Exemplary standing data collected using the Posture Differentiating Instrumented Insole; only one second of data is shown.

Time [s]	Medial Midfoot - Sensor 15	Central Forefoot - Sensor 8	Medial Hindfoot - Sensor 19	Lateral Midfoot - Sensor 11	Lateral Forefoot - Sensor 18
STANDING					
0.07	653	889	937	891	765
0.13	680	893	923	887	784
0.20	684	896	923	890	799
0.27	714	901	919	888	809
0.33	720	908	900	889	832
0.40	717	921	861	888	856
0.47	676	930	860	888	863
0.53	689	932	867	891	863
0.60	710	934	877	892	856
0.67	719	933	891	891	837
0.73	723	929	900	890	816
0.80	730	926	910	889	818
0.87	743	926	916	889	827
0.93	752	927	919	890	824
1.00	746	925	918	890	822

Table 10 Exemplary walking data collected using the Posture Differentiating Instrumented Insole; only one second of data is shown.

Time [s]	Medial Midfoot - Sensor 15	Central Forefoot - Sensor 8	Medial Hindfoot - Sensor 19	Lateral Midfoot - Sensor 11	Lateral Forefoot - Sensor 18
WALKING					
0.07	0	441	0	0	0
0.13	0	0	0	0	0
0.20	0	139	0	0	0
0.27	0	372	0	0	0
0.33	0	479	826	554	0
0.40	208	702	988	948	218
0.47	844	904	985	968	867
0.53	863	953	958	959	932
0.60	834	969	926	952	961
0.67	626	982	726	893	978
0.73	0	990	439	410	956
0.80	0	869	0	0	0
0.87	0	0	0	0	0
0.93	0	0	0	0	0
1.00	0	85	0	0	0

When examined over a full six-minute trial (Figure 17), it is clear qualitatively that the three postures are distinct even when observing the raw, uncalibrated FSR data. During sitting, the highest loading values were in the hindfoot (Figure 17e). Additionally, both the central and lateral forefoot (Figure 17a-b) displayed consistent loading though to a lesser extent when compared to the hindfoot. The midfoot (Figure 17c-d) was inactive during sitting. Less noise was present in the raw signal during standing when compared to sitting. Standing loads were consistent amongst all five sensors presented, with the hindfoot (Figure 17e) and central/lateral forefoot (Figure 17a-b) demonstrating more pressure than the medial/lateral midfoot (Figure 17c-d). Walking displayed the highest loads amongst the three postures across all five regions shown. Additionally, the temporal characteristics of walking were distinguishable. On the whole, the midfoot sensors (Figure 17c-d) demonstrated the greatest contrasts between the three postures.
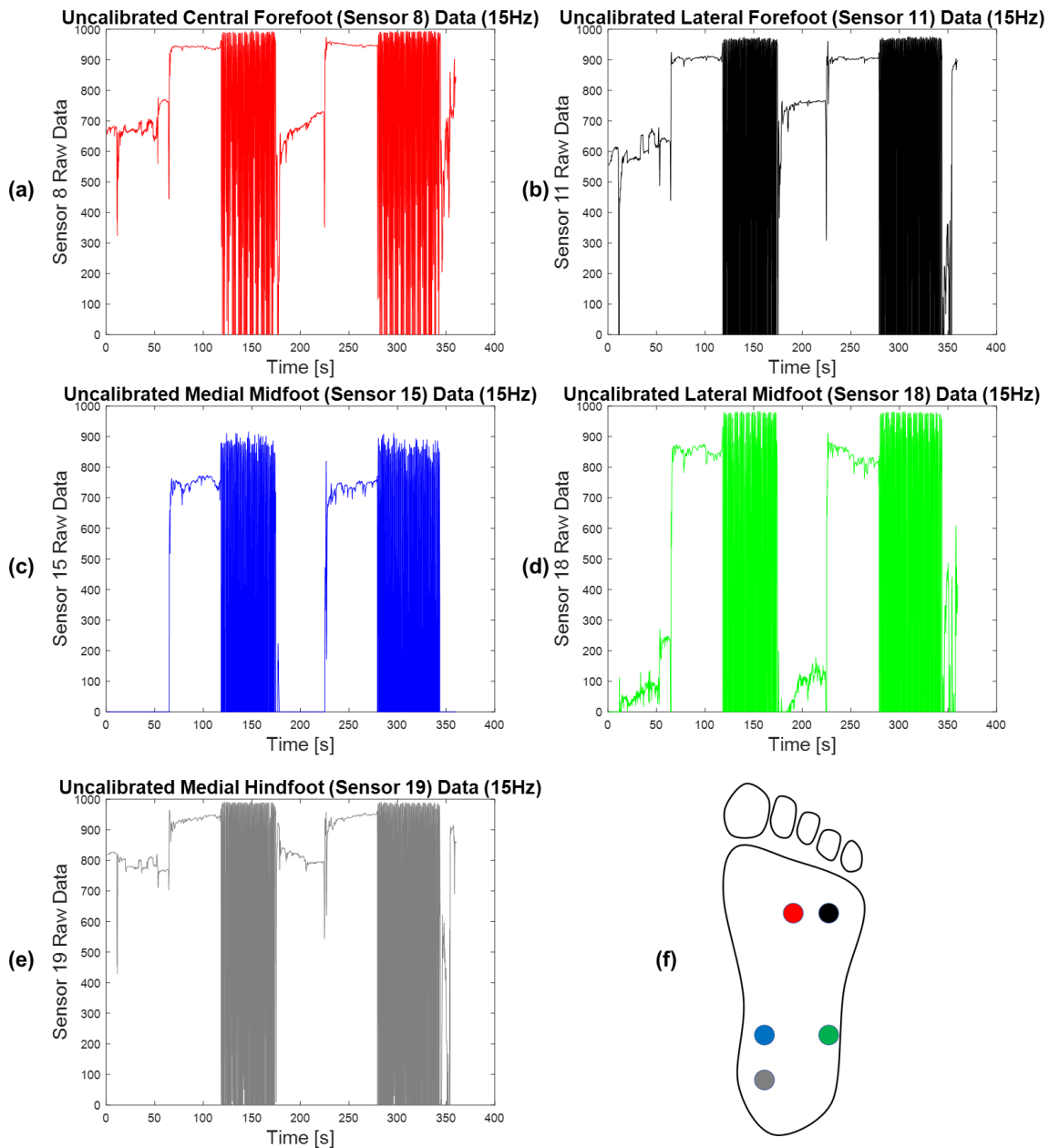
Figure 17 **Exemplary raw data collected using the Posture Differentiating Instrumented Insole; values range from 0-1023 and represent the non-linear force response of five FSRs. Six minutes of data is shown collected at five different locations: (a) the central forefoot, (b) lateral forefoot, (c) medial midfoot, (d) lateral midfoot) and (e) medial hindfoot. Order of activities was Sitting-Standing-Walking-Sitting-Standing-Walking. Coloured curves indicate sensors common to both the simFSR system final outcomes (chapter 3) and the PDI² initial prototype. Black and grey curves denote sensors used in the PDI² initial prototype but not in the final outcomes of the simFSR system. (f) provides an approximate location breakdown of the five sensors showcased with colours corresponding to the associated curves. Foot outline and sensor size are not-to-scale.**

4.3.2. Comparison of simFSR system to PDI^2 system

By converting the raw data collected with the PDI^2 system (Figure 17) to on/off characteristics using an on/off boundary of 50 raw units, an initial comparison can be made between the simFSR system and the PDI^2 system (Figure 18). Of the three sensors compared, the central forefoot (sensor 8, Figure 16b) demonstrated the most variability between the two systems (Figure 18a-b). During both instances sitting, the simFSR system sensor at the central forefoot (Figure 18a) was completely off whereas it was consistently on at the same location when using the PDI^2 system (Figure 18b). The medial and lateral midfoot (sensors 15 and 18, Figure 16b) showed substantial agreement when comparing the simFSR system to the PDI^2 system (Figure 18c-f). Sitting was generally inactive ('off') in the medial midfoot and active ('on') in the lateral midfoot using both systems. Standing had constant activation in both systems across the medial and lateral midfoot sensors while the temporal characteristic of walking was again captured using both systems at both midfoot locations.
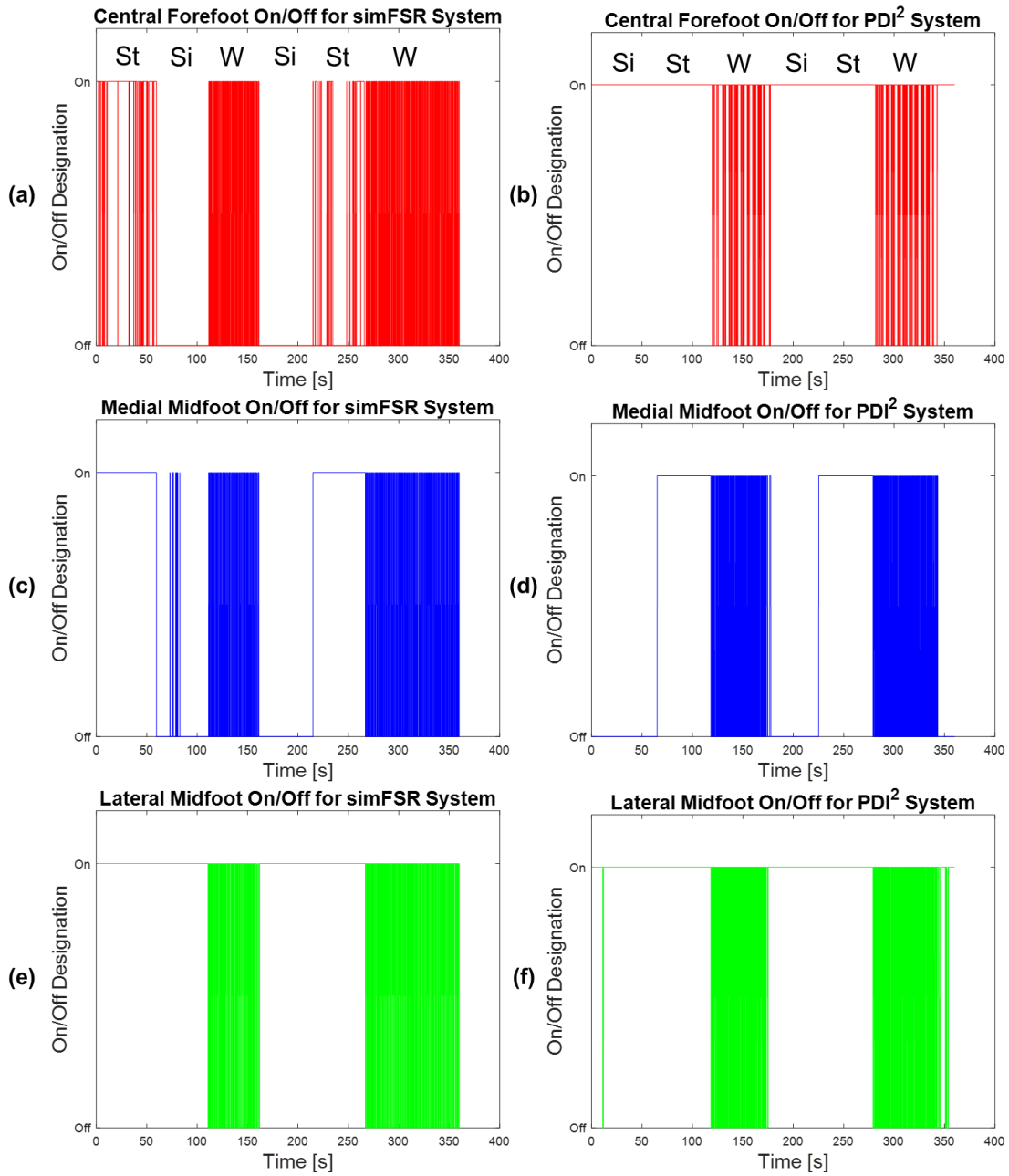
Figure 18   Exemplary on/off characteristics from the simFSR system (a,c,e) and the PDI^2 system (b,d,f). Six minutes of data was collected at three different locations: (a,b) central forefoot, (b,d) medial midfoot, and (e,f) lateral midfoot. Order of activities is showcased on the top of plots (a) and (b); note that Si,St and W represent sitting, standing and walking, respectively.

4.4. Discussion

4.4.1. Data Characteristics

The lack of loading in the medial midfoot during sitting may be due to the medial longitudinal arch, which could elevate the plantar aspect of the foot in that location enough to unload the sensor during sitting. The lack of loading in the lateral forefoot was unexpected, as the lateral forefoot is adjacent to the central forefoot, which recorded a value consistently during sitting. One possibility is that this trial is only representative of a single participant, and a combination of foot shape, shoe type, and personal plantar loading pattern could aggregate to result in the lack of loading witnessed. During standing (Table 9), loading was collected across all five of the sensors consistently. This could be subject specific as only one participant was tested, but all uncalibrated values during standing across the five sensor locations were within 300 raw values of each other (650-950), demonstrating that no sensor was damaged or completely inactive during the trial. Sensor-to-sensor variability could also contribute to the variations. During walking (Table 10), a clear differential between swing and stance was seen, even within the one second exemplary data set. The ability for low-cost sensors to provide feedback with resolution capable of segmenting several points within the stance phase of gait is impressive, and demonstrates the potential for these sensors to be used moving forward in subsequent prototypes.

When considering the characteristics of the full six-minute trial (Figure 17), the three postures (sitting, standing and walking) can be qualitatively distinguished. The greatest loads during sitting were in the hindfoot, which parallels outcomes from the characterization study (Chapter 2). The central and lateral forefoot show less loading when compared to the hindfoot, which is expected as the forefoot is minimally recruited during sitting as balance is not a concern. The midfoot was inactive during sitting which suggests that in this participant the medial and lateral longitudinal arches reduced sensor contact. This may be because the participant trialed in Figure 17 had a supinated foot posture index. The lateral midfoot is more actively engaged than the medial midfoot suggesting a supinated foot may be causing the observed loading (Figure 17c-d). Because the midfoot is loaded intermittently due to the medial and lateral longitudinal arches, the differential between the three postures increased suggesting it may delineate the postures better than locations loaded consistently throughout the three postures, such as the hindfoot and forefoot. When using a calibrated system, such as the F-Scan, consistently loaded

locations such as the hindfoot, medial forefoot and hallux are advantageous as they display the most consistent signal and subsequently can be used to differentiate the postures based on pressure magnitude. If magnitude is removed and raw data is observed (Figure 17), regions of inconsistent contact prove to be of more use when distinguishing the postures. However, these are preliminary conclusions based on a single trial. Further testing is required to draw more generalizable conclusions.

4.4.2. Comparing simFSR system to PDI^2 system

The central forefoot sensor demonstrated that greatest variability between the simFSR and the PDI^2 systems. Although this could be due to subject-specific loading, the most probable reason for this deviation is likely rooted in the different on/off boundary values used for both systems; because the PDI^2 system used a lower threshold for what constituted 'on', the sensor was more active even during sitting where the forefoot is not expected to be as engaged. The low on/off threshold likely also contributed to the consistent loading during standing using the PDI^2 system as when compared with the simFSR system. Walking was consistent between the two systems at the central forefoot location as both systems captured the temporal nature even when only analyzing on/off characteristics.

The medial and lateral midfoot showed better agreement when comparing the simFSR system to the PDI^2 system (Figure 18c-f) than the central forefoot sensor. The agreement between the two midfoot sensors using both the simFSR system and the PDI^2 system suggests that given that the simFSR system was used to construct a classification scheme able to classify the three postures as high accuracy, the PDI^2 system should be able to do the same if an appropriate classification scheme was developed using data from more participants.

On the whole, the PDI^2 system demonstrated the potential to distinguish between sitting, standing and walking using both uncalibrated data (Table 8-Table 10 and Figure 17) and on/off characteristics (Figure 18b,d,e). Although the initial testing regime presents data of only one participant, the results showcase the potential of the PDI^2 system to gather data of similar character to the simFSR system. Further testing using more participants is warranted and a formal testing regime similar to the one presented in chapter 2 is advised. Additionally, further testing would also allow for the development of a classification scheme similar to previous work presented in this thesis (chapter 3), ultimately concluding if the novel system can utilize machine

learning to classify sitting, standing and walking at high accuracies using only on/off
characteristics.

.

Chapter 5.

Contributions & Conclusions

5.1. Contribution Overview

This thesis was motivated by the need to improve current methods for quantifying behaviors at work. The studies presented here represent a systematic analysis of the physiology of plantar loading during workplace postures, the application of machine learning to classify workplace postures, the identification of simulated sensor locations that are most likely to be able to differentiate these postures and finally, the development of an insole prototype with sensors positioned using the insights gained from the first two studies.

The first study focused on substantiating the claim that plantar pressure is a viable means of characterizing common workplace postures by identifying the critical biomechanical features specific to each posture. Laboratory experiments were conducted to characterize the pedobarographic patterns specific to common workplace postures: walking (dynamic WBR), standing (static WBR) and sitting (static non-WBR). Although a number of studies have compared characteristics or changes of these three postures in various populations [36,133,163-169], to the authors' knowledge, no previous studies have investigated which pedobarographic characteristics best distinguish the postures in a healthy population. Additionally, much of the current literature restricts various subject-specific characteristics (e.g. shoe type, walking speed) which may compromise the ecological validity of their results. Results suggest that it is possible to differentiate both WBR from non-WBR postures and static from dynamic behaviours through plantar pressure. In addition, ten foot region/measurement parameter combinations were found to differentiate all three postures concurrently.

The second study aimed to utilize machine learning to isolate specific regions of the foot with the best potential to differentiate workplace postures. Data collected in the first study was resampled from 960 sensors providing calibrated pressure data at 75Hz (i.e. a lab-grade system) to 24 sensors providing on/off data at 15Hz (simulating a low-cost FSR-based insole system). With the validation of plantar pressure as a differentiation tool completed in Study 1, Study 2 sought to identify the lower limit of necessary information needed to classify the three postures. Five different variables—window length, overlap and output metric, feature selection

method, and machine learning algorithm used—were manipulated to first identify the optimal method to employ machine learning for this application. Following the implementation refinement, the number of simulated sensors present was tested using ranked sensor locations; the top ten sensor locations were tested using five machine learning algorithms, followed by the top nine, and so on, until the single sensor ranked as carrying the most information about the postures was tested. Results suggest that five sensors can classify the postures correctly over 99% of the time, while three strategically placed sensors can classify the postures correctly over 98% of the time. Of the top five sensors chosen, three (central forefoot, lateral forefoot and lateral midfoot) align with regions that were found to differentiate all three postures simultaneously in Study 1. Of the top three sensors chosen, the central forefoot and lateral midfoot regions were also identified as critical in Study 1, but the medial midfoot (Sensor 15, Figure 16) was not. The discrepancy here may be associated with the fact that Study 1 used data across the entire medial midfoot, whereas Study 2 used the posterior region of the medial midfoot to assess on/off characteristics of Sensor 15. Because the posterior region of the medial midfoot was used and subsequently selected as critical using the machine learning algorithm, it can be postulated that the posterior part of this mask may be more like the medial heel, which was found to simultaneously differentiate the postures in Study 1.

A novel *Posture Differentiating Instrumented Insole* (PDI^2) was developed as a first-generation prototype in the path towards a deployable tool for quantifying sedentary behaviours at work. This work sought to initiate the development of a new, low-cost deployable technology, and a subsequent new line of research, using the PDI^2 system to quantify sedentary behaviors at work. The PDI^2 system was developed using off-the-shelf components in an attempt to minimize the system cost while collecting the minimum amount of data needed to classify the three postures. Although similar instrumented shoe-based systems have been used previously for posture classification [36,131,134,135,137,148], the PDI^2 concept system has been specifically developed for this application, costs less, and provides longer collection periods by minimizing the amount of data needed. Further work is needed to develop and implement the machine learning classification algorithms suited for this system.

5.2. Future Research Directions

5.2.1. Insole Development

As the current prototype of the PDI^2 system is the first generation for this application, several developmental modifications may be considered moving forward in order to distinguish the system from the *SmartStep* [36,137,170], the nearest competitor system in the space. The suggested modifications include:

1. **Protoboard Miniaturization**: To decrease size and reduce wired connection wear, progression of the system to a printed circuit board is ideal.

2. **FSR Sensor Selection**: The current FSR sensors used in the PDI^2 system (*Interlink 402 FSRs*) were selected based on previous experiences working with the sensors within our lab group. The size of these sensors (0.5" diameter) may be beneficial for keeping sensor locations robust, but smaller sensors could be considered if sensor saturation could be avoided.

3. **Embedding of Sensors within Insole**: Currently, sensors and associated leads are sandwiched between two polymer insoles to 'hide' the electronics and minimize any user impact. Custom manufacturing of sensors in an insole shaped layer could result in a packaged solution with a single point of connection that reduces the opportunity for wire breakage and discomfort due to the wired connections. Alternatively, optimization of wiring schematics based on outcomes from Study 2 coupled with slot milling could potentially hide sensor wires and tails.

4. **Packaging of Electronics**: To make the system 'useable' in a worker population, a case structure or dongle must be developed to comfortably hide the PDI^2 data acquisition unit. An effective case design would not only shield the unit from accidental adjustment but could also minimize user avoidance due to appearance or bulk.

5. **Insole Sizing**: To keep system cost down, it is ideal to not custom fit the PDI^2 system to each user; resultantly, a sizing regime suitable to most people is needed. As insole size changes however, sensor locations will also need to change. Solving this problem could be done through a modular insole, or a sliding element. A further

sensitivity study of sensor locations would also provide clarity on the need for precise sensor positioning for each shoe size.

5.2.2. Subject-Specific Fidgeting

This work focused solely on characterizing steady-state postures which was necessary to facilitate the start of this research stream. However, the author acknowledges that this is not wholly representative of a typical person over an extended duration. Each person adjusts their body to achieve comfort when maintaining a posture over an extended period. This could include things like crossing their legs or shifting weight to one foot while offloading the other. Review of literature and investigation with the PDI^2 system must address this in the future to ensure accurate classification.

5.2.3. Posture Differentiation at Work

Tracking sedentary behaviours at work is challenging; questionnaires are not sufficiently accurate [21,22], commercial activity trackers show limited potential [37,38,171], and other methods such as video monitoring are resource intensive. The main goal for this research was to establish sufficient evidence for a novel insole technology to be designed with the intention of eventually deploying it into the workplace. Now that a prototype of the system physically exists, planning can begin to structure what the eventual deployment of the system into a worker population might look like. Once the system is deployed, various reliability and validation studies should be conducted to evaluate measurement repeatability within a real-world population.

5.2.4. Future Clinical Implications

The overarching goal of this work is to establish or refute any associated link between WBR at work and PF, thus resolving the current ambiguities [27]. Upon execution of the previously listed studies, a longitudinal observational study of workers in at-risk professions and the association with PF could refute or support any link between WBR and PF.

5.3. Limitations of the Research

Although this work attempted to address key limitations within each study specifically, several key limitations still exist. During data collection, a relatively small sample size was used, and although this is similar to other works in posture characterization [166,172,173] and posture classification through machine learning [36,131,146,148], more data with larger variations in subject characteristics could result in more robust outcomes. Further, by only using one participant for analysis of the PDI^2 system, results must be interpreted hesitantly until further formal testing can be conducted. Additionally, all postures analyzed were steady-state and did not contain any fidgeting or transitions; this must be considered when interpreting this work and should be addressed in future works. Lastly, the data collected in this study was collected with only one in-shoe pressure measurement system. Replication studies using other in-shoe pressure measurement systems, specifically the Pedar system by Novel, which is arguably the most-used in-shoe system, could further validate these results.

5.4. Significance

The studies conducted in this thesis lay the groundwork for an evidence-based low-cost instrumented insole system. The most significant outcomes from this work are:

1. Identifying various biomechanical characteristics which differ between the three workplace postures and conveying on a fundamental level that using an insole as a behaviour tracker is appropriate.

2. Identifying the minimal number and configuration of FSRs needed to classify the postures by computationally simulating a low-cost instrumented insole system, which proved that sitting, standing, and walking could be distinguished at high accuracy using as little as three sensors without any inertial measurement units or calibration of the FSRs.

3. Developing the first generation PDI^2 system prototype. This work took the idea of a low-cost instrument insole system and produced an evidence-based prototype that has the potential to classify common workplace postures at high accuracies.

Taken together these results show that plantar pressure based metrics reduced to on/off contact data have the potential to classify workplace postures in a highly accurate cost-effective way. This work is novel in its comprehensive assessment of plantar pressure characteristics and use of machine learning to inform a low-cost insole design specifically for differentiation of three common workplace postures.

References

[1] Parent-Thirion A, Vermeylen G, van Houten G, Lyly-Yrjänäinen M, Biletta I, Cabrita J. Fifth European Working Conditions Survey overview report . 2012;EF1182.

[2] Anton D, Weeks D. Prevalence of work-related musculoskeletal symptoms among grocery workers. Int J Ind Ergonomics 2016;54:139-45.

[3] Crawford F, Thomson C. Interventions for treating plantar heel pain. The Cochrane database of systematic reviews 20033:CD000416.

[4] Riddle DL, Pulisic M, Pidcoe P, Johnson RE. Risk Factors for Plantar Fasciitis: a Matched Case-Control Study. Journal of Bone & Joint Surgery, American Volume 2003;85-A5:872.

[5] Gautham P, Nuhmani S, Kachanathu SJ. Plantar fasciitis - an update. Bangladesh Journal of Medical Science 2015;141:3-8.

[6] Thomas MJ, Roddy E, Zhang W, Menz HB, Hannan MT, Peat GM. The population prevalence of foot and ankle pain in middle and old age: a systematic review. Pain 2011;15212:2870-80.

[7] Jefferson JR. The Effect of Cushioning Insoles on Back and Lower Extremity Pain in an Industrial Setting. Workplace Health & Safety 2013;6110:451-7.

[8] Werner RA, Gell N, Hartigan A, Wiggerman N. Risk Factors for Plantar Fasciitis Among Assembly Plant Workers. PM & R 2010;22:110; 110,116; 116.

[9] Sheikhzadeh A, Gore C, Zuckerman JD, Nordin M. Perioperating nurses and technicians' perceptions of ergonomic risk factors in the surgical environment. Appl Ergon 2009;405:833-9.

[10] Hou J, Shiao JS. Risk Factors for Musculoskeletal Discomfort in Nurses. Journal of Nursing Research 2006;143:228-36.

[11] Tong KB, Furia J. Economic burden of plantar fasciitis treatment in the United States. Am J Orthop 2010;395:227.

[12] Singh D, Angel J, Bentley G, Trevino SG. Fortnightly Review: Plantar Fasciitis. BMJ: British Medical Journal 1997;3157101:172-5.

[13] Atkins D, D Atkins, F Crawford, J Edwards, M Lambert. A systematic review of treatments for the painful heel. Rheumatology (Oxford) 2010;3810:968; 968.

[14] Davies MS, Weiss GA, Saxby TS. Plantar fasciitis: how successful is surgical intervention? Foot Ankle Int 1999;2012:803-7.

[15] McPoil TG, Martin RL, Cornwall MW, Wukich DK, Irrgang JJ, Godges JJ. Heel pain--plantar fasciitis: clinical practice guildelines linked to the international classification of function, disability, and health from the orthopaedic section of the American Physical Therapy Association. J Orthop Sports Phys Ther 2008;384:A1.

[16] Anonymous Discussion Paper: Plantar Fasciitis Due to Prolonged Weight Bearing. 2014.

[17] Morfitt G. The Workers' Compensation Board of British Columbia Resolution to the Board of Directors RE: Plantar Fascitis. 2015;2015/10/22-02.

[18] Major M, Vézina N. Analysis of worker strategies: A comprehensive understanding for the prevention of work related musculoskeletal disorders. Int J Ind Ergonomics 2015;48:149-57.

[19] Stock S, Nicolakakis N, Raïq H, Messing K, Lippel K, Turcot A. Underreporting work absences for nontraumatic work-related musculoskeletal disorders to workers' compensation: results of a 2007-2008 survey of the Québec working population. Am J Public Health 2014;1043:e94-e101.

[20] Urda JL, Larouere B, Verba SD, Lynn JS. Comparison of subjective and objective measures of office workers' sedentary time. Preventive Medicine Reports 2017;8Supplement C:163-8.

[21] Pedersen SJ, Kitic CM, Bird M, Mainsbridge CP, Cooley PD. Is self-reporting workplace activity worthwhile? Validity and reliability of occupational sitting and physical activity questionnaire in desk-based workers. BMC Public Health 2016;161:836.

[22] Wick K, Faude O, Schwager S, Zahner L, Donath L. Deviation between self-reported and measured occupational physical activity levels in office employees: effects of age and body composition. Int Arch Occup Environ Health 2016;894:575.

[23] Wearing SC, Smeathers JE, Yates B, Sullivan PM, Urry SR, Dubois P. Sagittal movement of the medial longitudinal arch is unchanged in plantar fasciitis. Med Sci Sports Exerc 2004;3610:1761-7.

[24] Beeson P. Plantar fasciopathy: Revisiting the risk factors. Foot & Ankle Surgery (Elsevier Science) 2014;203:160-5.

[25] Wang T, Lin Z, Day RE, Gardiner B, Landao- Bassonga E, Rubenson J, Kirk TB, Smith DW, Lloyd DG, Hardisty G, Wang A, Zheng Q, Zheng MH. Programmable mechanical stimulation influences tendon homeostasis in a bioreactor system. Biotechnol Bioeng 2013;1105:1495-507.

[26] Reed L, Battistutta D, Young J, Newman B. Prevalence and risk factors for foot and ankle musculoskeletal disorders experienced by nurses. BMC MUSCULOSKELETAL DISORDERS 2014;151:196-.

[27] Waclawski ER, Beach J, Milne A, Yacyshyn E, Dryden DM. Systematic review: plantar fasciitis and prolonged weight bearing. Occupational Medicine 2015;652:97-106.

[28] Sullivan J, Burns J, Adams R, Pappas E, Crosbie J. Musculoskeletal and Activity-Related Factors Associated With Plantar Heel Pain. Foot & Ankle International 2015;361:37-45.

[29] Busschaert C, De Bourdeaudhuij I, Van Holle V, Chastin SFM, Cardon G, De Cocker K. Reliability and validity of three questionnaires measuring context-specific sedentary behaviour and associated correlates in adolescents, adults and older adults. The international journal of behavioral nutrition and physical activity 2015;12:117.

[30] Clark BK, Lynch BM, Winkler EA, Gardiner PA, Healy GN, Dunstan DW, Owen N. Validity of a multi-context sitting questionnaire across demographically diverse population groups: AusDiab3. The international journal of behavioral nutrition and physical activity 2015;121:148.

[31] Kurtze N, Rangul V, Hustvedt B, Flanders WD. Reliability and validity of self-reported physical activity in the Nord-Trøndelag Health Study — HUNT 1. Scand J Public Health 2008;361:52-61.

[32] Loannidis JPA. Implausible results in human nutrition research. BMJ 2013;347nov14 3:6698

[33] Schoeller DA, Thomas D, Archer E, Heymsfield SB, Blair SN, Goran MI, Hill JO, Atkinson RL, Corkey BE, Foreyt J, Dhurandhar NV, Kral JG, Hall KD, Hansen BC, Heitmann BL, Ravussin E, Allison DB. Self-report-based estimates of energy intake offer an inadequate basis for scientific conclusions. Am J Clin Nutr 2013;976:1413-5.

[34] Taber DR, Stevens J, Murray DM, Elder JP, Webber LS, Jobe JB, Lytle LA. The Effect of a Physical Activity Intervention on Bias in Self-Reported Activity. Ann Epidemiol 2009;195:316-22.

[35] Klein DA, Levine E, Walsh BT, Sazonov ES. Validation of two novel monitoring devices to measure physical activity in healthy women. In: International Converence of the IEEE Engineering in Medicine and Biology Society; 2014. p. 1727-30.

[36] Sazonov ES, Fulk G, Hill J, Schutz Y, Browning R. Monitoring of Posture Allocations and Activities by a Shoe-Based Wearable Sensor. IEEE Transactions on Biomedical Engineering 2011;584:983-90.

[37] Montgomery-Downs HE, Insana SP, Bond JA. Movement toward a novel activity monitoring device. Sleep and Breathing 2012;163:913-7.

[38] Smith L, Hamer M, Ucci M, Marmot A, Gardner B, Sawyer A, Wardle J, Fisher A. Weekday and weekend patterns of objectively measured sitting, standing, and stepping in a sample of office-based workers: the active buildings study. BMC Public Health 2015;151:9-.

[39] Tadigadapa S, Najafi N. Reliability of micro-electro-mechanical systems (MEMS). In: ; 2001. p. 197-205.

[40] Rodriguez-Martin D, Perez-Lopez C, Sama A, Cabestany J, Catala A. A Wearable Inertial Measurement Unit for Long-Term Monitoring in the Dependency Care Area. SENSORS 2013;1310:14079-104.

[41] Ompusunggu AP, Bey-Temsamani A. 2-Level error (drift) compensation for low-cost MEMS-based inertial measurement unit (IMU). Microsystem Technologies 2016;227:1601-12.

[42] Altun K, Barshan B, Tunçel O. Comparative study on classifying human activities with miniature inertial and magnetic sensors. Pattern Recognit 2010;4310:3605-20.

[43] Leutheuser H, Schuldhaus D, Eskofier BM. Hierarchical, multi-sensor based classification of daily life activities: comparison with state-of-the-art algorithms using a benchmark dataset. PloS one 2013;810:e75196.

[44] Khan SH, Sohail M. Activity monitoring of workers using single wearable inertial sensor. In: ; 2013. p. 60-7.

[45] Awais M, Palmerini L, Bourke A, Ihlen E, Helbostad J, Chiari L. Performance Evaluation of State of the Art Systems for Physical Activity Classification of Older Subjects Using Inertial Sensors in a Real Life Scenario: A Benchmark Study. Sensors 2016;1612:2105.

[46] Fulk GD, Edgar SR, Bierwirth R, Hart P, Lopez-Meyer P, Sazonov E. Identifying Activity Levels and Steps of People With Stroke Using a Novel Shoe-Based Sensor. Journal of Neurologic Physical Therapy 2012;362:100-7.

[47] Gray H. Anatomy of the Human Body. 20th ed. Philadelphia: Lea & Febiger; 1918 .

[48] OpenStax College. Bones of the Foot. OpenStax, Anatomy & Physiology. OpenStax CNX 2014;2017December 11.

[49] Modesto M, Gille U. The skeleton of the foot. 2010.

[50] Lucas R, Cornwall M. Influence of foot posture on the functioning of the windlass mechanism. The Foot 2017;30:38-42.

[51] Bolgla LA, Malone TR. Plantar fasciitis and the windlass mechanism: a biomechanical link to clinical practice. Journal of athletic training 2004;391:77.

[52] Kappel-Bargas A, Woolf RD, Cornwall MW, McPoil TG. The windlass mechanism during normal walking and passive first metatarsalphalangeal joint extension. Clin Biomech 1998;133:190-4.

[53] Fuller EA. The windlass mechanism of the foot. A mechanical model to explain pathology. J Am Podiatr Med Assoc 2000;901:35.

[54] Wearing SC, Smeathers JE, Urry SR, Hennig EM, Hills AP. The Pathomechanics of Plantar Fasciitis. Sports Medicine 2006;367:585-611.

[55] Kogler G, Solomonidis S, Paul J. Biomechanics of longitudinal arch support mechanisms in foot orthoses and their effect on plantar aponeurosis strain. Clin Biomech 1996;115:243-52.

[56] Gramatikoff K. The Windlass Mechanism. 2007.

[57] Mitchell C. Pedestrian mobility and safety: a key to independence for older people. Topics in Geriatric Rehabilitation 2006;221:45.

[58] Inman VT, Ralston HJ, Todd F, Lieberman JC. Human walking. Baltimore: Williams & Wilkins; 1981 .

[59] Winter DA. Kinematic and kinetic patterns in human gait: Variability and compensating effects. Human Movement Science 1984;31:51-76.

[60] Blanc Y, Balmer C, Landis T, Vingerhoets F. Temporal parameters and patterns of the foot roll over during walking: normative data for healthy adults. Gait Posture 1999;102:97-108.

[61] Chipotng. Gait Cycle as proposed by Jaquelin Perry 1992. 2017;2017December 11.

[62] Natali AN, Forestiero A, Carniel EL, Pavan PG, Dal Zovo C. Investigation of foot plantar pressure: experimental and numerical analysis. Med Biol Eng Comput 2010;4812:1167-74.

[63] Erdemir A, Hamel AJ, Fauth AR, Piazza SJ, Sharkey NA. Dynamic Loading of the Plantar Aponeurosis in Walking. The Journal of Bone & Joint Surgery 2004;863:546-52.

[64] Sarrafian SK. Functional characteristics of the foot and plantar aponeurosis under tibiotalar loading. Foot Ankle 1987;81:4.

[65] Warren BL. Plantar fasciitis in runners. Treatment and prevention. Sports Med 1990;105:338.

[66] Stecco C, Corradin M, Macchi V, Morra A, Porzionato A, Biz C, De Caro R. Plantar fascia anatomy and its relationship with Achilles tendon and paratenon. J Anat 2013;2236:665-76.

[67] Wright DG, Rennels DC. A study of elastic properties of plantar fascia. The Journal of bone and joint surgery.American volume 1964;46:482.

[68] Gefen A. The in Vivo Elastic Properties of the Plantar Fascia during the Contact Phase of Walking. Foot & Ankle International 2003;243:238-44.

[69] Kitaoka HB, Luo ZP, Growney ES, Berglund LJ, An K. Material Properties of the Plantar Aponeurosis. Foot & Ankle International 1994;1510:557-60.

[70] Wu C, Chang K, Mio S, Chen W, Wang T. Sonoelastography of the plantar fascia. Radiology 2011;2592:502-7.

[71] Gallego PH, Craig ME, Duffin AC, Bennetts B, Jenkins AJ, Hofer S, Lam A, Donaghue KC. Association Between p.Leu54Met Polymorphism at the Paraoxonase-1 Gene and Plantar Fascia Thickness in Young Subjects With Type 1 Diabetes. Diabetes Care 2008;318:1585-9.

[72] Northcoast Footcare. Plantar Fasciitis: What is really happening in your heel. 2015;2017December 11.

[73] Buchbinder R. Plantar Fasciitis. N Engl J Med 2004;35021:2159-66.

[74] Shetty VD, Dhillon M, Hegde C, Jagtap P, Shetty S. A study to compare the efficacy of corticosteroid therapy with platelet-rich plasma therapy in recalcitrant plantar fasciitis: a preliminary report. Foot and ankle surgery : official journal of the European Society of Foot and Ankle Surgeons 2014;201:10-3.

[75] Maffulli N, Khan K, Puddu G. Overuse tendon conditions: Time to change a confusing terminology. Arthroscopy: The Journal of Arthroscopic and Related Surgery 1998;148:840-3.

[76] Thomas JL, Thomas JL, Christensen JC, Kravitz SR, Mendicino RW. The Diagnosis and Treatment of Heel Pain: A Clinical Practice Guideline–Revision 2010. The Journal of foot and ankle surgery 2010;493:S1; S1,S19; S19.

[77] Stephens MM, Walker G. Heel pain: an overview of its aetiology and management. Foot and Ankle Surgery 1997;32:51-60.

[78] Orchard J. Plantar fasciitis. BMJ: British Medical Journal 2012;3457878:35-40.

[79] McPoil TG, Martin RL, Cornwall MW, Wukich DK, Irrgang JJ, Godges JJ. Heel pain--plantar fasciitis: clinical practice guildelines linked to the international classification of function, disability, and health from the orthopaedic section of the American Physical Therapy Association. J Orthop Sports Phys Ther 2008;384:A1.

[80] Puttaswamaiah R, Chandran P. Degenerative plantar fasciitis: A review of current concepts. The Foot 2007;171:3-9.

[81] Young CC, Rutherford DS, Niedfeldt MW. Treatment of plantar fasciitis. Am Fam Physician 2001;633:467; 467.

[82] Tsai W, Wang C, Tang F, Hsu T. Treatment of proximal plantar fasciitis with ultrasound-guided steroid injection. Arch Phys Med Rehabil 2000;8110:1416; 1416,1421; 1421.

[83] Stuber K, Kristmanson K. Conservative therapy for plantar fasciitis: a narrative review of randomized controlled trials. The Journal of the Canadian Chiropractic Association 2006;502:118.

[84] Rompe JD, Furia J, Weil L, Maffulli N. Shock wave therapy for chronic plantar fasciopathy. Br Med Bull 2007;81-821:183-208.

[85] McNally EG, Shetty S. Plantar Fascia: Imaging Diagnosis and Guided Treatment. Semin Musculoskelet Radiol 2010;143:334-43.

[86] Thing J, Maruthappu M, Rogers J. Diagnosis and management of plantar fasciitis in primary care. The British journal of general practice : the journal of the Royal College of General Practitioners 2012;62601:443-4.

[87] Tahririan MA, Motififard M, Naghi Tahmasebi M, Siavashi B. Plantar fasciitis. Journal of Research in Medical Sciences 2012;178:799-804.

[88] Bergenuud H, Lingarde F, Nilsson B. Prevalence and Coincidence of Degenerative Changes of the Hands and Feet in Middle Age and Their Relationship to Occupational Work Load, Intelligence, and Social Background. Clin Orthop 1989;&NA;239:306; 306,310; 310.

[89] Rome K, Campbell R, Flint A, Haslock I. Heel Pad Thickness—A Contributing Factor Associated with Plantar Heel Pain in Young Adults. Foot & Ankle International 2002;232:142-7.

[90] Prichasuk S, Mulpruek P, Siriwongpairat P. The heel-pad compressibility. Clin Orthop 1994300:197-200.

[91] Captain Danielle L. Scher, Lieutenant Colonel Philip J. BelmontJr, Bear MR, Mountcastle SB, Orr JD, Major Brett D. Owens. The Incidence of Plantar Fasciitis in the United States Military. The Journal of Bone & Joint Surgery 2009;9112:2867-72.

[92] Irving D, Cook J, Young M, Menz H. Obesity and pronated foot type may increase the risk of chronic plantar heel pain: a matched case-control study. BMC Musculoskeletal Disorders 2007;841.

[93] Rano JA, Fallat LM, Savoy-Moore RT. Correlation of heel pain with body mass index and other characteristics of heel pain. The Journal of Foot and Ankle Surgery 2001;406:351-6.

[94] Frey C, Zamora J. The Effects of Obesity on Orthopaedic Foot and Ankle Pathology. Foot & Ankle International 2007;289:996-9.

[95] Hill J,J J., Cutting PJ. Heel pain and body weight. Foot Ankle 1989;95:254.

[96] Pascual Huerta J, Alarcón García JM. Effect of gender, age and anthropometric variables on plantar fascia thickness at different locations in asymptomatic subjects. Eur J Radiol 2007;623:449-53.

[97] League AC. Current Concepts Review: Plantar Fasciitis. Foot & Ankle International 2008;293:358-66.

[98] Bolívar YA, Munuera PV, Padillo JP. Relationship Between Tightness of the Posterior Muscles of the Lower Limb and Plantar Fasciitis. Foot & Ankle International 2013;341:42-8.

[99] Johal KS, Milner SA. Plantar fasciitis and the calcaneal spur: Fact or fiction? Foot and Ankle Surgery 2012;181:39-41.

[100] Geppert MJ, Mizel MS. Management of heel pain in the inflammatory arthritides. Clin Orthop 1998;349349:93-9.

[101] Collins M, Raleigh SM. Genetic Risk Factors for Musculoskeletal Soft Tissue Injuries. Genetics and Sports 2009;54:136.

[102] Cham R, Redfern MS. Effect of Flooring on Standing Comfort and Fatigue. Hum Factors 2001;433:381; 381,391; 391.

[103] Rajput B, Abboud RJ. Common ignorance, major problem: the role of footwear in plantar fasciitis. The Foot 2004;144:214-8.

[104] Taunton JE, Ryan MB, Clement DB, McKenzie DC, Lloyd-Smith DR, Zumbo BD. A retrospective case-control analysis of 2002 running injuries. Br J Sports Med 2002;362:95-101.

[105] Rome K, Howe T, Haslock I. Risk factors associated with the development of plantar heel pain in athletes. Foot (Edinburgh, Scotland) 2001;113:119; 119,125; 125.

[106] D'Souza JC, Franzblau A, Werner RA. Review of Epidemiologic Studies on Occupational Factors and Lower Extremity Musculoskeletal and Vascular Disorders and Symptoms. J Occup Rehabil 2005;152:129-65.

[107] Messing K, Tissot F, Stock S. Distal Lower-Extremity Pain and Work Postures in the Quebec Population. Am J Public Health 2008;984:705-13.

[108] Gill L, Kiebzak G. Outcome of nonsurgical treatment for plantar fasciitis. Foot & ankle international 1996;179:527; 527,532; 532.

[109] Garcia M, Läubli T, Martin BJ. Long-Term Muscle Fatigue After Standing Work. Human Factors: The Journal of Human Factors and Ergonomics Society 2015;577:1162-73.

[110] Nealy R, McCaskill C, Conaway MR, Burns SM. The aching feet of nurses: an exploratory study. Medsurg nursing : official journal of the Academy of Medical-Surgical Nurses 2012;216:354.

[111] Cham R, Redfern MS. Effect of Flooring on Standing Comfort and Fatigue. Human Factors: The Journal of the Human Factors and Ergonomics Society 2001;433:381-91.

[112] Redfern MS, Cham R. The Influence of Flooring on Standing Comfort and Fatigue. AIHAJ - American Industrial Hygiene Association 2000;615:700-8.

[113] Castillo-Retamal M, Hinckson EA. Measuring physical activity and sedentary behaviour at work: a review. Work (Reading, Mass.) 2011;404:345.

[114] Spittaels H, Bourdeaudhuij d, Ilse, Brug H, Vandelanotte C. Effectiveness of an online computer-tailored physical activity intervention in a real-life setting. Health Educ Res 2007;223:385-96.

[115] Kaleta D, Makowiec-Dąbrowska T, Jegier A. Occupational And Leisure-Time Energy Expenditure And Body Mass Index. Int J Occup Med Environ Health 2007;201:9-16.

[116] Kruger J, Yore MM, Ainsworth BE, Macera CA. Is Participation in Occupational Physical Activity Associated With Lifestyle Physical Activity Levels? Journal of Occupational and Environmental Medicine 2006;4811:1143-8.

[117] Mummery WK, Schofield GM, Steele R, Eakin EG, Brown WJ. Occupational Sitting Time and Overweight and Obesity in Australian Workers. Am J Prev Med 2005;292:91-7.

[118] Prince SA, Adamo KB, Hamel ME, Hardt J, Connor Gorber S, Tremblay M. A comparison of direct versus self-report measures for assessing physical activity in adults: a systematic review. The international journal of behavioral nutrition and physical activity 2008;51:56-.

[119] Chau JY, Van Der Ploeg HP, Dunn S, Kurko J, Bauman AE. Validity of the occupational sitting and physical activity questionnaire. Med Sci Sports Exerc 2012;441:118-25.

[120] Laperrière E, Messing K, Couture V, Stock S. Validation of questions on working posture among those who stand during most of the work day. Int J Ind Ergonomics 2005;354:371-8.

[121] Mukhopadhyay SC. Wearable Sensors for Human Activity Monitoring: A Review. IEEE Sensors Journal 2015;153:1321-30.

[122] Malhi K, Mukhopadhyay SC, Schnepper J, Haefke M, Ewald H. A Zigbee-Based Wearable Physiological Parameters Monitoring System. IEEE Sensors Journal 2012;123:423-30.

[123] Edwards J. Wireless Sensors Relay Medical Insight to Patients and Caregivers [Special Reports]. IEEE Signal Process Mag 2012;293:8-12.

[124] Aziz O, Robinovitch SN. An Analysis of the Accuracy of Wearable Sensors for Classifying the Causes of Falls in Humans. IEEE Transactions on Neural Systems and Rehabilitation Engineering 2011;196:670-6.

[125] Aziz O, Park EJ, Mori G, Robinovitch SN. Distinguishing the causes of falls in humans using an array of wearable tri-axial accelerometers. Gait Posture 2014;391:506-12.

[126] Shany T, Redmond SJ, Narayanan MR, Lovell NH. Sensors-Based Wearable Systems for Monitoring of Human Movement and Falls. IEEE Sensors Journal 2012;123:658-70.

[127] Kan Y, Chen C. A Wearable Inertial Sensor Node for Body Motion Analysis. IEEE Sensors Journal 2012;123:651-7.

[128] D'Angelo LT, Neuhaeuser J, Zhao Y, Lueth TC. SIMPLE-Use-Sensor Set for Wearable Movement and Interaction Research. IEEE Sensors Journal 2014;144:1207-15.

[129] Chuo Y, Marzencki M, Hung B, Jaggernauth C, Tavakolian K, Lin P, Kaminska B. Mechanically Flexible Wireless Multisensor Platform for Human Physical Activity and Vitals Monitoring. IEEE Transactions on Biomedical Circuits and Systems 2010;45:281-94.

[130] Sazonov ES, Hegde N, Tang W. Development of SmartStep: An insole-based physical activity monitor. In: ; 2013. p. 7209-12.

[131] Sazonova N, Browning R, Sazonov E. Accurate Prediction of Energy Expenditure Using a Shoe-Based Activity Monitor. Med Sci Sports Exerc 2011;437:1312; 1312,1321; 1321.

[132] Chen M, Huang B, Lee KK, Xu Y. An Intelligent Shoe-Integrated System for Plantar Pressure Measurement. In: ; 2006. p. 416-21.

[133] Hellstrom PAR, Åkerberg A, Ekström M, Folke M. Walking Intensity Estimation with a Portable Pedobarography System. Stud Health Technol Inform 2016;224:27.

[134] Jacobs DA, Ferris DP. Evaluation of a Low-Cost Pneumatic Plantar Pressure Insole for Predicting Ground Contact Kinetics. Journal of applied biomechanics 2016;322:215.

[135] Shu L, Hua T, Wang Y, Li Q, Feng DD, Tao X. In-Shoe Plantar Pressure Measurement and Analysis System Based on Fabric Pressure Sensing Array. IEEE Transactions on Information Technology in Biomedicine 2010;143:767-75.

[136] Fulk GD, Sazonov E. Using sensors to measure activity in people with stroke. Topics in stroke rehabilitation 2011;186:746-57.

[137] Edgar SR, Swyka T, Fulk G, Sazonov ES. Wearable shoe-based device for rehabilitation of stroke patients. In: ; 2010. p. 3772-5.

[138] Abdul Hadi Abdul Razak, Zayegh A, Begg RK, Wahab Y. Foot Plantar Pressure Measurement System: A Review. Sensors 2012;127:9884-912.

[139] Bishop CM. Pattern recognition and machine learning. New York: Springer; 2006 .

[140] Witten IH, Frank E, Hall MA, Pal CJ. Data mining: practical machine learning tools and techniques. 4th revis ed. Cambridge, MA: Morgan Kaufmann Publisher; 2016 .

[141] Preece SJ, Goulermas JY, Kenney LPJ, Howard D, Meijer K, Crompton R. Activity identification using body-mounted sensors—a review of classification techniques. Physiol Meas 2009;304:R1-R33.

[142] Frank RJ, Davey N, Hunt SP. Time Series Prediction and Neural Networks. Journal of Intelligent and Robotic Systems 2001;311:91-103.

[143] Leon F, Zaharia MH. Stacked Heterogeneous Neural Networks for Time Series Forecasting. Mathematical Problems in Engineering 2010;2010:1-20.

[144] Yoshida S, Hatano K, Takimoto E, Takeda M. Adaptive Online Prediction Using Weighted Windows. IEICE Trans Inf Syst 2011;E94-D10:1917-23.

[145] Wu W, Dasgupta S, Ramirez EE, Peterson C, Norman GJ. Classification accuracies of physical activities using smartphone motion sensors. Journal of medical Internet research 2012;145:e130.

[146] Moufawad el Achkar C, Lenoble-Hoskovec C, Paraschiv-Ionescu A, Major K, Büla C, Aminian K. Instrumented shoes for activity classification in the elderly. Gait Posture 2016;44:12-7.

[147] Aziz O, Robinovitch SN. An Analysis of the Accuracy of Wearable Sensors for Classifying the Causes of Falls in Humans. IEEE Transactions on Neural Systems and Rehabilitation Engineering 2011;196:670-6.

[148] Archer CM, Lach J, Chen S, Abel MF, Bennett BC. Activity classification in users of ankle foot orthoses. Gait Posture 2014;391:111-7.

[149] Preece SJ, Goulermas JY, Kenney LPJ, Howard D. A Comparison of Feature Extraction Methods for the Classification of Dynamic Activities From Accelerometer Data. IEEE Transactions on Biomedical Engineering 2009;563:871-9.

[150] Arif M, Kattan A, Ahamed SI. Classification of physical activities using wearable sensors. Intelligent Automation & Soft Computing 2017;231:21-30.

[151] Bastian T, Maire A, Dugas J, Ataya A, Villars C, Gris F, Perrin E, Caritu Y, Doron M, Blanc S, Jallon P, Simon C. Automatic identification of physical activity types and sedentary behaviors from triaxial accelerometer: laboratory-based calibrations are not enough. Journal of applied physiology (Bethesda, Md.: 1985) 2015;1186:716-22.

[152] Rosenberg D, Gdobole S, Ellis K, Di C, Lacroix A, Natarajan L, Kerr J. Classifiers for Accelerometer-Measured Behaviors in Older Women. Medicine & Science in Sports & Exercise 2017;493:610-6.

[153] Fiorini L, Cavallo F, Dario P, Eavis A, Caleb-Solly P. Unsupervised Machine Learning for Developing Personalised Behaviour Models Using Activity Data. Sensors 2017;175:1034.

[154] Howcroft J, Kofman J, Lemaire ED. Feature selection for elderly faller classification based on wearable sensors. Journal of Neuroengineering and Rehabilitation 2017;14.

[155] Zhang J, Wang S. A fast leave-one-out cross-validation for SVM-like family. Neural Computing and Applications 2016;276:1717-30.

[156] Shao Z, Er MJ, Wang N. An Efficient Leave-One-Out Cross-Validation-Based Extreme Learning Machine (ELOO-ELM) With Minimal User Intervention. IEEE Transactions on Cybernetics 2016;468:1939-51.

[157] Stone M. Cross-Validatory Choice and Assessment of Statistical Predictions. Journal of the Royal Statistical Society.Series B (Methodological) 1974;362:111-47.

[158] Shao J. Linear Model Selection by Cross-Validation. Journal of the American Statistical Association 1993;88422:486-94.

[159] Rogers WH, Wagner TJ. A Finite Sample Distribution-Free Performance Bound for Local Discrimination Rules. The Annals of Statistics 1978;63:506-14.

[160] Uematsu A, Inoue K, Hobara H, Kobayashi H, Iwamoto Y, Hortobagyi T, Suzuki S. Preferred step frequency minimizes veering during natural human walking. Neurosci Lett 2011;5053:291-3.

[161] Boyle J. Wireless technologies and patient safety in hospitals. Telemedicine journal and e-health : the official journal of the American Telemedicine Association 2006;123:373.

[162] Chuckpaiwong B, Nunley JA, Mall NA, Queen RM. The effect of foot type on in-shoe plantar pressure during walking and running. Gait Posture 2008;283:405-11.

[163] Chung M, Wang M. Gender and walking speed effects on plantar pressure distribution for adults aged 20-60 years. Ergonomics 2012;552:194-200.

[164] Cimolin V, Veronica Cimolin, Paolo Capodaglio, Nicola Cau, Manuela Galli. Foot-type analysis and plantar pressure differences between obese and nonobese adolescents during upright standing. International journal of rehabilitation research 2015;391:87-91.

[165] Kim J, Kim K, Gubler C. Comparisons of Plantar Pressure Distributions between the Dominant and Non-dominant Sides of Older Women during Walking. Journal of Physical Therapy Science 2013;253:313-5.

[166] Pau M, Galli M, Celletti C, Morico G, Leban B, Albertini G, Camerota F. Plantar pressure patterns in women affected by Ehlers-Danlos syndrome while standing and walking. Res Dev Disabil 2013;3411:3720-6.

[167] Lee S, Chou C, Hou Y, Wang Y, Yang C, Guo L. The effects of changes in step width on plantar foot pressure patterns of young female subjects during walking. Journal of Mechanics in Medicine and Biology 2011;115:1071-83.

[168] Sullivan J, Burns J, Adams R, Pappas E, Crosbie J. Plantar heel pain and foot loading during normal walking. Gait Posture 2015;412:688-93.

[169] Hegde N, Sazonov ES. SmartStep 2.0 - A completely wireless, versatile insole monitoring system. In: ; 2015. p. 746-9.

[170] Kozey-Keadle S, Libertine A, Lyden K, Staudenmayer J, Freedson PS. Validation of wearable monitors for assessing sedentary behavior. Med Sci Sports Exerc 2011;438:1561.

[171] Gurney JK, Kersting UG, Rosenbaum D. Between-day reliability of repeated plantar pressure distribution measurements in a normal population. Gait Posture 2008;274:706-9.

[172] Rao S, Carter S. Regional plantar pressure during walking, stair ascent and descent. Gait Posture 2012;362:265.

[173] Wafai L, Zayegh A, Woulfe J, Aziz SM, Begg R. Identification of Foot Pathologies Based on Plantar Pressure Asymmetry. Sensors (Basel, Switzerland) 2015;158:20392-408.

[174] Stebbins JA, Harrington ME, Giacomozzi C, Thompson N, Zavatsky A, Theologis TN. Assessment of sub-division of plantar pressure measurement in children. Gait Posture 2005;224:372-6.

[175] Ellis SJ, Stoecklein H, Yu JC, Syrkin G, Hillstrom H, Deland JT. The Accuracy of an Automasking Algorithm in Plantar Pressure Measurements. HSS Journal 2011;71:57-63.

[176] Cavanagh PR, Ulbrecht JS. Clinical plantar pressure measurement in diabetes: rationale and methodology. The Foot 1994;43:123-35.

[177] Sterzing T, Frommhold C, Rosenbaum D. In-shoe plantar pressure distribution and lower extremity muscle activity patterns of backward compared to forward running on a treadmill. Gait Posture 2016;46:135-41.

[178] Bennetts CJ, Owings TM, Erdemir A, Botek G, Cavanagh PR. Clustering and classification of regional peak plantar pressures of diabetic feet. J Biomech 2013;461:19-25.

[179] Chua YK, Quek RKK, Kong PW. Basketball lay-up - foot loading characteristics and the number of trials necessary to obtain stable plantar pressure variables. Sports Biomechanics 2017;161:13-22.

Appendix A – Standard Operating Procedures for Study 1

Simon Fraser University, Surrey Campus, NeuroSpine Laboratory

Updated: November 8, 2017

Author: Kohle Merry

Principal Investigator: Dr. Carolyn J. Sparrey

Study Number (as per SFU Office of Research Ethics): 2016s0326

Introduction

This SOP outlines the protocol used to collect sitting, standing and walking data using an insole-based plantar pressure measurement system, specifically the F-Scan in-shoe system (Tekscan Inc, Boston, USA).

Materials

Table 1   Materials used in Sitting, Standing and Walking Data Acquisition Study

Equipment	Amount	Provider	Description
Tape (1-sided)	1 Roll	Retail store	Used to mark 'X's on the floor for distinguishing ends of the walking course, as well as the location for standing to be done.
Desks/Tables	2	-	Need to be roughly the same height. Used to support materials for the attention-diversion task.
Office Chair	2	-	Used for the sitting component. Chair used for this study had a 46cm floor-seat height.
Deck of Cards	5	Retail store	Ideally need to be the same brand of cards to ensure uniform appearance.
Timer	1	-	Used to time the trials.
Video Camera	1	-	Used to video tape the trials for validation purposes. A GoPro camera was used in this study.
Wireless F-Scan in-shoe system	1	Tekscan Inc.	One data acquisition unit (wireless) was used. Multiple pairs of F-Scan insole sensors were used, and are only reusable for approximately 5-15 trials depending on the use. Insoles were trimmed to fit.
Data Acquisition Laptop	1	-	Needs to have the appropriate F-Scan software downloaded. Note that the wired F-Scan system has a CD version of the software and is registered to Dr. Ed Park (University of Victoria) whereas the wireless version only has a digital copy of the software and is registered to Dr. Ed Park (SFU). The system will not work if the wrong software is used.
Tape (2-sided)	1 Roll	Retail Store	Used to minimize relative motion of the insoles.
Scale	1	-	Used to weigh the participant for calibration of insoles.

Experimental Overview

The purpose of the protocol is to provide distinct phases of sitting, standing or walking activities in focused or distracted situations to determine the plantar pressures associated with each activity. In line with SFU DORE protocol 2016s0326 data collection is structured into three distinct trials performed ten minutes apart, each consisting of a six-minute collection phase. Two trials have no task associated with them (Trials 1 & 3) whereas one trial has an attention-diversion task (sorting cards by colour) for the participants to do while going through the three postures (Trial 2).

Trials 1 & 3 each consist of six, one-minute activity blocks (sitting, standing, or walking) in which each activity is executed twice and the order of activities is randomized. Sitting is conducted in a standard rigid plastic office chair (46cm floor-seat height) while walking was performed at a self-selected speed over a 10m walkway (adjacent hallway to lab 3980); upon reaching the end of

the walkway, participants should turn in a self-selected manner and continue this repetition until the completion of the activity block. Participants should be warned approximately five seconds before the conclusion of each activity. At the start of each activity the participant will perform a right-footed stomp to sync plantar pressure and video data. Video of the participant's feet (for data privacy) will be captured over the entire test and used to validate the activity classifications.

Trials 2 consists of three, two-minute activity blocks (sitting, standing, or walking) in which each activity is executed while sorting cards by colour. The order of activities will be randomized. Cards will be moved from a designated starting position to a designated final position; only the colour of the cards matters while the numeric value serves no purpose. Sitting will be conducted in the same standard plastic office chair (46cm floor-seat height) used in Trials 1 and 3. Walking will be performed at a self-selected speed over a 5m walkway; upon reaching the end of the walkway, participants either pick-up or drop-off a card, and then turned in a self-selected manner and continue this repetition until the completion of the activity block. Similarly, during the sitting and standing activities, participants move cards from the starting positions to the final positions, alternating between red and black. Participants will be warned approximately five seconds before the conclusion of each activity. At the start of each activity the participant will perform a right-footed stomp. Video of the participant's feet will be capture for the duration of the test.

Experimental Setup

Equipment for the experiments is housed is SRY 3960. The room should be booked using the shared calendar to ensure sufficient experimental space. Trials will be carried out in SRY 3960 and the adjacent hallway.

Trials 1 & 3 (No Task)

Two trials are conducted with no task issued to the participants; the experimental setup can be found in Figure 1 below.
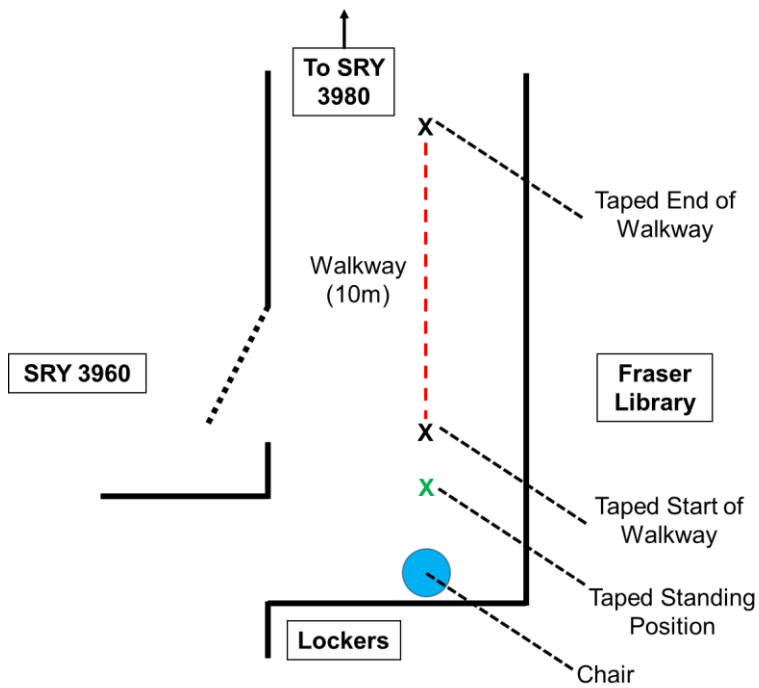
Figure *1*   **Experimental setup for Trials 1 & 3 (No Task)**

Trial 2 (Attention-Diversion Task)

One trial is conducted with an attention-diversion task issued to the participants (sorting cards by colour); the experimental setup can be found in Figure 2 below.
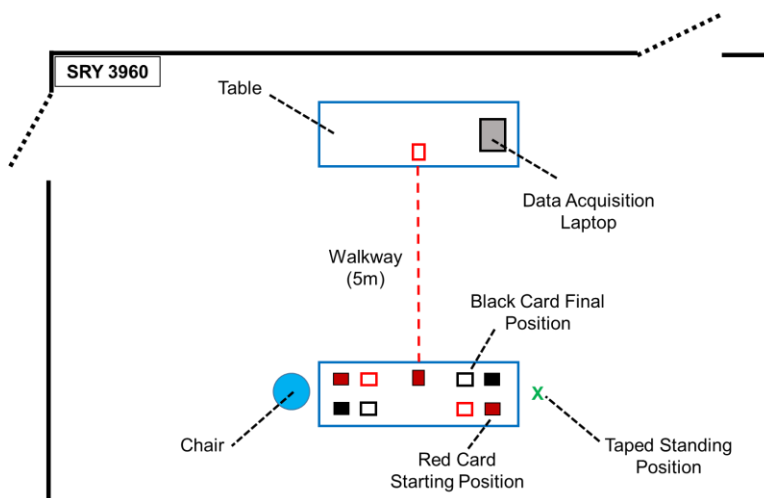

Figure 2   **Experimental setup for Trial 2 (Attention-Diversion Task)**

Experimental Protocol

The study should be run according to the following protocol; note that underlined features designate an associated form.

1. Introduction and greeting
2. Study explanation (study purpose/rationale, introduce testing equipment, risks and benefits of study, review study protocol)
3. <u>Consent Form</u> review (participant reviews form & signs)
4. <u>Participant Profile Form</u>
5. Foot Posture Index analysis conducted by study administrator (See FPI manual) and recorded on the <u>FPI Scoring Table</u>
6. F-Scan setup
   6.1. Size insoles appropriately
   6.2. Weigh participant (no shoes)
   6.3. Velcro cuffs (should be noticeably tight)
   6.4. Ankle unit attachment to Velcro cuffs
   6.5. Belt attachment/sizing
   6.6. Ethernet cable connections: ankle units to belt
   6.7. Tape bottom of insole sensors in 3 locations (medial midfoot, toes, heel) and put sensors in shoes
   6.8. Connect insole sensors to ankle units via. sensor leash
   6.9. Participant puts on shoes slowly, holding back of the sensor to reduce movement
   6.10. Power up system and sync with data collection laptop (see F-Scan user manual)
   6.11. Enter patient info into software, click new recording to start a new trial
   6.12. Set up capture parameters (75Hz collection frequency, 400s collection time [6 min of data collection plus 40s buffer room], 15s trigger delay to get participant into place, etc.)
   6.13. System calibration (*Step Calibration* – see F-Scan user manual)
7. Video camera setup (GoPro mounted to *GoPro Vertical Surface Mount* to be held in hand and carried by test administrator during trial, 720p/120fps video collection mode, etc.)
   7.1. Note that the associated app, *GoPro (formerly Capture)*, can be downloaded onto a mobile device from either the Apple app store or the Google Play store.
8. Data collection period
   8.1. Start camera capture (button on camera)
      8.1.1. Camera is held by the test administrator and follows the participants feet in real-time to sync data and note any abnormalities
   8.2. Start F-Scan capture (done via software UI; set a trigger delay of 15s)
   8.3. Trial 1, in hallway →Capture 400s of data
      8.3.1. Order of activities is predefined by the test administrator, and written on the <u>Trial Ordering Form</u>. Randomization is carried out independently for each trial. Within Trials 1 & 3, randomization is spliced into two sets, each comprising

three minutes of collection (e.g. Randomize min 1-3 [Si,St,W] then randomize min 4-6 [Si,St,W]), then two orders are joined together to compose a trial. No back-to-back activities can exist, with the single exception of minutes 3 & 4, the joining point of the two segments (e.g. first block [Si,St,W] and block two is [W,St,Si] results in trial [Si,St,W,W,St,Si]). In this example, participant would conduct two minutes of continuous walking from minutes 2-4 with no stomp in between. Randomization is carried out through random number generation between 1-9, with 1-3 denoting sitting, 4-6 denoting walking, and 7-9 denoting standing. Participants are told of the activity sequence to be carried out before each trial.

8.3.2. Timing of activities is shielded from participants, and is carried out using a standard smartphone timer. Upon hearing the *beep* from the F-Scan belt signaling the start of an activity, the timer is started. Timing is meant to approximate a minute of data collection per posture. Participants are prompted through a 5-4-3-2-1 countdown to switch activities when 55s of an activity has elapsed. Because the transition period encroached into the subsequent minute, timing is modified as best as possible to accommodate this; an additional 40s of collection time is used to counteract the transition times. Trial is concluded once the F-Scan belt *beeps* again, signifying that the 400s has elapsed.

8.4. Turn off camera (F-Scan automatically shuts down after 400s capture duration complete—this is signified with an audible *beep* from the F-Scan belt).

8.5. Ten-minute break; participant is permitted to self-select which posture(s) they assume for the break.

8.6. Trial 2, in SRY 3960 →Start F-Scan, camera, Capture 400s of data

8.6.1. Prior to the start of the trial, test administrator demonstrates the sorting task to the participant. Sorting during sitting and standing consists of two piles, sorted by colour, face up, approximately four inches from the desk edge, and approximately six inches apart (Figure 2, NTS). Roughly 50 cards are placed in each pile (i.e. 50 red, 50 black), totaling 100 cards for sitting and 100 cards for standing. One card from each pile is then placed approximately four inches towards the table center from each larger pile, denoting the final position of the cards. Participants are asked to move cards, one at a time, alternating between red and black, from the starting position of each pile to the final position, denoted initially by the single card. During the walking trial, only one pile of red (or black) cards is used. The initial position with approximately 25 cards of the same colour are placed on the same table as the sitting and standing cards. One card is moved to the opposite table, to denote the final location for the walking cards. Participants again move one card at a time from one table to the other. Walking speed and turning direction/speed are self-selected. Cards are also sorted at self-selected speeds. In most cases, participants will not run out of cards, however, if they do run out, they are asked to sit/stand/or walk similar to trials 1 & 3 for the remaining duration of the trial.

   8.6.2. Camera is again held by the test administrator throughout the trial, targeting the participant's feet.

  8.7. Turn off camera (F-Scan automatically shuts down after capture duration complete)

  8.8. Ten-minute break; participant is permitted to self-select which posture(s) they assume for the break

  8.9. Trial 3, in hallway → Start F-Scan, camera, Capture 400s of data

  8.10. Turn off camera (F-Scan automatically shuts down after capture duration complete)

9. Remove F-Scan system from participant

10. Participant debrief (explain next steps to be performed and answering participant questions if any)

11. Reimburse participant

  11.1. Money transfer and receipt signing

Data Retention & Storage

Following the completion of the experimental protocol, the following elements should be in the study administrator's possession:

1. 3 sets of F-Scan trial data (.fsx), corresponding to 3 separate trials
2. 3 sets of ASCII F-Scan trial data (.csv), corresponding to 3 separate trials
3. 3 videos, corresponding to 3 separate trials
4. A signed copy of the <u>Consent Form</u>
5. A completed <u>Participant Profile Form</u>
6. A completed <u>FPI Scoring Table Form</u>
7. A completed Trial Ordering Form

Pending any requests of the participant to withdraw their data from the study, participant data (paper and electronic), including video data, shall be kept for 5 years. The consent form is stored in a locked filing cabinet in a separate office at the study location, only accessible by the primary investigators and the co-investigators conducting the study. Only the consent forms contain identifying subject data; all other documents and electronic data are denoted through a participant ID of the format 'SSWXX', where X's denote a two-digit number from 0-10.

The personal profile forms, FPI scoring table forms, and trial ordering forms are stored in a locked filing cabinet within a passcard protected laboratory at the study location. The electronic participant data from the F-Scan system, as well as the trial video, are kept on a password protected secured server (SFU Vault) at the study location, accessible only by the primary investigators and the co-investigators conducting the study.

Associated Study Forms

The following forms are associated with this study are appended to the end of this document.

1. Consent Form (not appended due to length—contact author for access)
2. Participant Profile Form
3. FPI Scoring Table Form
4. Trial Ordering Form
5. NSERC2016 SSW Receipt Template

Additional Sources

The following additional documents are associated with this study and should be consulted when necessary:

1. F-Scan User Manual (v. 6.51x)
2. *The Foot Posture Index* Manual (six item version FPI-6)

Contact Information

Any questions should be directed to the author, Mr. Kohle Merry at *kmerry@sfu.ca*

Participant Profile Form

Differentiation of Foot Contact Parameters between Sitting, Standing and Walking

School of Mechatronic Systems Engineering

250-13450 102 Avenue, Surrey, BC, V3T 0A3

Investigator Contact Information

Dr. Carolyn Sparrey	Dr. Edward Park	Mr. Kohle Merry
Co – Principal Investigator	Co – Principal Investigator	Co – Investigator
250-13450 102 Avenue	250-13450 102 Avenue	250-13450 102 Avenue
Surrey BC CANADA V3T 0A3 1 (778) [...]	Surrey BC CANADA V3T 0A3 1 (778) 782 [...]	Surrey BC CANADA V3T 0A3 1 (778) 998 [...]
[...]@sfu.ca	[...]@sfu.ca	[...]@sfu.ca

The following profile collects personal health information as it is relevant to the study; please fill out the following to the best of your abilities. If you have any questions, please consult the test administrator. If you are not comfortable answering a question, please leave it blank.

Subject ID: _____

Date: _____

Test Administrator: _____

Location: _____

Age (years): _____

Weight (lbs): _____ **Height**: _____(ft) _____(in)

Gender: M   F   Other

Dominant Foot: R   L

Shoe Size: _____

The following section is to be completed by the study investigator.

Foot Posture Index (FPI): _____

1) Talar head palpation

Score	-2	-1	0	1	2
	Talar head palpable on lateral side/but not on medial side	Talar head palpable on lateral side/slightly palpable on medial side	Talar head equally palpable on lateral and medial side	Talar head slightly palpable on lateral side/ palpable on medial side	Talar head not palpable on lateral side/ but palpable on medial side

2) Supra and infra lateral malleolar curvature

Score	-2	-1	0	1	2
	Curve below the malleolus either straight or convex	Curve below the malleolus concave, but flatter/ more shallow than the curve above the malleolus	Both infra and supra malleolar curves roughly equal	Curve below malleolus more concave than curve above malleolus	Curve below malleolus *markedly* more concave than curve above malleolus

3) Calcaneal frontal plane position

Score	-2	-1	0	1	2
	More than an estimated 5° inverted (varus)	Between vertical and an estimated 5° inverted (varus)	Vertical	Between vertical and an estimated 5° everted (valgus)	More than an estimated 5° everted (valgus)

4) Prominence in the region of the talonavicular joint (TNJ)

Score	-2	-1	0	1	2
	Area of TNJ markedly concave	Area of TNJ slightly, but definitely concave	Area of TNJ flat	Area of TNJ bulging slightly	Area of TNJ bulging markedly

5) Congruence of the medial longitudinal arch

Score	-2	-1	0	1	2
	Arch high and acutely angled towards the posterior end of the medial arch	Arch moderately high and slightly acute posteriorly	Arch height normal and concentrically curved	Arch lowered with some flattening in the central portion	Arch very low with severe flattening in the central portion – arch making ground contact

6) Abduction/Adduction of the forefoot

Score	-2	-1	0	1	2
	No lateral toes visible. Medial toes clearly visible	Medial toes clearly more visible than lateral	Medial and lateral toes equally visible	Lateral toes clearly more visible than medial	No medial toes visible. Lateral toes clearly visible

131

Date: _____   Study Ordering Form   Subject ID: _____

<u>Min 1-6:</u>
    1. _____
    2. _____
    3. _____
    4. _____
    5. _____
    6. _____

<u>Min 7-12:</u>
    1. _____
    2. _____
    3. _____

<u>Min 12-18:</u>
    1. _____
    2. _____
    3. _____
    4. _____
    5. _____
    6. _____

Project Title:
Differentiation of Foot Contact Parameters between Sitting, Standing and Walking

Principle Investigators: *Dr. Carolyn Sparrey & Dr. Edward Park*

By signing this receipt you confirm that you have received $25.00 for your participation in the study named above.

Participant name: Participant Phone Number:

_____   _____

Participant signature: Participant Email Address:

_____   _____

_____

Appendix B – Extended Methods for Study 1

These extended methods are intended to provide clarity and specific details of the techniques used to conduct the plantar pressure insole study that could not fit in the standard journal paper format.

Trimming F-Scan Insoles to Fit

The F-Scan system (Tekscan Inc, Boston, USA) is comprised primarily of three elements: The F-Scan software, the data acquisition unit, and the insole-based sensors. The insole sensors are comprised of 960 (pre-trimming) resistive sensing elements (known as 'sensels') embedded into a Mylar substrate. The F-Scan insoles are particularly unique in that they are only 0.15mm thick, making them extremely discreet compared to most other commercial in-shoe pressure measurement systems. Additionally, the thinness of the F-Scan insole provides another advantage in that the sensors are shipped as templates, which are then trimmed to fit as needed.
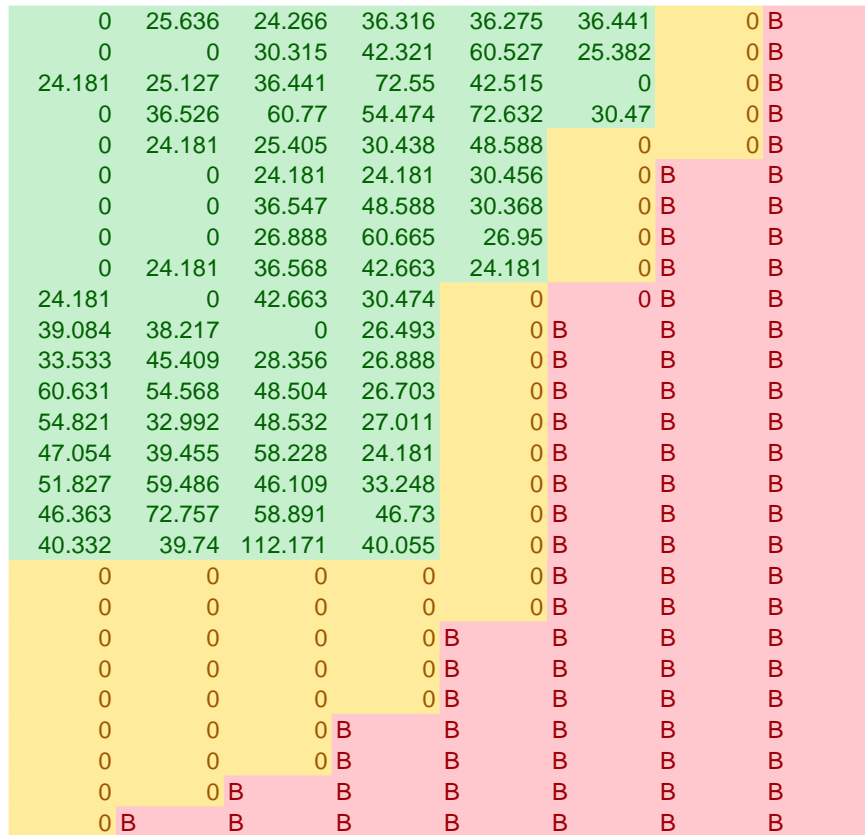
Trimming the F-Scan insoles to fit a specific shoe-size was straightforward as the templates are marked with lines denoting various common sizes on them; however, because foot shape is not always uniform, it was noticed that despite the shoe size of the insole matching the participant's shoe size, the insole did not always fit perfectly. An especially wide foot was difficult to size appropriately as the length may fit correctly, but the insole may be too narrow therefore not covering the entire plantar aspect of the foot. Conversely, if the insole was cut to fit the width, often the length would be too long and bunching of the insole would occur near the toes/heel. To adapt for certain participants where this was the case, non-standard insole sizes were cut; for example, if a participant had a M10 shoe size with an especially wide foot, the M10 outline would be followed towards the heel and toe areas, but the midfoot and forefoot would be trimmed especially wide to accommodate.

Bunching of the insole was also found to be an issue in many cases. When placing the insole sensor into the participant's shoes (post-trimming), double-sided tape was used in an attempt to hold it in place and eliminate subsequent relative motion. Even still, when participants were putting their shoes on, if they did not proceed quite slowly and hold the posterior of the insole, the insole tended to shift anteriorly and would resultantly curl

around the toes, thus reducing the number of sensors under the heel. To compensate for this, participants were instructed to proceed very slowly when putting their shoes on and to hold the posterior of the insole with their fingers, while sliding on their shoe as if using their fingers as a shoe-horn. Based on the used sensors, it appeared there was still some bunching around the toe areas during some tests, but an attempt was concisely made to mitigate this throughout.

Identifying the Foot Outline

When data is exported from the F-Scan system, it is exported as a .csv file where each frame of the data collection period is represented by a 60 x 21 matrix of calibrated pressure values. Within the 60 x 21 matrix, some values are given a default 'NaN' or 'Not a Number' value to approximate the shape of an insole from a rectangular matrix; these are known as filler elements (Figure 1). If inside the matrix and not given a NaN designation, one must assume the rest of the matrix is a combination of active sensel elements, which form the trimmed sensor and are under the foot, and inactive sensel elements, which are trimmed off sensels designated with a zero value (Figure 1). The challenge found with this labeling system is the active/inactive designation is not labeled, making it difficult to identify the true foot outline; an inactive sensor designated with a default zero value could just as easily be an active sensor not currently loaded by the participant.

0	25.636	24.266	36.316	36.275	36.441	0	B
0	0	30.315	42.321	60.527	25.382	0	B
24.181	25.127	36.441	72.55	42.515	0	0	B
0	36.526	60.77	54.474	72.632	30.47	0	B
0	24.181	25.405	30.438	48.588	0	0	B
0	0	24.181	24.181	30.456		0	B ... B
0	0	36.547	48.588	30.368		0	B ... B
0	0	26.888	60.665	26.95		0	B ... B
0	24.181	36.568	42.663	24.181		0	B ... B
24.181	0	42.663	30.474	0		0	B ... B
39.084	38.217	0	26.493	0	B	B	B
33.533	45.409	28.356	26.888	0	B	B	B
60.631	54.568	48.504	26.703	0	B	B	B
54.821	32.992	48.532	27.011	0	B	B	B
47.054	39.455	58.228	24.181	0	B	B	B
51.827	59.486	46.109	33.248	0	B	B	B
46.363	72.757	58.891	46.73	0	B	B	B
40.332	39.74	112.171	40.055	0	B	B	B
0	0	0	0	0	B	B	B
0	0	0	0	0	B	B	B
0	0	0	0	B	B	B	B
0	0	0	0	B	B	B	B
0	0	0	0	B	B	B	B
0	0	0	B	B	B	B	B
0	0	0	B	B	B	B	B
0	0	B	B	B	B	B	B
0	B	B	B	B	B	B	B

Legend		
Active Sensels	Inactive Sensels (Trimmed Off)	Filler Elements

Figure 1   Exemplary F-Scan insole outline with sensel values denoting pressure in kPa. Segment pictured is the lateral heel of a right foot.

This problem was resolved by first converting all 'NaN' values, labeled as 'B' in Figure 1, to zero values. Following this, all sensel readings within the 60 x 21 matrix were summed over an entire trial (~six minutes), creating a new 60 x 21 matrix with the total pressure values recorded by a sensel during a trial summed (Figure 2a-b). When pressure elements were summed over an entire trial, the footprint consisting of only active sensels emerged (Figure 2). Subsequent measurements were then able to be made to segment the foot into specific regions for subsequent analysis.

(a)
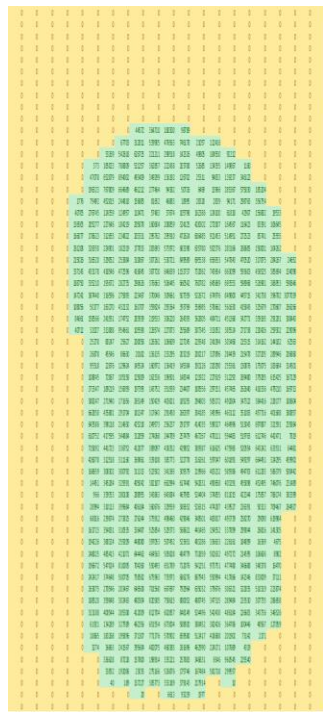
598327	464996	513043	697887	321591	235864	0	0
478111	594483	519763	612746	442471	7819	0	0
616625	475965	520554	643242	633531	64481	0	0
597047	601891	549297	664451	324295	459902	0	0
403232	589386	494703	611283	586379	500442	0	0
490658	403291	455898	452495	746076	231489	0	0
374855	811015	422344	175857	786174	383399	0	0
474287	439527	236391	50313	709467	264927	0	0
483817	493739	258270	29090	619984	0	0	0
154552	337899	299044	26816	141305	0	0	0
336633	226161	184899	16369	4675	0	0	0
502632	497272	214595	106606	8982	0	0	0
973751	477480	346688	348378	16470	0	0	0
550994	417866	142346	833009	37111	0	0	0
379676	306321	322835	510319	223874	0	0	0
347315	289484	233530	307735	286658	0	0	0
542438	486184	226603	343736	346526	0	0	0
382426	364786	100446	48567	127059	0	0	0
418688	201902	73142	2171	0	0	0	0
224171	107689	4319	0	0	0	0	0
6546	960545	225540	0	0	0	0	0
581718	299557	0	0	0	0	0	0
0	10	0	0	0	0	0	0
0	0	0	0	0	0	0	0
0	0	0	0	0	0	0	0

(b)

Figure 2 **Exemplary footprint extracted from exported F-Scan data. (a) 60 x 21 Matrix containing summed pressure values over an entire trial. Yellow cells contain a zero value while green cells contain a non-zero value (b) Isolated lateral heel region from (a) for readability**

Segmenting the Foot

Regionally deconstructing the plantar aspect of the foot presented several challenges. Firstly, most in-shoe pressure measurement systems have automated algorithms for identifying the foot outline and designating foot regions, known as 'masks'. Data analysis done within the commercial software accompanying the system is convenient for the user as the software segments the foot into masks automatically (Figure 3). However, further manipulation of the masked data can be difficult. Conducting analyses with exported data provides more freedom and is therefore preferred in some cases; however, the user must then define how to segment the foot. To protect intellectual property, most commercial measurement systems do not detail how their respective software packages segment the foot. As a result, much of the current literature is scattered on how to do this and no 'gold standard' is defined [172-179]; this is problematic as labels such as 'midfoot pressures' may not be describing the same midfoot region as another study, making comparisons invalid. To standardize the foot masks as much as possible this work used a masking method created by the company

Novel, which sells the Pedar in-shoe measurement system. Novel's auto-segmentation method, known as the PRC masking method, uses the foot length, foot width at the metatarsals, and an axis spanning the heel center to the center of the second toe to regionally divide the foot [172,177]. Because of the wide-spread use of the Pedar insoles in the literature, this method was selected.
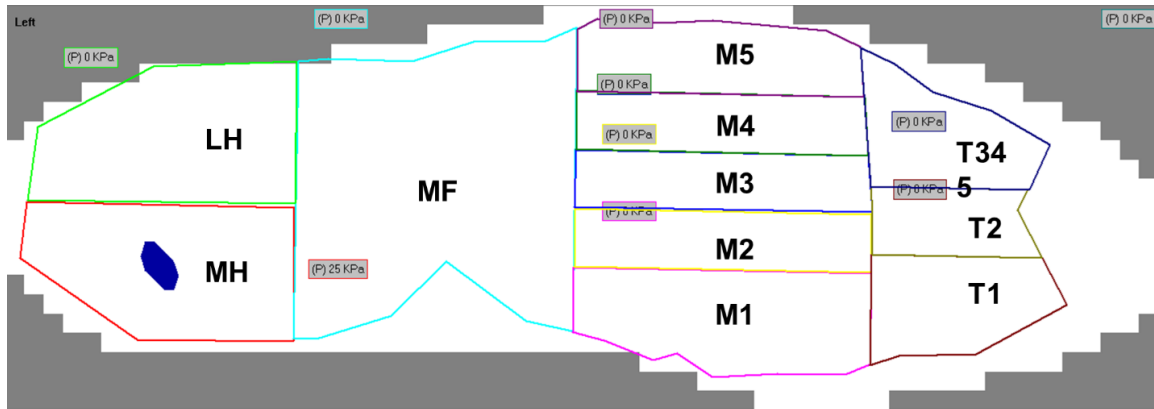

Figure 3   **Exemplary F-Scan regional foot breakdown as produced within the F-Scan software package**

One shortcoming of the PRC masking method is that the various descriptions of the segmentation method do not describe how the toe/forefoot boundary is established [3,6]. To account for this, a method was devised to identify the space between the interphalangeal joint (IP) and the metatarsophalangeal joint (MCP) of the great toe, which is an approximate dividing point between the hallux and the medial forefoot. This area was expected to be the region of lowest plantar pressure between the two joints as they protrude more on the plantar side of the foot causing them to load more significantly during the various postures (Figure 4a-b). Therefore, the MCP- IP space was defined by the inflection point where cumulative pressure begins to increase (traveling towards the MCP joint) again after decreasing when moving away from the prominence created by the IP joint.
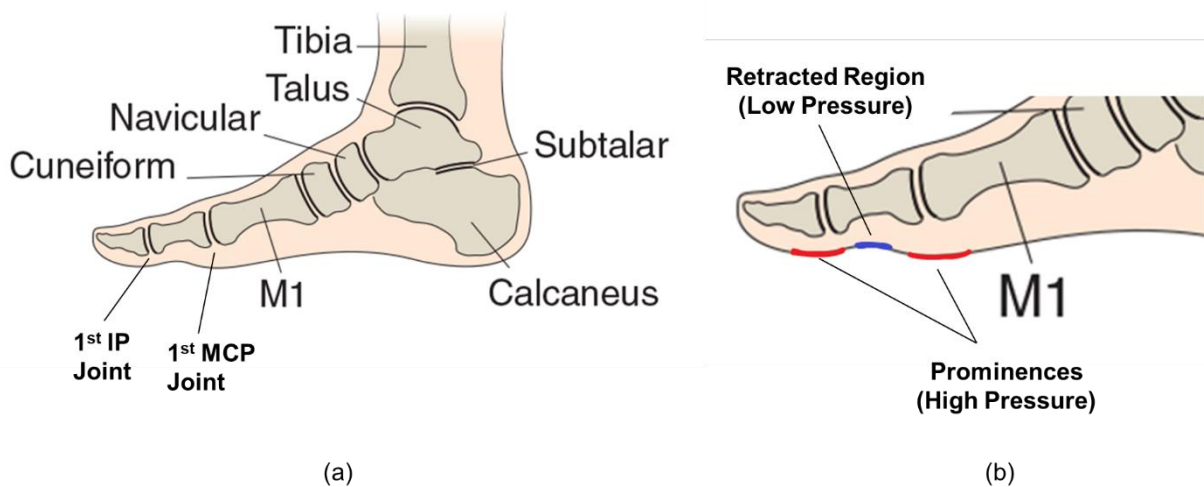
Figure 4   **Sagittal view of the right foot from the medial side. (a) Bony anatomy with emphasis placed on the first interphalangeal joint (IP) and the first metatarsophalangeal joint (MCP). (b) Regions of pressure created by the bony prominences. Red areas denote higher contact pressure while blue areas denote low pressure regions.**

To find this point using the F-Scan data, the IP joint of the hallux was approximated by mathematically determining the sensel element of highest cumulative pressure within a defined search box; the search area was automatically defined as the expected location of the hallux, and confirmed visually. Upon finding the sensel which corresponded to the center of the hallux, a column of sensels was extracted from the center of the hallux to approximately halfway up the medial forefoot. To isolate the center of the retracted space between the two joints, the gradient was taken along the extracted column of sensels, therefore describing the rate of change of the summed pressure values between the approximated IP and MCP joint locations (Figure 5). In Figure 5, rows one to ten are inactive sensels and therefore do not yield a summed pressure value. Upon reaching row ten, the summed pressure begins to increase resulting in an associated positive gradient until approximately row 13, where the pressure peaks and begins to decrease; this peak in pressure can be identified as roughly the IP joint of the hallux. Moving posteriorly, the pressure begins to drop until approximately row 16, where pressure again begins to rise towards the second prominence (the MCP joint). The valley created at approximately row 16 in this case can be distinguished as the retracted region between the two joints (Figure 4b), approximating the gap between the toes and the forefoot. Moving forward in segmentation, row 16, in this case, was subsequently used as the horizontal toe/forefoot boundary for the hallux and T2. Because of the

sloped nature of the foot from toes three to five, a compensation was made to create an angular boundary dividing the T35 region from the lateral midfoot. The T2/T35/CFF/LFF intersection point (Figure 6) was used as the medial boundary point, while another point was selected on the most lateral active sensel the row located 10% of the foot length below the toe/forefoot boundary (Figure 6a-b). The points were then connected by a diagonal row of sensels approximating a slope of negative one.
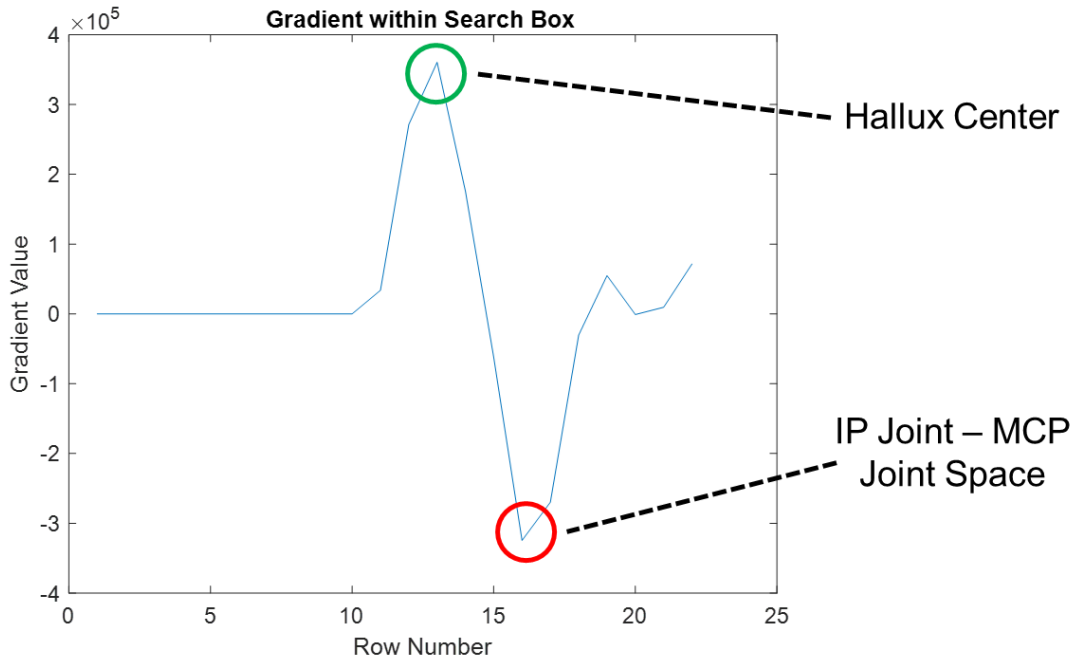

Figure 5   **Plot of the gradient ascertained from summer pressure values over a single trial; this plot was used to identify the Toe/Forefoot Boundary**
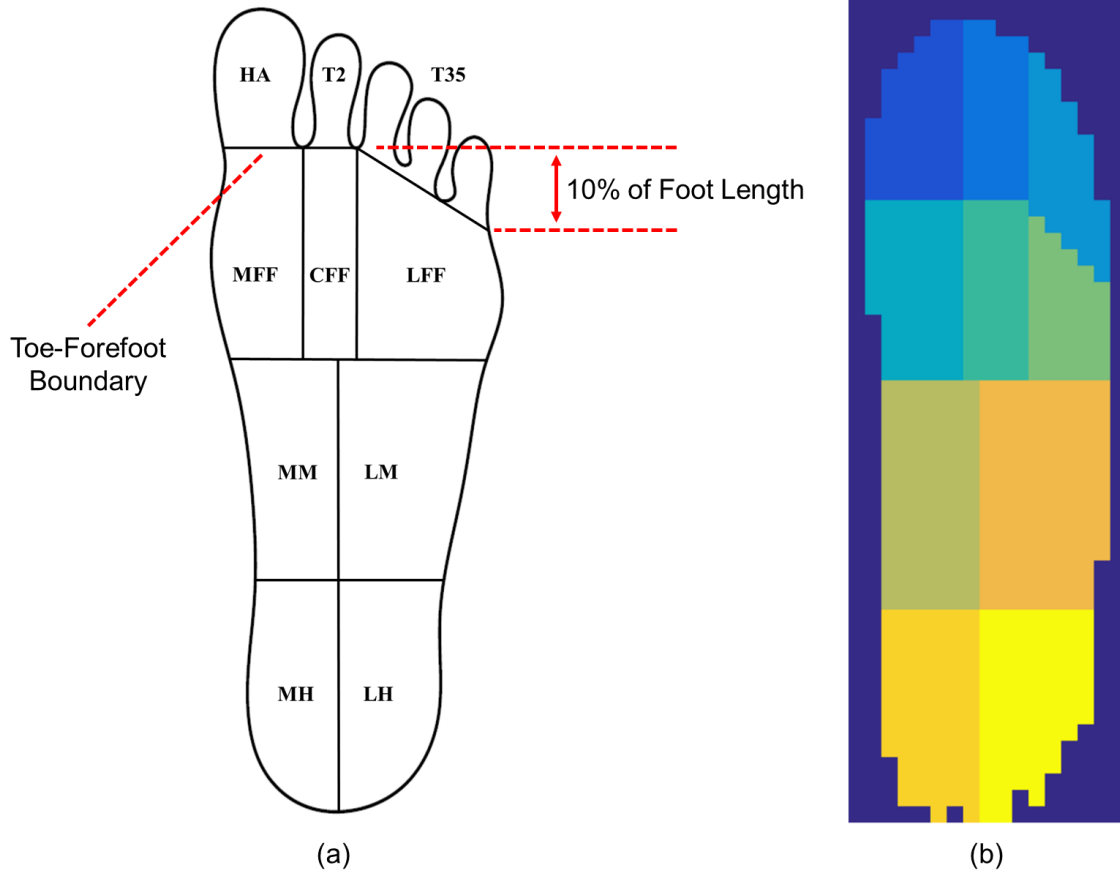
Figure 6 **Toe-Forefoot boundary depiction through (a) a diagram of the right foot and (b) an exemplary image from study one after foot segmentation was carried out**

Dead F-Scan Sensel Elements

Although it is advantageous in some regard to have an insole as thin as the F-Scan systems (0.15mm), the insole resultantly has limitations in terms of durability and longevity. The manufacturer states that an insole should last approximately 5-15 uses depending on the application. Towards the end of that lifespan, some of the sensel elements 'die' and no longer read pressure values. Dead sensels are not usually visible by eye and were typically found when examining real-time data prior to the start of a trial. If single sensels located in an area obviously under the plantar aspect of the foot were deemed to be inactive, the trial was continued and the sensel was removed during subsequent data analysis. On occasion, however, there were several sensels within a region attached to one another creating a 'gap' in a certain foot region; this gap was generally visible on the real-time F-Scan software interface prior to testing. If a gap

existed consisting of more than a single sensel, the insole was switched out and replaced with a new one.

Automated Detection of Activity Start Points

When collecting the posture data during the experimental portion of this work, a right-foot stomp was intended to denote the start of an activity and sync the video data to the pressure data. Once in a comfortable position, the participant was asked to give a small stomp using only their right foot to denote the start of a posture. The stomp created a sharp peak in the plantar pressure profile (Figure 7), which helped distinguish the start of an activity period from the transient transition phase.
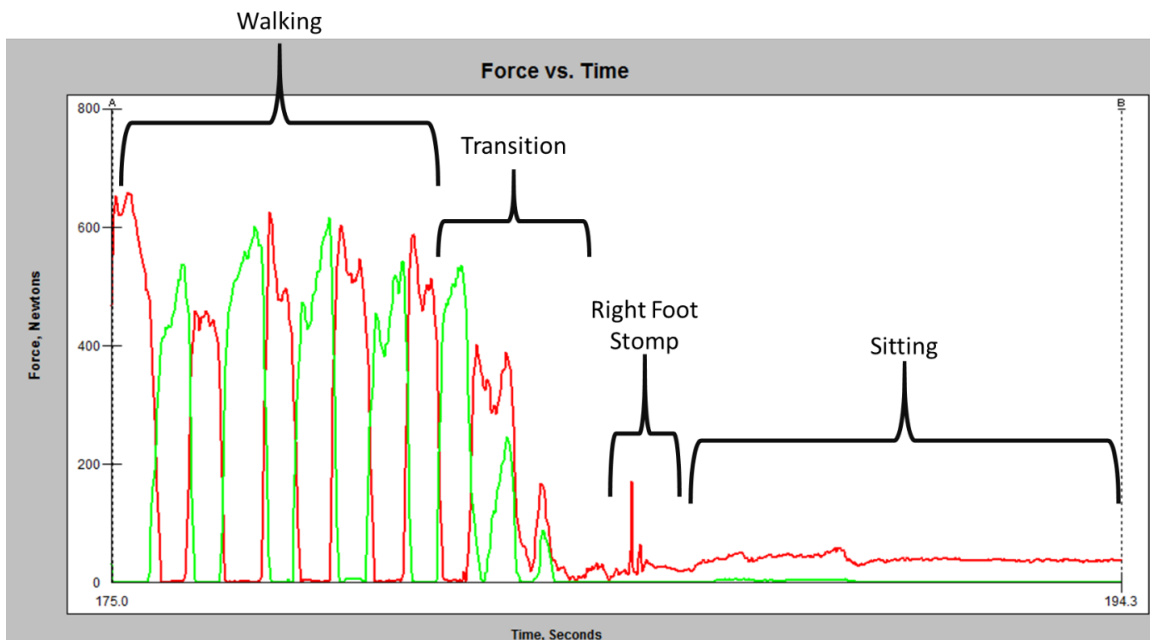
Figure 7   Exemplary data showcasing right-foot stomp denoting the start of an activity. Note that red data represents the right foot while green represents the left.

Rather than code the video data for validation of activities, it was postulated that the pressure data could be analyzed to extract the timestamp of each stomp denoting the starting of each of the six activities. Further, it was believed that because of the nature of the stomp in comparison to the other postures, the gradient, or the rate of change of pressure in this case, would be a feasible way to isolate these peaks. To do this, regional pressure data over the entire heel was first averaged as this region yielded the strongest signal throughout all the activities. The gradient was taken over the entire

activity collection phase (~six minutes) (Figure 8a). A threshold value was established through trial and error to filter out much of the steady state character of a posture in addition to some noise (Figure 8b). Lastly, a peak-finder function was used to identify peaks in the noise-reduced gradient profile which either had a substantial number of zeros behind or in front of them; values with many zeros either in front or behind them were representative of the start or end of a steady-state posture (Figure 8c). When these 'critical timestamps' were then overlaid on the corresponding pressure profile, the results were generally quite promising (Figure 9), demonstrating the potential in this method. However, upon investigation of all participants, noise associated with some participant's steady state posture data, specifically during standing, was found to be indistinguishable from the right-foot stomp. Two exemplary cases of this can be found in Figure 10a-b where distinctions in time are not as representative of activity start/end points when compared to Figure 9. Specifically, the first instance of sitting and the first instance of standing in Figure 10a are skewed, as well as the second instance of standing in Figure 10b. Because of the associated unreliability of this method, it was ultimately concluded that coding of videos was more reliable and because of the small number of subjects was used to accurately define the activity start/end points. For a larger data set it would be advantageous to revisit a pressure based activity distinction method as video coding would become prohibitively time consuming.
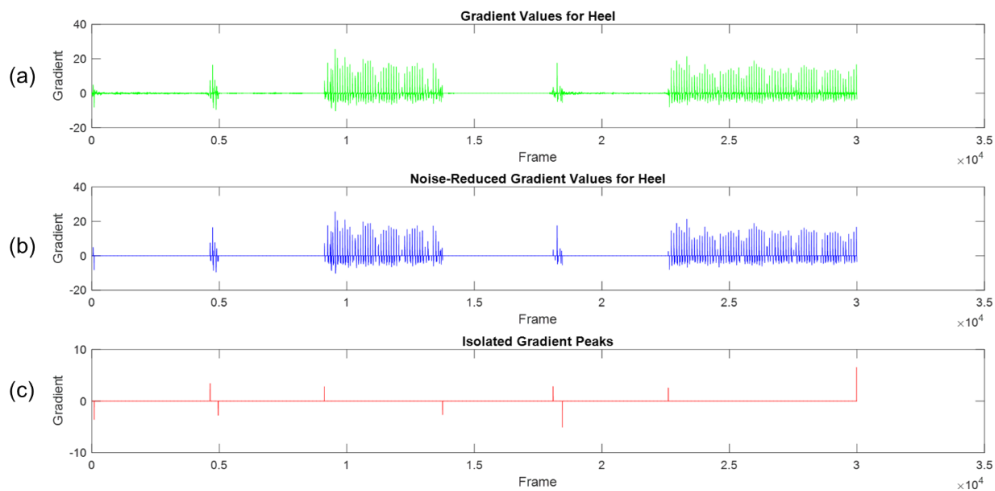

Figure 8   **Exemplary reduction steps involved in isolating critical timestamps in the data set. Note that order of activities was stand-sit-walk-sit-stand-walk. (a) Gradient data from the average pressure of the heel (b) Gradient data after filtering (c) Isolated peaks denoting critical timestamps in the trial.**
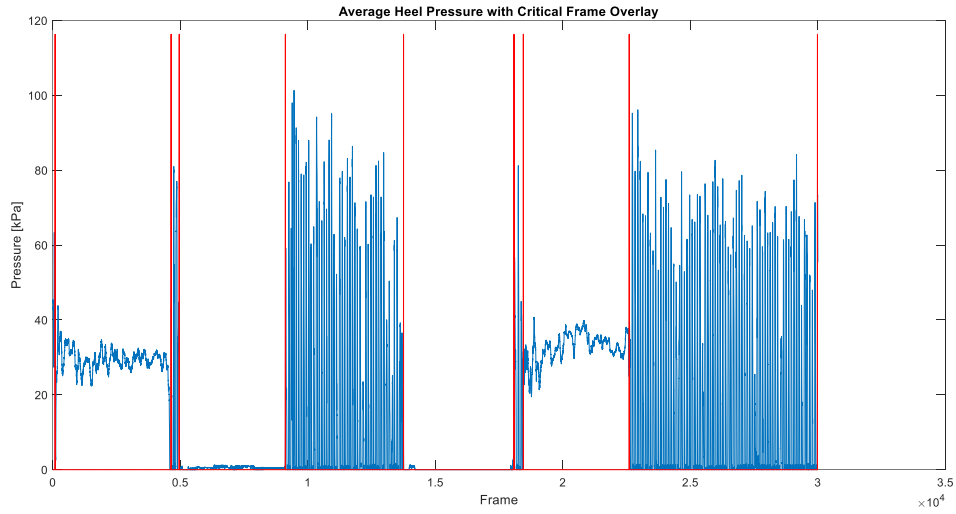
Figure 9   **Exemplary average heel pressure plot with critical timestamps overlaid. Blue denotes the pressure profile while red vertical lines showcase the identified times corresponding to the start or end of an activity. Order of activities was standing-sitting-walking-sitting-standing-walking.**
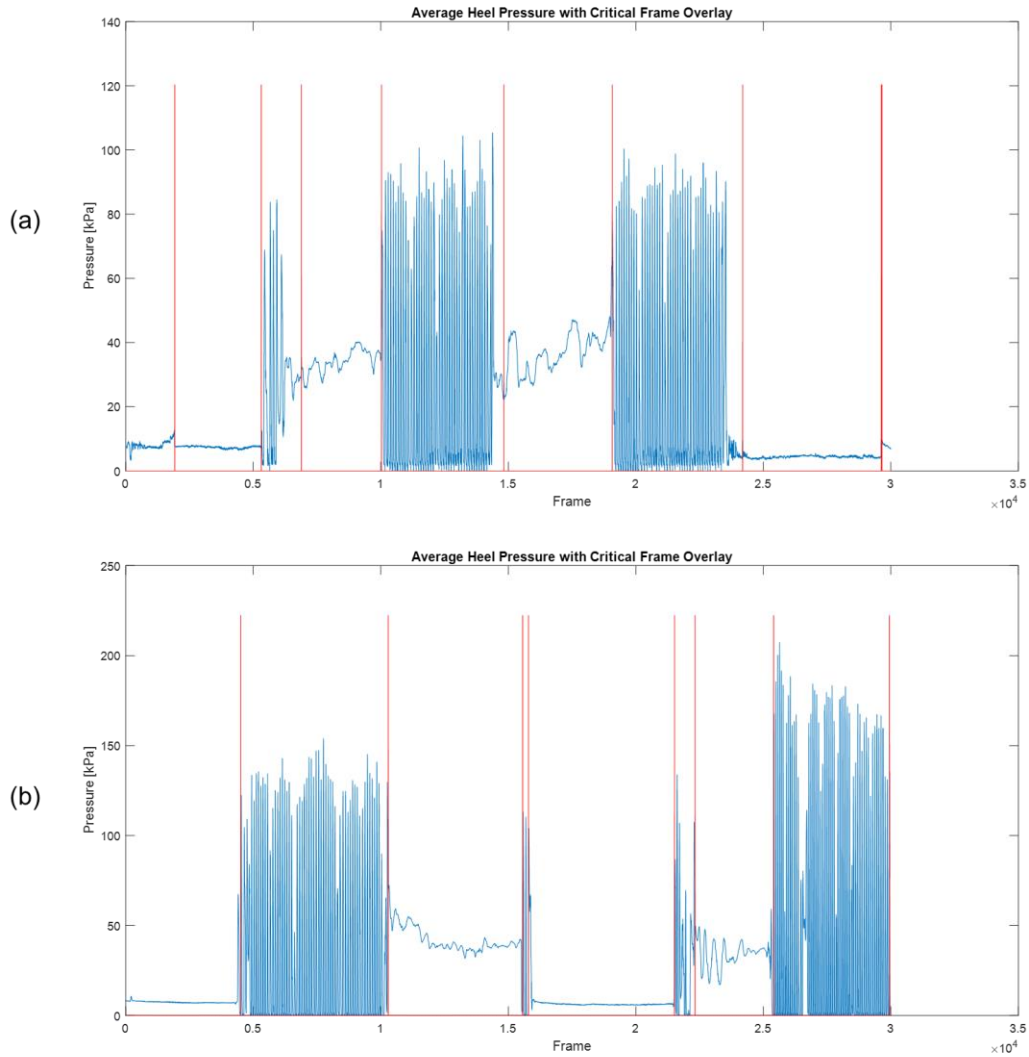
Figure 10 Exemplary average heel pressure plot with critical timestamps overlaid. Blue denotes the pressure profile while red vertical lines showcase the identified times corresponding to the start or end of an activity. (a) Activity order was sitting-standing-walking-standing-walking-sitting (b) Activity order was sitting-walking-standing-sitting-standing-walking

Measurement Parameters: Force-Time Integral & Pressure-Time Integral

A thorough literature was conducted to identify potential metrics of plantar pressure to be used in the classification schemes. In particular, temporal metrics were desired to differentiate standing and walking patterns. Two examples of these metrics are the force-time integral and the pressure-time integral. Force-time and pressure-time integrals represent the cumulative effects of force or pressure over time, respectively, and are measured in [N s] or [kPa s]. These metrics were thought to be suitable for this

145

study because the cumulative loading placed on the plantar fascia is thought to be a contributing factor for plantar fasciitis. Therefore, distinguishing the differences in cumulative force or pressure during standing and walking could yield valuable results. A force-time integral (FTI) is calculated as the area under the average force plot for a given foot region, whereas a pressure-time integral (PTI) is calculated as the area under the average pressure plot for a given region. After further investigation into the literature, it was ultimately concluded that FTI and PTI are used almost completely during dynamic activity analysis only. For example, Chuckpaiwong and colleagues [163] used FTI to analyze the effect of foot type on in-shoe pressure during walking and running. Additionally, Chua and colleagues [180] utilized PTI to describe the behaviour of both feet during particular steps of a basketball lay-up. To the authors' knowledge, no study has used FTI or PTI to analyze static postures. Since FTI/PTI are calculated from force or pressure plots, respectively, over an entire activity there would only be six FTI/PTI values representing an entire six-minute trial, one denoting the integral for each posture instance. For a representative trial, there are six curves as opposed to having time-series data available (Figure 11a-b). Because of the lack of resolution in time when compared with other metrics, FTI and PTI parameters served no purpose in this study and were therefore excluded from subsequent analysis.
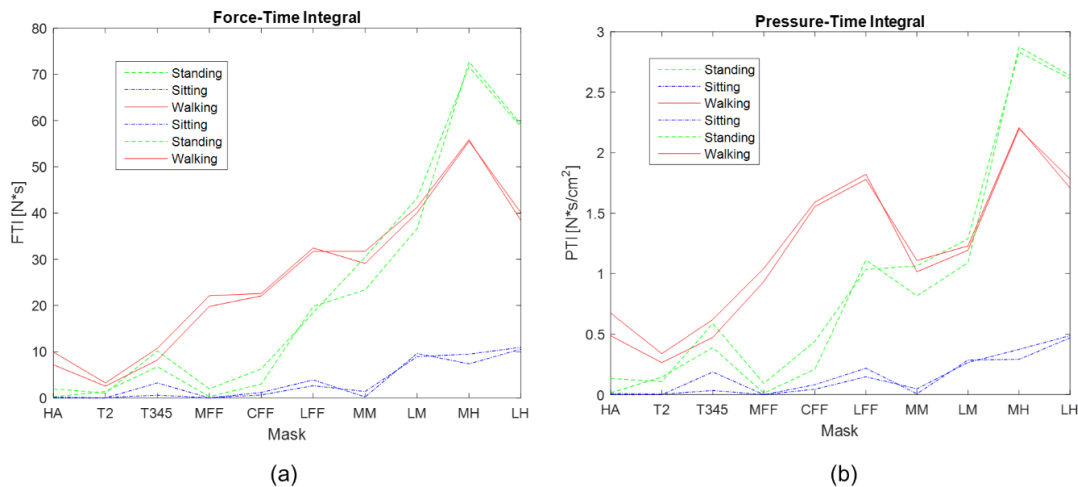

(a)   (b)

Figure 11   Exemplary plots of (a) Force-Time Integrals and (b) Pressure-Time Integrals for a representative six-minute trial.

146

Measurement Parameters: Fourier Transform

A Fourier Transform (FT) is a function decomposition method which deconstructs a function of time into the various frequencies that compose it. Upon conducting a FT, both the magnitude and phase of various frequencies can be compared to determine fundamental characteristics of the original signal. It was postulated that a FT could be useful in this application as the temporal characteristics of gait are a notable feature that distinguishes it from the other postures; conversion of the average pressure signal in time to the frequency domain could yield useful data which could be used to distinguish the postures.

A script was written to use a Fast-Fourier Transform to deconstruct the various posture-specific regional pressure signals into their fundamental frequencies. Results demonstrated that there was indeed evident differences between the three postures, but not enough significant differences to warrant subsequent use of the FT. During sitting and standing (Figure 12a-b), very little frequency data was extracted from the original signal. Conversely, during walking (Figure 12c), several key frequencies are distinguishable between 0-5Hz, although there is quite a bit of noise within the signal. It was concluded that frequency analysis could not reliably distinguish sitting from standing, making it an non-ideal method. Ultimately, the overlapping sliding window approach was instead used to extract the temporal characteristics from walking, while also establishing differences between sitting and standing.
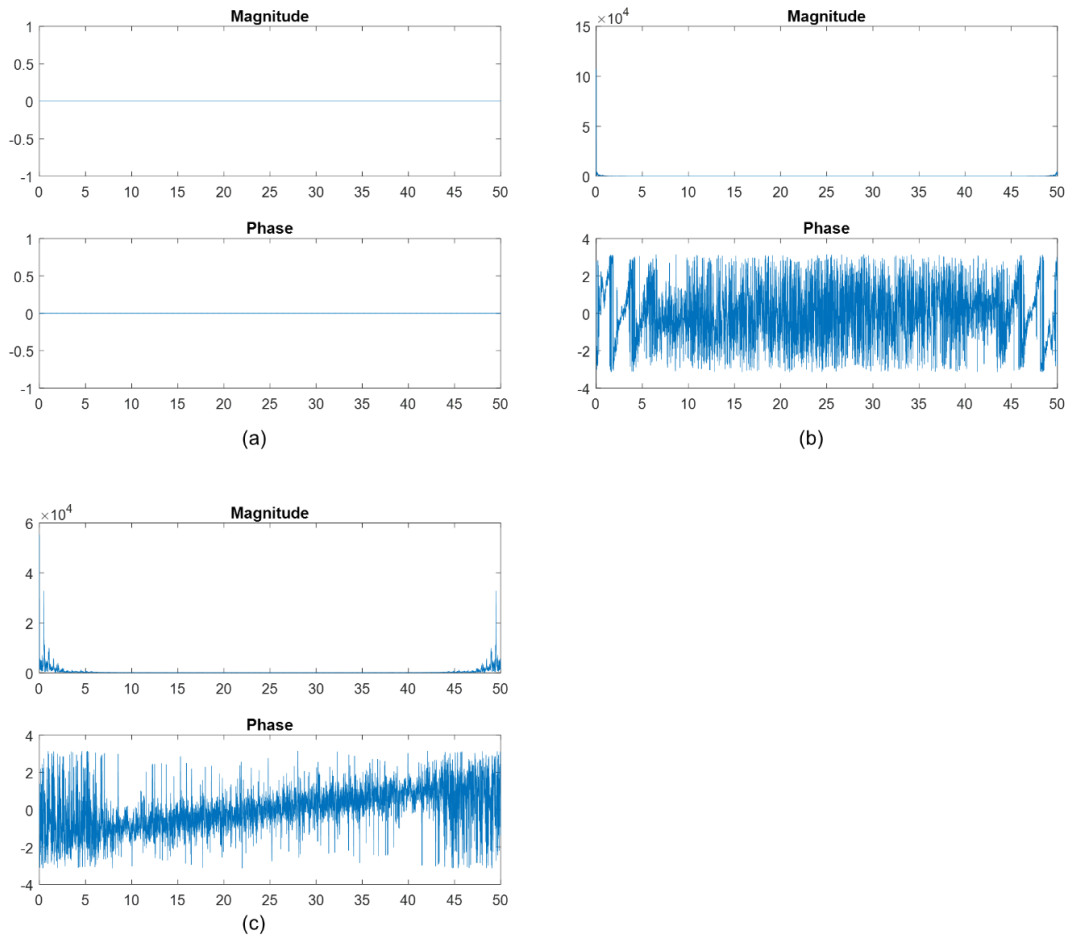
Figure 12 **Exemplary fast fourier transform plots of the magnitude and phase during (a) sitting (b) standing and (c) walking for the average pressure of the lateral heel**

Appendix C – Extended Methods for Study 2

These extended methods are intended to provide clarity and specific details of the techniques used to conduct the machine learning analysis study that could not fit in the standard journal paper format.

Simulating an FSR Sensor

To identify the minimal number and location of FSR sensors needed to accurately classify sitting, standing and walking, it was necessary to determine how to approximate an FSR sensor using the plantar pressure data obtained through the F-Scan system. Previous projects in the lab worked with the *Interlink 402* FSRs (Figure 1a), so as a preliminary choice it was decided to move forward with that sensor while looking at different options in parallel. The Interlink 402 FSR sensor has a 0.5" diameter sensor head which translates to a sensor area of $1.29cm^2$. In comparison, each resistive sensel element (Figure 1b) has a sensel area of $0.062cm^2$; therefore, five sensel elements has a cumulative area of $0.31cm^2$. Although the area of the interlink sensor is over four times larger than that of five F-Scan sensels, the sensor area does not matter as the spacing of the five F-Scan sensels was selected to sufficiently cover the span of the Interlink 402 FSR area (Figure 1c). As a best approximation, it was determined that using five sensel elements arranged in a cross shape was the closest match for the Interlink sensor (Figure 1c).
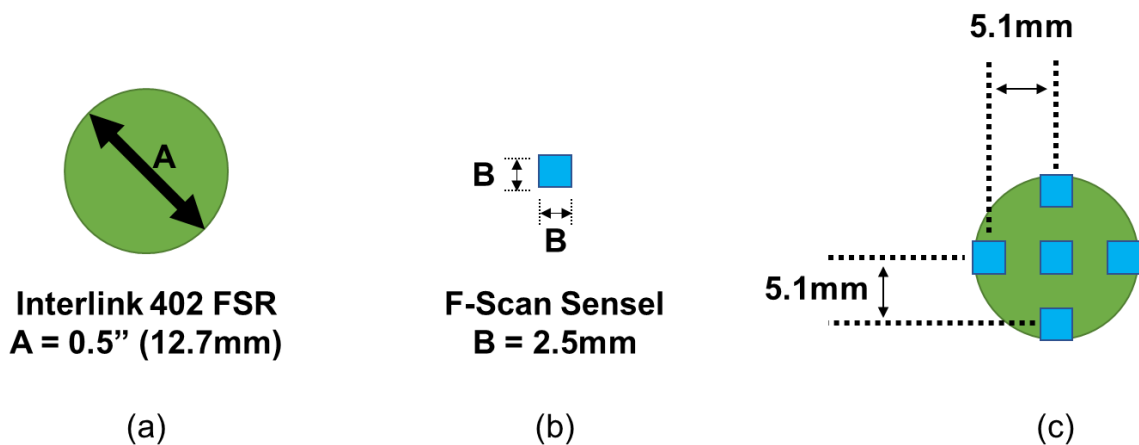

Figure 1   **Comparison of the (a) Interlink 402 FSR and (b) F-Scan Sensel Elements. (c) Approximated overlap showcasing the composition of a simulated FSR**

Defining the Number and Locations of Simulated FSR Sensors

After deciding on the closest approximation of the Interlink FSR using the F-Scan sensels, the next step to determine how to distribute the simulated FSRs ('simFSRs') over the plantar aspect of the foot. Although this problem seems trivial on the surface, complexities arise when multiple individuals are brought into the picture; because all participants have different sized feet, sensor locations must be scalable to draw generalized conclusions from the analysis. Therefore, for the sake of this work, the same number and locations of sensors must fit both the largest and smallest feet. Logically then, it makes sense to look at the participant with the smallest feet, which in this case was a women's 7. Using the foot outline captured with the F-Scan system, the foot length of this participant was 24.9cm and the foot width across the metatarsals was 7.6cm, which translates to 49 and 15 sensels, respectively. As Figure 1c shows, the sensel elements span slightly beyond the sides of the Interlink FSR; resultantly, to avoid overlap and leave room for manufacturing (e.g. sensor tails, wiring channels, etc.), the closest any two simFSR centers can be is to have three sensels between them, two forming the sides of each simFSR and a single sensel gap between them. Additionally, no simFSR can hang off the edge, so at least one sensel must be between a simFSR center and the edge of the insole; in an ideal case, two spaces between the edge is better.

Using these spacing rules, the number of sensors can be determined along the length of the participant's foot. An insole 49 sensels long reduces to 44 sensels when two sensels worth of room are left at either end. Following this, it is known that each simFSR is three sensels long, and is separated from an adjacent one by a single sensel space. Dividing this up results in a maximum of 11 simFSRs (3 sensel diameter/simFSR x 11 simFSRs = 33 sensels + 11 gaps of a single sensel = 44 rows). Doing the same thing with the 15 sensels comprising the width, 15 reduces to 13 after a single sensel gap on either side, then 13 sensels results in 3 simFSRs (3 sensels diameter/simFSR x 3 simFSRs = 9 sensels + 3 gaps of a single sensel = 12 rows). Because of this, theoretically 33 simFSRs are potentially discernible. In practice, however, the foot shape is not a perfect rectangle and therefore roughly six sensors are lost in the narrowing of the posterior half of the foot, bringing the possible sensor total to 27. Additionally, because the foot masks were used to define the locations of the simFSRs, several subsequent gaps were created around the edges of masks in an attempt to avoid simFSRs lying across two

regions. The one exception to this rule existed at the toe/forefoot boundary in several cases. Because the hallux is tapered along the anterior edge, it was a challenge to place two simFSRs within that mask; to compensate, one of the medial forefoot simFSRs was moved anteriorly to span the gap more evenly. The same compensation method was employed for T2 and the central forefoot. Because of the gaps existing between some masks, ultimately three simFSRs were lost, bringing the total to 24 simFSRs for each participant (Figure 2). It may be postulated that one could extract the entire 33 possible simFSRs from each participant if this process was further refined. In this case, a balance was struck between having enough simFSRs to span the majority of the foot, time spent defining the locations, and making several compensations for gaps/atypical data/dead sensels beneath a simFSR. These simFSR locations should adequately convey the information necessary to classify the three postures. More simFSRs may provide an additional level of detail, but based on previous studies that could classify postures using 5 FSRs [36,46,136] the locations specified were expected to adequately classify the postures and this was subsequently proved by the results of Study 2.
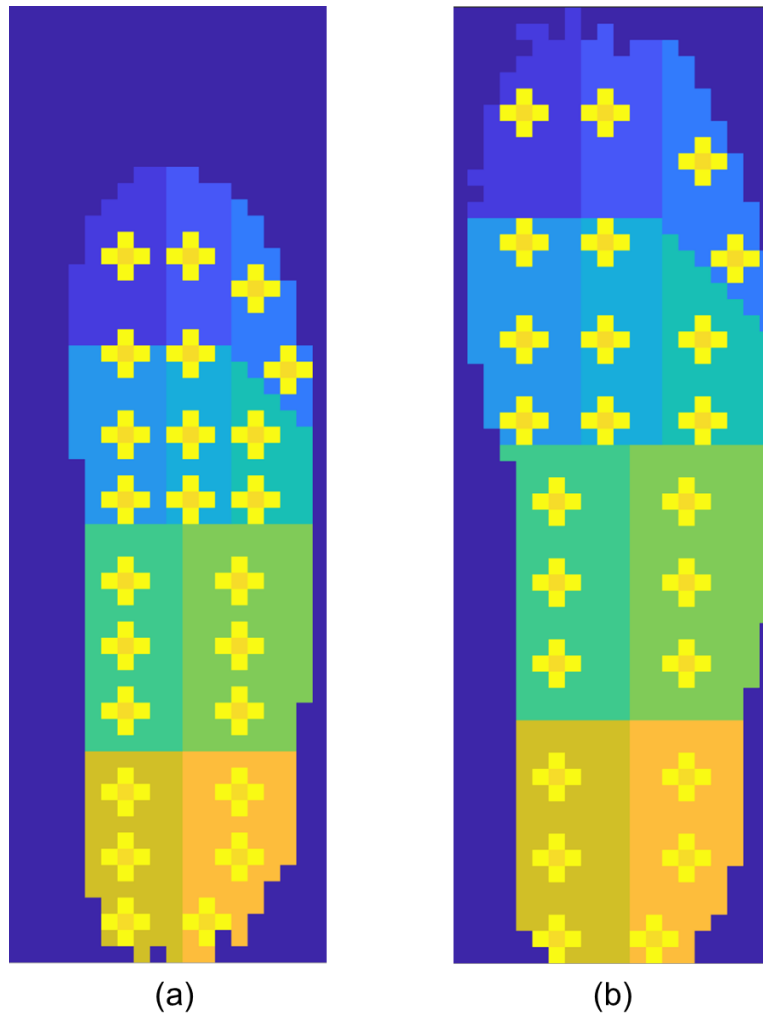
Figure 2   Exemplary footprints showcasing the foot masks and simulated FSRs for (a) the smallest participant (Women's 7) and (b) the largest participant (Men's 12)

The last component of defining the sensor locations is how each simFSR was specifically located within the insole using mathematical definitions to ensure repeatability and ease of scaling between subjects. To place the sensors, three sensors were first placed at the center of the hallux, second toe, and third to fifth toe regions (sensors 1,2,3) (Figure 3). A fourth sensor was then placed in the third to fifth toe region at an offset of 10% of the foot length in the posterior direction, and 10% of the foot width in the lateral direction (sensor 4). Sensors were placed at the center of the remaining anatomical masks (sensors 5,8,11,13,16,19,22). Remaining sensors were placed at an offset 10% of the foot length in the anterior/posterior directions from the center sensor in each mask along the longitudinal axis of the foot. Two sensor locations (sensors 6 & 9) were moved an additional 8% anteriorly to compensate for the large toe-forefoot sensor

gap. Only two sensors were defined for the lateral forefoot to compensate for the diagonal T35/LFF boundary. Sensor 24 was also moved medially 10% of the foot width. Note that 10% was selected through trial and error to avoid sensors spanning multiple masks, with the exception of simFSR 6 and 9. Additionally, 10% of the foot length was thought to be an easy number to follow when locating the proposed sensor locations during the manufacturing process.
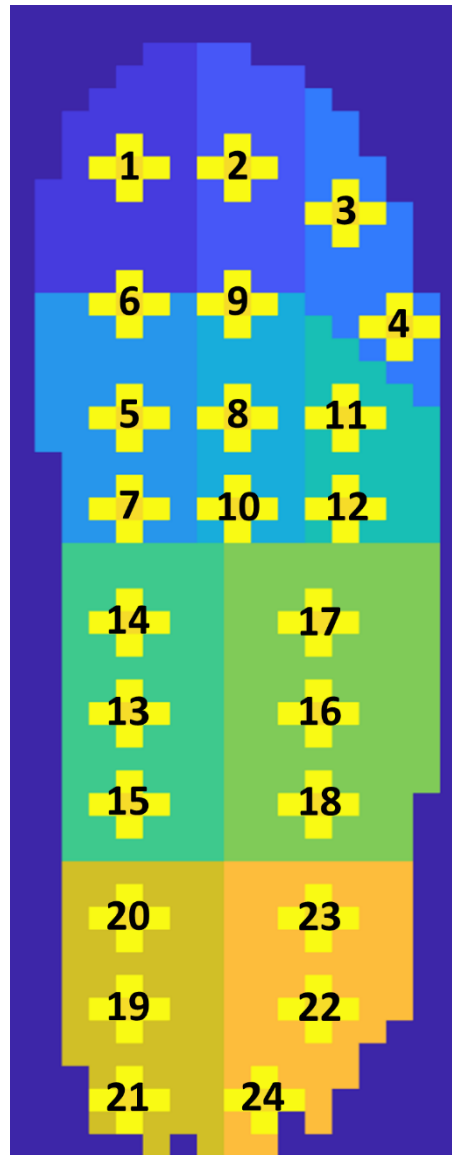

Figure 3   Exemplary foot outline with numbered simulated FSR sensors noted